SOLVED PROBLEMS

ELECTRO-OPTICAL INSTRUMENTATION:

SENSING AND MEASURING WITH LASERS

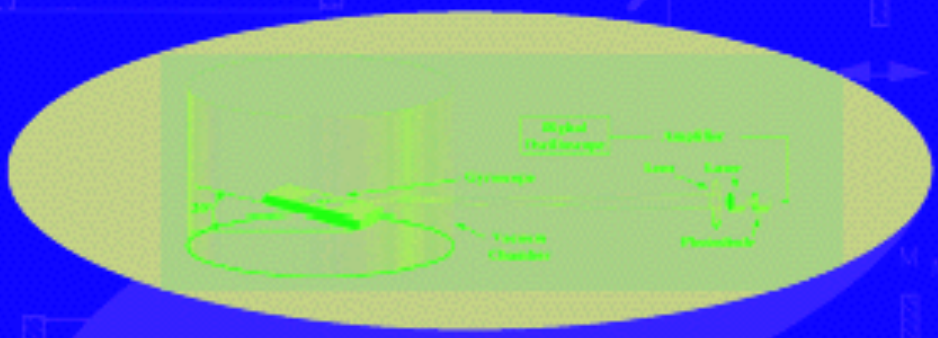

SILVANO DONATI

Electro-Optical Instrumentation

Solved Problems

Silvano Donati

University of Pavia

Prentice Hall PTR
Upper Saddle River, NJ 07458

Foreword

As promised in the Introduction of my book *'Electrooptical Instrumentation'*, I have prepared a number of solved problems to complement the main text, and with pleasure I make this booklet freely available to instructors and students through my website http://unipv.it/donati.
I have tried to arrange a mix of problems and questions ranging from very easy to rather difficult.
My main aim has been trying to convey to the student the design attitude of the instrumentation engineer who is continuously confronted with a variety of potential solutions and trade-offs to solve the problem at hand.
Many exercises start from numerical examples already presented in smaller font in the text, and develop the design in some detail, showing also the 'what happens if' of several possible choices.
I hope the material may be useful to colleagues and students. For any comment and suggestion, as well as to point out errors or inadequacies, please e-mail me at: silvano.donati@unipv.it.
For instructors, I have prepared the PowerPoint slides of the book. They are a set of 400 slides and those using the book in a course can ask me the password to download the slides from my website.

Index

Questions and Problems, Chapter 1 2
Questions and Problems, Chapter 2 4
Questions and Problems, Chapter 3 15
Questions and Problems, Chapter 4 35
Questions and Problems, Chapter 5 54
Questions and Problems, Chapter 6 63
Questions and Problems, Chapter 7 66
Questions and Problems, Chapter 8 77

Questions and Hints, Chapter 1

Q1-1 *Why do we speak of electro-optical instrumentation and not of laser instrumentation or, simply, of optics ?*

Answ.: No doubt that the laser and optics plays a central role in the development of the novel electro-optical instrumentation. However, parallel to the importance of the properties of the laser radiation, much credit shall be given to the new measurement methods, which are specific and distinctive of this new discipline, as it will be appreciated in the book.

Q1-2 *In the LURE experiment, how can they succeed in aiming the Apollo landing site even without seeing it ?*

Answ.: Following a clever proposal of Curry (see [1] of Chapt.1), they used a small (2" diameter) corner cube mounted internal to the telescope tube. When the laser pulse is fired out the telescope, the corner cube reflects back a small portion of the beam to the eyepiece of the telescope, thus identifying the aimed area with a small spot superposed to the moon image. The diffraction limit of the corner cube, $\theta=1.22\lambda/D\approx 2$ arc-sec is comparable to the divergence of the laser beam transmitted across the atmosphere.

Q1-3 *How can the Mars orbiting telemeter be able measuring the surface profile from an orbit that is elliptical (that is, not exactly circular)?*

Answ.: The raw telemetry data are transmitted to earth and processed to correct the height error due to the ellipticity of the orbit.

Q1-4 *After the He-Ne RLG was developed into a device deployed in the field and demonstrating the physical principle underlying the Sagnac measurement, what further understanding or benefit is really gained with the FOG gyroscope?*

Ans.: No progress in physical science is actually gained with the FOG respect to the RLG. Despite that, the progress in engineering is great if we consider that the sensor becomes much lighter, scalable in size, and potentially cheaper. For the same reason, efforts are pursued with the new MEMS-based technology.

Q1-5 *About experiments with interferometers, reported resolution or accuracy in the range of picometers or less is much smaller than the atomic size at the target surface. Is that correct, no issue about it ?*

Ans.: There is no physical limitation to the smallest displacement measurable on a surface, provided the spot size involves a number of atoms large enough to average the atomic-size ripple to the desired accuracy.

Problems, Chapter 2

P2-1 *How small is the beam waist of a typical L=20-cm long He-Ne laser?*

Answ.: We shall calculate the beam waist using Eq.A1-5 (Appendix A1). With the reasonable assumption of a plano-concave mirror cavity, with $R_1 = \infty$ and $R_2 = 2L = 40$ cm, so that K=2, and $m = \sqrt{(K-1)} = 1$ we get a beam waist:

$w_{0L} = \sqrt{[(\lambda/\pi)mL]} = \sqrt{[(0.000633/3.14) \times 1 \times 2000]} = \sqrt{0.402} = 0.63$ mm.

The waist is located at the plane mirror. Usually, we prefer to have the output mirror plane, and let the substrate be slightly wedged (in this way the second-surface reflection is deviated out from the useful beam.
So, the waist is located just at the output mirror.

P2-2 *Using the He-Ne laser of P2-1 for alignment purposes, how small can the beam size be maintained on a total path length of 10 m ? Which telescope is needed to project it ?*

Answ.: We can magnify or de-magnify the beam waist w_{0L} to fit properly into the distance 2z=10 m, as shown in figure.
Doing so, we obtain a beam size (Eq.2.4):
$w_0 = \sqrt{(\lambda z/\pi)} = \sqrt{(0.000633 \times 10000/3.14)} = \sqrt{2.015} = 1.42$ mm. This is the minimum size we can achieve at Z, the middle point of the 10-m distance.
At the boarders of the path, the beam size is (page 14)
$w_{-z} = w_{+z} = \sqrt{2}\, w_0 = 1.41 \times 1.42 = 2$ mm.

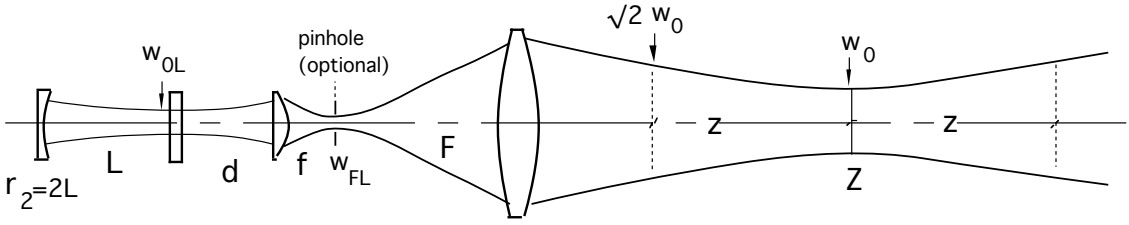

Figure 1

Now, let us consider the telescope we shall use. Suppose we start (see figure 1) with an intermediate optical element (the eyepiece of the telescope) placed at a distance d=100-mm from the beam waist.
As all the distances involved are much larger than beam sizes, the magnifications are given by the distance ratios (see figure 2). Thus, going out from the laser we arrive at the eyepiece focal plane with $w_{0F} = w_{0L}(f/d)$ and the objective conjugates this to a spot size: $w_0 = w_{0F}\,(z/F)$.

The total magnification is (see figure below): $m_{tot}=w_0/w_{0L}=$ (z/F)(f/d)= (z/d)/M =1.42/0.45= 3.15, where M=F/f is the telescope magnification.

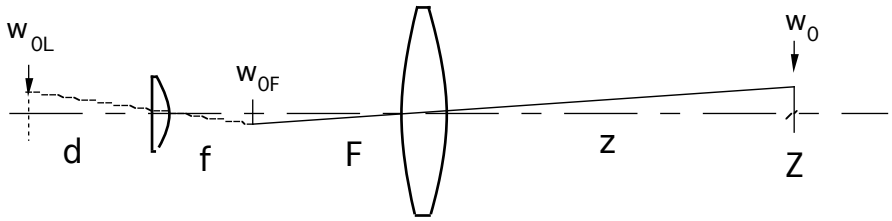

Figure 2

By inserting in $m_{tot}=w_0/w_{0L}=(z/d)/M$ the ratio z/d= 5000/100=50 and w_0/w_{0L} =1.42/0.63=2.25 we solve for M with the result M=50/2.25=22.18.
The telescope providing it may be implemented by an objective lens with, say, F=100-mm focal length and an eyepiece with f= F/M=100/22.2= 4.5 mm focal length. Or, we may prefer use a larger focal length (and hence telescope tube) F=200 mm to accommodate an easier focal length of the eyepiece, f=200/22.92= 9 mm.
The design of the telescope is not complete until we specify also the diameters needed to contain the beam being transmitted. In a Gaussian beam with spot size w_0, the fraction of total power which is contained in a radius r is $P(r)/P_{tot}=1-\exp -r^2/2\ w_0^2$. Thus, to get at least the 99% of the power (figure 3), and avoid cutting out the tail of the beam distribution, *Figure 3*

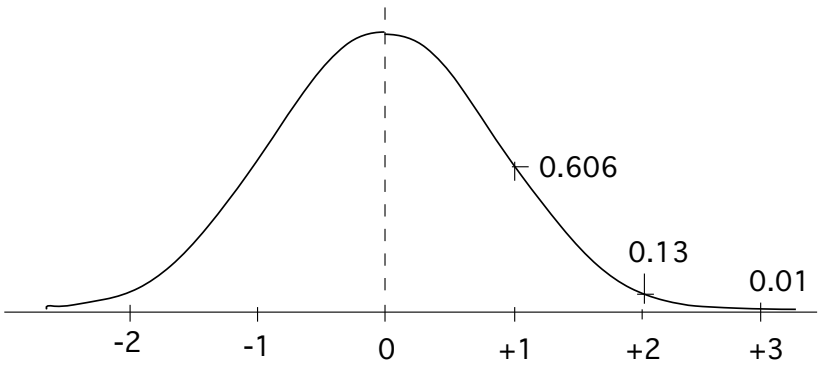

we have to work with a lens diameter D=6w. At the telescope eyepiece, the beam size is w_{0L}=0.63 mm plus the negligibly small increase due to divergence on the d=100-mm path. So the minimum diameter of the eyepiece is $D_{eyep}=6\times0.63=$ 3.8 mm.
At the objective, the waist is magnified by a factor F/f= 22.2 and thus we need $D_{object}=3.8\times22.2=85$ mm, a rather bulky lens.

P2-3 *Instead of the telescope used in Probl.2-2, could we use a single lens ? What is the advantage or disadvantage of both choices?*

Answ.:To use a single lens, we have to obtain the total magnification $m_{tot}=w_0/w_{0L}$ =3.15 in a single step. This requires a ratio z/d=3.15 or, using z=10m, a distance d=10/3.15= 317 cm. Clearly, this is a very unsuitable figure to work with. Now, the advantage of having a factor M (=22.2) of distance d reduction, provided by the collimating telescope is readily appreciated.

P2-4 *What about the beam size if we remove the telescope and let the beam propagate, using just the intrinsic collimation of the laser beam?*

Answ.: Removing the telescope and starting with the size w_{0L} of beam at the laser output mirror, we get a beam size (see Eq.2.1):

$w(z) = [w_{0L}^2+(\lambda z/\pi w_{0L})^2\ ]^{1/2}$

Inserting z=10 m and w_{0L}=0.63 mm in it, we get a spot size:

$w(10m) = [(0.63)^2+(0.000633 \times 10^4/3.14\times 0.63)^2\ ]^{1/2}= [0.397+(3.18)^2]^{1/2}$

As we can see from this equation, the second term coming from the angular divergence of the beam is dominant over the first. So we get
w(10m)= 3.18 mm, about twice the beam size of the minimum diffraction case (Probl.2-2).
Worth noting, at increasing distance z the above said trend continues, and it is even more disadvantageous to remove the telescope. On the other hand, if distance is small, for example z=1m, then we would obtain:

$w(1m) = [0.397+(0.318)^2]^{1/2}$=0.71 mm,

whereas the minimum spot size (Probl.2-2) is recalculated as

$w_0= \sqrt{(\lambda z/\pi)} = \sqrt{(0.000633\times 1000/3.14)} = \sqrt{0.2015} = 0.448$ mm,

and we may wonder if the telescope is really needed, in this case which, however, is definitely not the best representative of the application made possible by the laser source.

P2-5 *How can I estimate the effect of air turbulence, in a real experiment with alignment beams propagated through the atmosphere ? Up to which distance L will the small spot size calculated previously still be obtained ?*

Answ.: For air turbulence, we go to Appendix A3.2, where the effect of scintillation and beam wandering is described.
About scintillation, that is corruption of the original Gaussian profile of the beam, the equation to employ is (page 417):

$\sigma_\phi^2 \approx C_n^2 k^{7/6} L^{11/6}$

where σ_{ϕ^2} is the phase variance induced by turbulence, $k=2\pi/\lambda$ and C_n is the structure constant.

To avoid scintillation, we may settle that σ_ϕ is small respect to the phase differences involved in keeping the Gaussian beam collimated. Like for a lens aberration, we may take $\sigma_\phi=0.1$ rad ($\approx 0.01\lambda$). Inserting $\lambda=0.633$ μm and L=10m, we get:

$C_n^2 = \sigma_\phi{}^2 / k^{7/6} L^{11/6} = 10^{-4} (10^7)^{-7/6} (10)^{-11/6} = 10^{-14}$ ($m^{-2/3}$)

Comparing with the data of page 417, we can see that this is the value describing medium-strength turbulence.

As the distance factor is proportional to the power $11/6\approx 2$, increasing L by a factor of 3 to L=30 m means that we need a weak turbulence. Reducing it to 0.3 m reveals that also a strong turbulence can be tolerated.

Beam wandering is characterized by a radius ρ_w, of the beam centroid deviation. The approximate expression for it is (page 417):

$\rho_w = w/(1 - 2.45\, C_n^2 k^{2/3} L^{11/6} w^{-11/6})$,

Requiring that $\rho_w < w$ is like setting $2.45\, C_n^2 k^{2/3} L^{11/6} w^{-11/6} << 1$. With the above data, we get for this quantity:

$2.45\, C_n^2 k^{2/3} L^{11/6} w^{-11/6} = 2.45\, 10^{-14} (10^7)^{2/3} (10)^{11/6} (1.42\, 10^{-3})^{-11/6} = 0.013$

and wandering is negligible. But, if L is increased to 100m, the term $L^{11/6}$ will increase by a factor 77 and the calculated quantity will now approach unity, making $\rho_w >> w$.

P2-6 *In the 4-quadrant pn photodiode of Fig.2-4 top the two output anodes do not appear electrically isolated between them, because of the finite resistance of the p region. Does this introduce any errors?*

Answ.: Indeed, if R_{transv} is the transversal resistance found between the anodes, we need to terminate the photodiodes on load resistances $R_l << R_{transv}$ for the error to be negligible. This is indeed provided by the low-impedance, virtual ground of the op-amps receiving the photocurrents of the quadrant photodiodes.

P2-7 *What is the dynamic range of position acquisition of the 4-quadrant photodiode ? What its minimum position change that can be detected? Can these two quantities be changed through design in a specific given device?*

Answ.: The maximum extent of displacement, or dynamic range DR is given by the device diameter D_{ph}, whereas the minimum change of position MCP near the zero coordinates is given by the width w_{dz} of the gap between

adjacent photodiodes. Both these quantities can be changed with an optical system in either use of the sensor shown in Fig.2-7.
In sensing of position-coordinates, we use a collimating telescope in front of the PSD, whose F/f ratio is the magnification of both DR and MCP.
In sensing of angle-coordinates, we will change the focal length F of the objective to adjust θ_x, $\theta_y = D_{ph}/F$ and the minimum $MC\theta = w_{dz}/F$.

Q2-8 *Could a photoconductor structure be employed in place of the photodiode structure to perform like a 4-quadrant detector ?*

Answ.: Provided that the thickness to diameter ratio is very small and that the dark resistance of the photoconductor is high, the structure could indeed work as well as the photodiode, and in addition, one would get a photoconductive internal gain (see *'Photodetectors'*, Ch.5.6)

Q2-9 *Why shall we consider three types of position sensing devices, the 4-quadrant, the PSD and the reticle-assisted? Isn't one superior to the others ?*

Answ.: Each device has one characteristic in which is superior to the others. The PSD has the best linearity, the 4-quadrant is easier to fabricate (no transversal resistance constraint, and even a photoconductor fits as well) and thus is the cheapest. The reticle-assisted position sensor can be implemented using a normal photodetector of circular geometry and so it has the widest range of λ covered, from UV to IR; in addition, it provides a numerical output without using an A/D converter.

Q2-10 *What is the fastest position sensing device among the three types of detectors ?*

Answ.: The reticle-assisted position sensor is the slowest because it requires a full rotation of the reticle to adjourn the output data. Excluding the frequency cutoff of the electronic circuits, both the 4-quadrant and the PSD possess the high frequency performance typical of a junction photodiode, and therefore are of the same (or comparable) speed of response.

Q2-11 *In the laser level, why to use a pentaprism to deflect the beam instead of a plain mirror inclined at 45° ?*

Answ.: The pentaprism arrangement deflects the beam exactly 90° off the incoming direction, irrespective of the incidence angle error which instead affects the simple mirror system.

Q2-12 *How collimated can the fan-beam at the output of the laser level be maintained at a distance z?*

Answ.: All the calculations developed in P2-1 to P2-5 apply to the case of the laser level. As the only difference, instead of spot size we have fan-beam thickness in this case.

Q2-13 *Can a semiconductor laser diode be used in place of the He-Ne to build a laser level?*

Answ.: Laser diode with a wavelength appropriate for visualization of the beam are readily available from different vendors. They are quaternary hetero-structures (GaInAsP grown on InP) diodes, and may provide up to 50 mW power at relatively low cost. Laser diodes require an anamorphic objective lens to circularize the beam, and this is frequently provided by the manufacturer. The M^2 factor (page 367) of the source is however not very close to unity, 1.8 to 2.5 being common values. This means that the spot size is larger than the expected diffraction limit, and this is a first point of concern.
When mounted in a mechanical fixture fastening it to the transmitting telescope, laser diodes perform appropriately as the optical source of the level. But, with ageing, the near field spot that is imaged by the objective lens may drift appreciably, resulting in a pointing error (typically 0.1 to 0.5 mrad after few thousand hours of operation); this is the second point of concern when using laser diodes.

Q2-14 *Is the automatic verticality servo really superior to the manual setting version of the laser level ?*

Answ.: Technically it is, because with it the laser level quickly attains the working condition and is ready to operate. In the practical implementation, however, the user frequently finds the manual system more friendly. In addition, the manual system is simpler and cheaper, so it is often preferred.

Q2-15 *In the wire diameter sensor, what about the shape of the photodetector that is needed at the focal plane to collect the scattered field efficiently ?*

Answ.: As sketched in the figure 4, if the wire is placed vertical (or parallel to the Y-axis), the diffraction distribution swings horizontal, or along the Z-axis, generating the cylindrical distribution for the diffracted power shown in figure.

To collect all the available light, we need then a rectangular-shaped photosensitive area for the detector PD. The height of the rectangle will be chosen equal to the beam width W and the thickness w_{det} will be chosen according to the desired resolution along Z or in angle, being $\theta = w_{det}/F$.

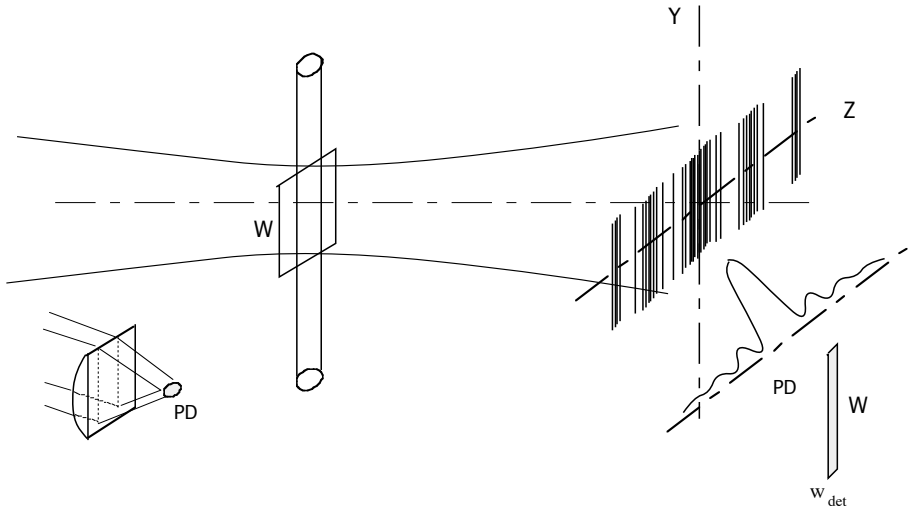

figure 4

Note that we don't actually require a rectangular shaped photodetector, because as shown in the lower left corner of figure, a cylindrical lens will suitably focus the rectangular (or fan) beam into a circular (or square) one, allowing us to use a detector with normal circular or square sensitive area.

P2-16 *In the wire diameter sensor, calculate the amplitude of the signal which is collected by the photodetector.*

Answ.: Let us start with a power P_0 supplied by the laser in the waist where the wire is located. Let W be the height of the waist cross section. Then, a total power $P_0(D/W)\,Q_{ext}$ is deviated off the beam (here Q_{ext} is the extinction factor discussed on page 410). As $D>>\lambda$, we are in the Mie scattering regime and it is $Q_{ext}\approx 2$. But, only half of the deviated power is the diffracted contribution, the other half being the power intercepted by the wire (page 410). Therefore, at the focal plane, the diffracted power has an amplitude $P_0(D/W)$ and an angular distribution $\mathrm{sinc}^2\theta D/\lambda$. As $\mathrm{sinc}^2\xi$ is normalized to

unity area respect to an integration over $\xi=\theta(D/\lambda)$ (see A5.15'), we write the power distribution as the product of the two above terms and of $(D/\lambda)^{-1}$: $P(\theta) = P_0(D/W)\ (\lambda/D)\ \mathrm{sinc}^2\theta D/\lambda$.
This quantity is normalized respect integration on θ. As the detector of size w_{det} presents an angle $\theta_{det}= w_{det}/F$ and the current coordinate is $z=\theta F$, we finally get for the power collected by the photodetector:
$P_{det}(z)= P(\theta)w_{det}/F= P_0(\lambda/W)(w_{det}/F)\ \mathrm{sinc}^2\ zD/F\lambda$
Letting numbers in this equation, for example w_{det}=0.1 mm, F=400 mm (as on page 28), W=10 mm, λ=1μm, we get that at sinc^2 =0.5 and with P_0= 20 mW the power reaching the detector is just P_{det}=20m 10^{-4} 2.5 10^{-4} 0.5= 0.25 nW, a value requiring suitable low-noise preamplification.

Q2-17 *In the wire diameter sensor, does the perpendicularity error affects the measurement?*

Answ.: If the wire is not perpendicular to the beam axis, as indicated in Fig.2-14, we may have two angle errors: one is the skew angle φ_{skew} the wire makes respect to the focal plane axis, the other is the tilt angle φ_{tilt} the wire makes respect to the plane of the drawing of Fig.2-14. The first error is inconsequential, insofar all the wire portions remain close to the beam waist (where they are illuminated by a plane wavefront). The second error amounts to rotate the diffracted distribution of an angle φ_{tilt} along the focal plane. Therefore, if the photodiode are wide enough transversally to collect the tilted diffracted field, no error is incurred, otherwise a distortion of the diffracted pattern sinc ξ will be suffered.

P2-18 *Is the measurement of first two zeroes width really the best way to extract the diameter information from the distribution of diffracted field?*

Answ.: Actually, we should apply the theory of the optimum filter to ascertain which signal treatment is the best. This has been carried out in connection to the timing problem of the pulsed telemeter (page 55 and ff). Let us suppose that the detected signal $E_0^2\ \mathrm{sinc}^2\theta D/\lambda$, is scanned by a CCD or other moving photodiode that performs a linear Z-scan, with z=vt. As $z=\theta F$ our signal becomes $E_0^2\ \mathrm{sinc}^2(vt/F)D/\lambda = f(t)$.
Now, the filter we shall cascade to the photodetector has the impulse (or Dirac-δ) response given by $f_{opt}(t)=[df(T-t)/dt]/f(T-t)$, where T is the time at which the measurement shall be performed, and the measurement consists in a zero crossing time-sorting.

If we look at the way the optimum filter $f_{opt}(t)$ weights the signal f(t), we find that the most important part of the signal is that contained in the up-going and down-going edges of the $sinc^2$ dependence.
Therefore, we can conclude that examining the zero crossings of the $sinc^2$ signal is reasonably close to the optimum filter treatment.

Q2-19 *Can any further information about the wire (such as absorption coefficient and index of refraction of the material) be inferred from the measurement of the diffracted field?*

Answ.: In the basic form depicted in Fig.2-14, no other feature of the wire other than the diameter can be inferred, because light entering and being refracted by the wire falls outside the detector and is lost. However, we can indeed find more information in the measurement if we collect also this contribution, i.e. the field refracted through the wire. To do so, we need to sandwich the wire between two flat glass plates, with transparent glue filling the space in between. Then, in addition to diameter, we can measure also the index of refraction profile, as useful in fiberoptics characterization.

Q2-20 *Can the spatial frequency (or the deniers) of a fabric be measured with the diffracted field setup of the diameter sensor ?*

Answ.: Indeed it can be measured. In the case of a X-Y spatial periodicity of the fabric Λ_x and Λ_y, the diffracted field has a periodicity $\theta_y=\lambda/\Lambda_x$ along the θ_y-axis of the focal plane and a periodicity $\theta_x=\lambda/\Lambda_y$ along the θ_x-axis (see page 425). The peaks of the periodic pattern are distributed according to Eq.2.8, that is, they are the $sinc^2\theta_x D_y/\lambda$ and $sinc^2\theta_y D_x/\lambda$ distributions associated to the diameters D_y and D_x of the wires along X and Y.

Q2-21 *In the particle size sensor, which errors may be caused by the scattering regime of the particles in the optical cell, and how can they be taken into account or be mitigated ?*

Answ.: First of all, we shall operate in the single scattering regime along the cell path length. Indeed, the angular distribution for multiple scattering is different from that of single scattering and this shall be avoided. Therefore, we will keep the optical density of the cell αL much less than 1, typically αL=0.1-0.2 max, as a rule of thumb. Such a value corresponds to a modest opacity of the cell when seen against a light source, one such that images can be clearly seen through the cell. Thus, it is important to check the concentration of particles in the cell before starting the measurement, and eventually adjust it.

Second, we note that Eq.2.9 is valid for a scattering factor independent from particle diameter, or Q_{ext}=const.. Going to page 410 and Fig.A3-6, we can see that this is true only for D=2r>>λ, that is, in the Mie region.
For D≈ λ or for D<λ, we can see that the scattering coefficient oscillates near Q_{ext}=2 and then becomes very small respect to 1 (the Rayleigh regime). We can correct for this dependence by inserting the factor Q_{ext}= Q_{ext}(λ/r,n) under the integral of Eq.2.9.
Third, measurement of the low-angle intensity affecting the large-D part of the distribution is disturbed by the superposition of a strong contribution of the undiffracted beam at θ=0. To expand the reach of the measurement near θ≈0, a good approach is the so-called reverse-Fourier filtering (illustrated in Fig.2-17) that can go down to θ≈1-mrad.

Q2-22 *In particle sizing measurements, which is the most effective method for extracting the desired particle distribution p(D) from the measured scattered intensity I(θ) ?*

Answ.: The least-square-method (LSM) is the best approach as a starting point, because it provides reasonable results even though not the most accurate, necessarily. A refinement to LSM is usually provided by one of the several available iterative methods, but in this case we need to supplement the experimental data I(θ) with some additional information about the expected distribution, so that the iteration can be stopped when the error respect to the true distribution reaches a minimum.

P2-23 *Estimate the magnitude of the signal received at the focal plane in a particle sizing measurement.*

Answ.: The calculation parallels that of problem P2-16. Let P_0 be the input optical power shed on the cell, and αL=0.1 the optical thickness of the cell, α=cA being the concentration (cm^{-3}) of the particles, A their effective cross-section, and L is the cell thickness.
Then, P_0αL is the total diffracted power, and is equal to the integral of the irradiance at the focal plane of the lens transforming the far-field in the focal-plane distribution. As an example, if we take P_0= 50 mW, and αL=0.1, this integral is 5mW.
Now, let us assume reasonable values for the detector size (or pixel if we use a CCD) and lens focal length. As a guideline, we may take a resolution a little bit finer than in a wire sensor (cf. problem P2-16), that is, let us

choose: w_{det}=0.04 mm and F=400 mm, so that we are sampling the θ−angles in steps of $\Delta\theta=w_{det}/F$=0.1-mrad.
Further, we may assume that the diameter distribution is centred around D=10 μm. At λ=1μm, this means that the average scattering angle is $\theta_{av}= \lambda/\pi D=1/3.14\times10=$ 30 mrad or, that scattered power is spread around θ_{av}=30 mrad.
Now, if we are interested to the magnitude of the received signal, to simplify the calculation we may assume a uniform the distribution of power between θ =0 and θ_{av}. The total corresponding solid angle is then $\theta_{av}^2/2$. Thus, the fraction of power collected by the detector [assumed a square of side w_{de}] is $\Delta\theta^2/(\theta_{av}^2/2)= (0.1^2/30^2 /2)= 2.2\ 10^{-6}$. Thus, the (average) power collected in each point of the distribution sampled by the detector is: $P_0\alpha L \times\Delta\theta^2/(\theta_{av}^2/2)=$ 5mW×2.2 10^{-6}= 11 nW. Again, we have to care about low-noise amplification of this signal with a suitable detector.

Problems and Questions, Chapter 3

P3-1 *Calculate the accuracy of a triangulation telemeter operating at distance of L=1 meter, using the following: a laser source with near-field spot size w_l =20 μm, a parallax base D=100 mm, a multi-element detector with pixel size (and period) p=10 μm, and an objective lens with focal length F=200 mm. Repeat the calculation for L= 0.3,3 and 10 meters.*

Answ.: To find the accuracy, we can use either Eqs.3.2 or the diagram in Fig.3-2. Let's start using the equations. First, we need calculate the angle error Δα. This quantity is determined by the largest between detector and source spot size, if we assume the conjugating objectives have the same focal length and work correctly (i.e. stay in focus). Then, the spot projected on the target is imaged back on the detector with the same size of the source, no matter how large it is on the target. As w_l>p, it is w_l to determine Δα, and it is: $\Delta\alpha = w_l /F$ = 20μm/200mm= 100μrad.
Now, we get from Eq.3.2':

$\Delta L/L=-(L/D)\ \Delta\alpha= -(1m/0.1m)\ 100\mu rad = 1\cdot 10^{-3}$ at L=1m.
and multiplying by L we get ΔL=1 mm (@ 1m).
Noting the L^2-dependence of ΔL in Eq.3.2, for the other distances we have: ΔL=100 μm (@ 0.31m), ΔL=10 mm (@ 3.1 m), and ΔL=100 mm (@ 10m).
As a comment, we may note that performance is good up to perhaps 1m, but the error is not so small at 3m.
Second, entering $\Delta\alpha$ =100μrad and D=0.1-m in the diagram of Fig.3-2, we sort out a -45° line as the one indicated with $\Delta\alpha/D$ =1mrad. This line supplies the relative accuracy (vertical scale) as well as the absolute accuracy (+45° dotted lines).
Of course, these are the same values calculated above but, worth being noted, we can visualise easily and quickly the range of accuracy covered by a given distance span, and, in addition, we can evaluate the effect of small changes to the parameters of the problem.

P3-2 *Evaluate how long has to be the detector used in Probl.3-1 to cover the distance range 1 to 10 m.*

Answ The parallax angle is α=atan D/L ($\approx$D/L for small α). As we can see from Fig.3-23, the detector width w_{CCD} needed to collect the spot at distance L is: w_{CCD} =F/ tanα = F D/L. Of course, the required size is small ($\approx$0) for large L ($\rightarrow\infty$) and thus we need to care only of the *minimum* distance. Using the data of Problem P3-1 and the minimum distance L=1-m we get: w_{CCD} = F D/L= 200 (0.1/1)=20 mm.
This is a large width for an array or multiple detector, yet an affordable value. But, if we had required L=0.3-m, the resulting width becomes prohibitively long. However, for L=0.3 m and at even shorter distance, accuracy is even too good and can be sacrificed – by let's say – a factor 10. Then, we can shorten the focal length of the objective lens by a factor 10 and keep the detector width w_{CCD} unaltered.

P3-3 *What do we need for $\Delta\alpha$ in order to keep the relative accuracy $\Delta L/L$ a constant, independent from the distance L ?*

Answ We shall increase the size of the individual element in the detector array, in such a way as to compensate the L-dependence. As seen from Eq.3-2, the relative accuracy at constant $\Delta\alpha$, $\Delta L/L=-(L/D)\Delta\alpha$ increases with L. To compensate the distance dependence we should arrange to get $\Delta\alpha$=W/L, where W is a constant. If we have a multiple detector with variable width, increasing with the radial distance R from the optical axis,

that is $w_{CCD}=\kappa R$ where κ is a constant, then we have $\Delta\alpha= w_{CCD}/F=\kappa R/F$. In addition, being $\tan\alpha\approx D/L=R/F$, we get by substitution: $\Delta\alpha=w_{CCD}/F=\kappa D/L$. Thus, we obtain for the relative accuracy $\Delta L/L=-(L/D)\Delta\alpha= \kappa$.

P3-4 *How many speckles are contained in the spot imaged back on the receiving photodetector of a triangulation telemeter ? Do they affect the accuracy of the instrument ?*

Answ Let us consider the ideal case of a spot size $w_{tar}=\sqrt{(\lambda L/\pi)}$ projected by a collimating telescope (Eq.2.4) on the target at distance L. The objective lens, of focal length F_{rec} and diameter D_{rec}, demagnifies the target spot size by a factor F_{rec}/L. The result on the photodetector plane is a spot of size $w_{fp}=w_{tar}\, F_{rec}/L= F_{rec}\sqrt{(\lambda/L\pi)}$ [this result is correct provided w_{fp} is larger than the diffraction limit of the objective, $\lambda\, F_{rec}/D_{rec}$].
On the focal plane, the subjective speckle (see Sect.5.1) has a transversal size $s_{f(fp)}=\lambda\, F_{rec}/D_{rec}$. Thus, the number of speckles inside the received spot is:
$N= [w_{fp}/s_{f(fp)}]^2= [F_{rec}\sqrt{(\lambda /L\pi)}/\lambda F_{rec}/D_{rec}]^2= D_{rec}^2/(\lambda L\pi)$
With L=3m, λ=1μm, D_{rec}=10mm, we get:
$N= 10^2 /[1\cdot 10^{-3}\ 3000\ 3.14]= 11$.
Such a small number of speckles actually may affect the accuracy of the measurement, because the speckle intensity is a negative-exponential distribution (Sect.5-1). Because of that, the collection of the speckle-spots has a centroid (or centre of mass) shifted of a random amount respect to the centre of the spot w_{fp}. The error decreases with $\sqrt{N}$, and is of the order of $w_{fp}/\sqrt{N}$. As L decreases, or the spot size on the target increases, the error becomes negligible.

P3-5 *In a direct-sight triangulation telemeter (as the one depicted in Fig.3-1) how can we incorporate an angle sensor capable of resolving less than the arc-minute of parallax angle α?*

Answ To appreciate 1 minute of arc, that is 1 part in 21600 across the circumference of an angle measuring wheel, or even more, go down to the arc-second of resolution, we take advantage of the Moire' reticles (see *"Photodetectors"*, Sect.9.3.4), which can resolve a fraction (usually $^1/_4$) of pitch p or spatial period of the black-and-white marks engraved on the wheel outer surface. With reasonable numbers, for example p=5μm and R=50 mm so that the circumference is 2πR=314 mm long, we get a resolution of 1 part in [314/0.005]·1/4= 251 200, or about 5 arc-sec.

P3-6 *Evaluate the background noise P_{bg} in a typical pulsed and sinewave modulated telemeter.*

Answ For a pulsed telemeter operating with a Nd-laser(λ=1.06μnm) we have a spectral irradiance (Fig.A3-3) $E_s \approx$ 500 W/m²μm in direct sunlight at AM1.5 (sun elevation 42°, taken as a conservative case). Other common design values we may assume are: Δλ=10nm (for an 80 to 90% transmission of the filter), NA=0.5, and d_r=0.2 mm. Writing the law-of-photography equation (in which the radiance is $R_s=\delta\,(1/\pi)E_s\Delta\lambda$) as:

$$P_{bg} = R_s\, A\Omega = \delta(1/\pi)E_s\Delta\lambda\, A\Omega$$
$$= \delta\, E_s\Delta\lambda\, NA^2\, (\pi\, d_r^2/4),$$

we may insert the above values, with δ=1 (as the worst case for background) and get

$$P_{bg} = 1\cdot 500\cdot 0.01\cdot 0.25\cdot (\pi\, 0.2^2\, 10^{-3x2}/4) = 1.25\cdot \pi\cdot 10^{-8} = 40 \text{ nW}.$$

The attenuation is $P_r/P_s = \delta(D_r/2L)^2$. Working at L=1 km with D_r=100 mm and δ=0.3 for the signal, we have $P_r/P_s = 0.075\ 10^{-8}$, that is, for a typical transmitted (peak) power of P_s =0.3MW, we get a received power P_r= 0.23 mW.

In addition, the I_{ph0} noise for an APD receiver at 100 MHz is evaluated from Fig.3-7 as 2 pA/√Hz. Multiplying by $\sqrt{B}/\eta\sqrt{\sigma}$, we get $P_{ph0}\approx$4 nW. Thus, we obtain the points labeled 'pulsed' in Fig.3-8, and we can see that it is the received signal shot-noise to prevail.

For a sine-wave modulated telemeter operating at λ=820 nm, we may have $E_s \approx$ 900 W/m²μm and P_{bg} approximately doubles at a value of 80nW.

The attenuation is now $P_r/P_s = D_r^2/4\theta_s^2L^2$. Working at L=100 m with D_r=100mm and θ_s=1 mrad, we have P_r/P_s= 0.25. That is, for a typical transmitted power of P_s =0.1 mW, we get a received power P_r=25 μW.

Again, using an APD receiver at 10 MHz, the noise spectral density is 0.2 pA/√Hz, and multiplying by $\sqrt{B}/\eta\sqrt{\sigma}$ with a bandwidth of 100 Hz now, we get $P_{ph0}\approx$5 pW.

Comment: in both cases, the largest noise is the shot-noise term of the received photons. This corresponds to have a good-design result. On the

contrary, if we had omitted the filter for the background or used too large a detector or noisy electronics, the I_{bg} or I_{ph0} values could easily be increased by one or two order of magnitudes and become the limiting factor of telemeter performance.

P3-7 *Calculate the accuracy of the threshold-crossing timing in a pulsed telemeter operating with a Gaussian waveform of standard deviation τ=5ns and with a peak received power of 1 mW.*

The Gaussian waveform for the pulse is written as:
$s(t/\tau)=[\sqrt{2\pi}]^{-1}\exp-(t/\tau)^2/2$,
and a standard deviation τ=5 ns means that the full-width-half-maximum of the pulse is 2.36×5ns=12ns. The Gaussian has a bandwidth factor equal to κ=0.13.
The optimum level for the threshold S_0 is found from the condition (see also Eq.3.16') $s(t/\tau)/s'^2(t/\tau)$=minimum, or by inserting the Gaussian function as $(t/\tau)^2[\sqrt{2\pi}]^{-1}\exp-(t/\tau)^2/2$ = max.
Differentiating with respect to t/τ and equating to zero, we find $(t/\tau)^2=2$ as the result. Accordingly, the optimum (fixed) threshold is $S_0 = s(\sqrt{2}) = 1/[e\sqrt{2\pi}] = 0.147$ and the signal slope is $s'^2=2S_0^2=0.043$.
The threshold-dependent factor is therefore:
$s(t/\tau)/s'^2(t/\tau)=S_0/s'^2=0.147/0.043=3.42$.
Assuming η=0.7 and being κ=0.13, the normalized time variance is calculated as:
$\sigma_t/(\tau/\sqrt{N_r})=[2\kappa/\eta\times3.42]^{1/2}= [2\times0.13/0.7\times3.42]^{1/2} =1.12$.
The timing accuracy then obtained is $\sigma_t = 5.7\text{ns}/\sqrt{N_r}$, which is a value very close to that ($5\text{ns}/\sqrt{N_r}$) given by the default approximation of Eq.3.16.
From the data of Fig.3-8, we may expect $P_r\approx$1mW as the typical received power of the pulsed telemeter, which corresponds to a number of photons $N_r\approx P_r\tau/h\nu=10^{-3}\times5.10^{-9}/2.10^{-19} \approx 2.5\ 10^7$. The accuracy of a single-shot measurement is then found as:
$\sigma_t^2=5.7\text{ns}/\sqrt{(2.5\cdot10^7)} =1.1$ ps,
a very good theoretical limit of performance, even beyond the capabilities of electronic circuits (usually in the range 10 to 50ps).

P3-8 *Repeat the calculation of Prob.P3-8 using a Gaussian-like waveform but with the leading edge faster that the trailing edge. Assume a realistic ratio 1.8 of the two.*

An asymmetric Gaussian, with the leading edge τ_{le} faster that the trailing edge τ_{te} is indeed a more realistic pulse waveform.

Repeating the calculation with $\tau_{te}/\tau_{le}=1.8$ and τ_{le} =5ns, we find that the accuracy worsens only by about 10%.

Q3-9 *What about the contribution of background noise to the timing accuracy ?*

Answ.: This contribution is given by the last factor in square brackets of Eq.3.16''. To make it negligible, we need the number of photons at threshold to be larger than the corresponding number of background and circuit photons. This is the case of examples discussed in Prob.P3-6.
In general we can say that, even when it is $N_{bg+ph0}>S_0/N_r$, there is still a $1/\sqrt{N_r}$ dependence for the timing accuracy, which improves resolution at increasing number of collected photons.

P3-10 *Evaluate the improvement that can be obtained by the optimum filter processing of the photodetected signal, in the case of a Gaussian waveform like in Probl.P3-6.*

Answ.: Using a Gaussian pulse waveform of the type:
$s(t/\tau)=[\sqrt{2\pi}]^{-1}\exp-(t/\tau)^2/2$, we can evaluate the timing term, that is:
$[\int_{0-\infty} S'^2/S\ d\tau]^{-1}$ as $\int_{0-\infty}\sqrt{(2\pi)}\ \tau^2\exp-(\tau^2/2)\ d\tau$ =1, or, the timing variance supplied by the optimum filter is $\sigma_{t\,(opt)}^2=\tau/\sqrt{N_r}(2\kappa/\eta)$ to be compared with that of the best fixed threshold crossing previously calculated as
$\sigma_t^2=\tau/\sqrt{N_r}(2\kappa/\eta)\ s(t/\tau)/s'^2(t/\tau) = 3.42\times\tau/\sqrt{N_r}(2\kappa/\eta)$.
Thus, the optimum filter yields an improvement by a factor 3.42 in variance, or $\sqrt{3.42}=1.85$ in time rms error.

Q3-11 *How important is, in sine-wave modulated telemeter, to use a modulation index m as close as possible to the maximum value of unity ?*

Answ.: Looking at the timing accuracy (Eq.3.25)we can see that the modulation index enters in the dependence in product with η, the quantum efficiency of the detector. Therefore, decreasing m has the same effect as decrease the quantum efficiency.

Q3-12 *Can a waveform different from the sinusoid be used in the sine-wave modulated telemeter, or a penalty is incurred when distortion of the sine-wave is appreciable ?*

Answ.: In principle we can use a waveform different from the sinusoid to modulate the power emitted by the source in a sine-wave telemeter. We need anyway to have a sinusoid available for the mixing operation required to be able recovering the relative phase. There are two problems to care about when using a distorted sinusoid: i) the loss of modulation index m (as the harmonics in the waveform decrease the amplitude of the fundamental component) and ii) the phase shift error amplitude of the fundamental

component which is incurred when even harmonics (which make the semi-periods waveforms different) are contained in the modulating signal.

Q3-13 *In a pulsed telemeter, couldn't we overcome the ambiguity problem by slowly increasing the repetition frequency at the switch-on of the instrument, so that we can determine if 1, 2 or more pulses are contained in the distance span under measurement ?*

Answ.: Yes, indeed this is a theoretically correct approach. However, it is rather complex to implement and does not bring so far, in a pulsed telemeter, unless we can go up to a large number n of pulses and are able to manage them automatically. On the other hand, the approach can work very well for a sine wave modulated telemeter, and indeed the frequency-sweep method (page 75) is the development of this idea.

Q3-14 *Discuss the advantage/disadvantage of using a single- versus double-objective optical system in the transceiver (transmitter-receiver) of a time-of-flight telemeter.*

Answ.: The single-objective has no parallax error nor dead zone in front of the instrument. This is important in short-range measurements.
On the other hand, the double-objective has no 3-dB loss in the splitting of outgoing and incoming beams. In addition, it can manage easily different requirements of lens size and focal length in transmission and reception. About power backscattered from the air, the single-objective is more sensitive than the double-objective arrangement.

P3-15 *Design a simple pulsed telemeter operating with the technique of start-stop clock counting, using a semiconductor source for a medium-range application (e.g., an altimeter working on a 0-2900 m span)*

Answ.: We may consider a P_0=20-W peak-power laser as the optical source of our telemeter. Such a device is a stack of probably 20-50 individual diodes, mounted in an array arrangement (see Fig.A1-18 as an example). Stacks are available from several vendors at wavelengths ranging from 630 to 1550 nm.
By pulsing the stack at a τ=30-ns pulse duration, we have $c\tau/2 = 3 \cdot 10^8$ m/s $\cdot 30\ 10^{-9}/2 = 4.5$ m, and using a clock frequency $f=M/\tau$, the length of resolution [cfr page 67] we obtain is $L_l = c\tau/2M = 4.5/M$ (m).
For example, we may assume M=4.5 and have $f_c = 4.5/30$ ns = 150 MHz, a very easy-to-follow value for a counter in a cheap IC technology. In length, the resolution is $L_l = c\tau/2M = 1$ m.
For a 2800-m span, the repetition frequency f_{PRF} of the pulses can be taken according to the safe value of $L_{NA} = 3000$ m yielding $f_{PRF} < c/2L = c/2L_{NA} = (3 \cdot 10^8 \text{ m/s})/2 \cdot 3000 = 0.5 \cdot 10^5 = 50$ kHz. The corresponding repetition period is $T_R = 20$ μs, and this value settles the duty factor of the laser at η = 30ns/ 20μs $= 1.5 \cdot 10^{-3}$, or, the mean power of the laser at $P_{AVE} = \eta\ P_0 = 1.5 \cdot 10^{-3} \cdot 20$ W=

30 mW, a Class B device, requiring safety measures when allowed to propagate at a distance.
Now, we can average the time-of-flight measurement on N_m successive measurements, and N_m will be chosen as the largest possible allowed by the application requirements. Typically, a few milliseconds will be quite acceptable even in fast-to-respond applications, (such as for an altimeter) whereas in a topographic instrument we could even go up to 1-10 s. Taking T_m= 2 ms we get $N_m = f_{PRF}\ T_m$= 50 kHz 2 ms= 100. Therefore, the accuracy is improved by a factor $\sqrt{N_m}$ = 10 compared to the value σ_t or σ_L of the single measurement.
If the error incurred in the measurement is just the roundoff error, then the accuracy is $\sigma_L = L_l/\sqrt{6N_m}$ =4.1 cm for the average of 100 measu-rement. Counting the periods of the clock at 150 MHz gives the distance of the last digit in units of length L_l= 1m. Then, accumulating the counts (adding the new result to the previous content) in a $5^1/_2$-digit register for N_m=100 measurements makes the least-significant digit represent a length L_l= 1cm.
Thus, the obtained resolution is adequate for the accuracy σ_L=4.1 cm found above [Note: resolution shall be always finer than actual accuracy, to get out all the information available in the measurement]

P3-16 *With the data of the pulsed telemeter of Probl.P3-15, calculate the accuracy of the timing measurement performed by threshold crossing on a 30-ns pulse with Gaussian waveform, at the distances 100, 300, 1000 and 3000 m. assume a diffuser with δ=1 and an objective lens with diameter D_r = 100 mm. Assume a quantum-limited performance set by the noise of the received power.*

Answ.: Starting with the peak power P_0=20 W and a Gaussian waveform with FWHM (full-width-half-maximun) of 30 ns, we obtain for the standardized time parameter τ= FWHM/2.36= 12.7 ns. [the factor 2.36 has already been used at p.54 line 3 as the ratio of FWHM to standard deviation σ).
In the calculations that follow, we consider the quantum noise contribution associated to the received photons, and neglect background and electronic noises.
Let us place the threshold of discrimination at the best value 0.147 for the Gaussian (see Problem P3-7) and thus we obtain $s(t/\tau)/s'^2(t/\tau)=S_0/s'^2=$ $=0.147/0.043=3.42$. With η=0.7 for the quantum efficiency of the photodetector, and being κ=0.13 for the Gaussian waveform, the normalized time variance is calculated as:

$$\sigma_t=(\tau/\sqrt{N_r})[2\kappa/\eta \cdot S_0/s'^2]^{-1/2} \text{ or}$$

$$\sigma_t/(\tau/\sqrt{N_r}) = [2\times0.13/0.7\times3.42]^{1/2} =1.12.$$

The timing accuracy is then obtained, being τ=12.7ns, as:

$$\sigma_t =1.12\times12.7 \text{ ns } /\sqrt{N_r} =14.2 \text{ ns } /\sqrt{N_r}$$

We shall now evaluate N_r, the number of detected photons. The power attenuation is (cfr Eq.3.5, 3.6a):

$P_r/P_0 = \delta D_r^2/4L^2$

$= 1 \cdot 0.1^2/4 \cdot 100^2 = 0.25 \cdot 10^{-6}$ (@ L=100 m)

so that $P_r = 0.25 \cdot 10^{-6} \cdot 20$ W $= 0.5 \cdot 10^{-5}$ W, and in addition, for the other values of distances:

$= 1 \cdot 0.1^2/4 \cdot 300^2 = 0.27 \cdot 10^{-7}$ (@ 300-m) so that $P_r = 0.54 \cdot 10^{-6}$ W,

$= 1 \cdot 0.1^2/4 \cdot 1000^2 = 0.25 \cdot 10^{-8}$ (@ 1000-m) so that $P_r = 0.5 \cdot 10^{-7}$ W,

$= 1 \cdot 0.1^2/4 \cdot 3000^2 = 0.27 \cdot 10^{-9}$ (@ 3000-m) so that $P_r = 0.54 \cdot 10^{-8}$ W.

Now, we can multiply the received power by and τ divide by $h\nu$ to get the number of received photons N_r.

Using λ=1μm so that [there are $(1.24)^{-1}$=0.8 photons per eV] :

$h\nu = 1.6 \cdot 10^{-19}/0.8 = 2 \cdot 10^{-19}$

and being τ=12.7 ns we get: $\tau/h\nu = 12.7 \cdot 10^{-9}/2 \cdot 10^{-19} = 0.635 \cdot 10^{11}$

Then, by multiplying for the above value of P_r we obtain:

$N_r = P_r \tau/h\nu = 0.5 \cdot 10^{-5} \cdot 0.635 \cdot 10^{11} =$

$= 0.32 \cdot 10^6$ (photons per pulse @ L=100 m)

and moreover: $N_r = 0.54 \cdot 10^{-6} \cdot 0.635 \cdot 10^{11} =$

$= 0.34 \cdot 10^5$ (photons per pulse @ L=300 m)

$N_r = 0.5 \cdot 10^{-7} \cdot 0.635 \cdot 10^{11} = 0.32 \cdot 10^4$ (photons per pulse @ L=1000 m)

$N_r = 0.54 \cdot 10^{-8} \cdot 0.635 \cdot 10^{11} = 0.34 \cdot 10^3$ (photons per pulse @ L=3000 m)

Finally, we can compute the timing accuracy at the various distances as:

$\sigma_t = 14.2$ ns $/\sqrt{N_r} = 14.2/\sqrt{(0.32 \cdot 10^6)} = 25$ ps (@ L=100 m),

or $\sigma_L = c\sigma_t/2 = 3 \cdot 10^8$ m/s $\cdot$ 25 ps/2= 3.7 mm (@ L=100 m);

and for the other distances:

$\sigma_t = 14.2$ ns $/\sqrt{N_r} = 14.2/\sqrt{(0.34 \cdot 10^5)} = 77$ ps (@ L=300 m),

or $\sigma_L = c\sigma_t/2 = 3 \cdot 10^8$ m/s $\cdot$ 77 ps/2= 11.6 mm (@ L=300 m);

$\sigma_t = 14.2$ ns $/\sqrt{N_r} = 14.2/\sqrt{(0.32 \cdot 10^4)} = 0.25$ ns (@ L=1000 m),

or $\sigma_L = c\sigma_t/2 = 3 \cdot 10^8$ m/s $\cdot$ 0.25 ns/2 = 37 mm (@ L=1000 m);

$\sigma_t = 14.2$ ns $/\sqrt{N_r} = 14.2/\sqrt{(0.34 \cdot 10^3)} = 0.77$ ns (@ L=3000 m),

or $\sigma_L = c\sigma_t/2 = 3 \cdot 10^8$ m/s $\cdot$ 0.77 ns/2= 116 mm (@ L=3000 m).

As we can see from these results, the timing accuracy is good at short distances but worsens at the largest distance to be covered.

Taking advantage of the $\sqrt{N_m}$ improvement in accuracy which is obtained by averaging on N_m measurements, we can decide to use $N_m = 10^2$. Doing so we obtain:

$\sigma_{tN} = 25$ ps $/\sqrt{N_m} = 2.5$ ps

and $\sigma_{LN} = \sigma_{LN}/\sqrt{N_m} = 37$ mm/10= 0.37 mm (@ L=100 m);

$\sigma_{tN} = 77$ ps $/\sqrt{N_m} = 7.7$ ps

and $\sigma_{LN} = 11.6$ mm $/\sqrt{N_m} = 1.16$ mm (@ L=300 m);

$\sigma_{tN} = 0.25$ ns $/\sqrt{N_m} = 25$ ps

and $\sigma_{LN} = 37$ mm/10= 3.7 mm (@ L=1000 m);

$\sigma_{tN} = 0.77$ ns $/\sqrt{N_m} = 77$ ps

and $\sigma_{LN} = 116$ mm $/\sqrt{N_m} = 11.6$ mm (@ L=3000 m).

As we can see, to keep σ_{LN} <1-cm we could as well decrease the number of measurement (and shorten the measurement time) for L<3000m.

P3-17 *Using the data of the pulsed telemeter of Probl.P3-15 and P3-16 check whether the quantum noise contribution associated to the received photons is larger than the background and electronic noises, so that these latter can be actually neglected.*

Answ.: The received powers at the several distances considered in Probl.3-15 are:

$P_r = 0.5 \cdot 10^{-5}$ W (@ L=100 m)
$= 0.54 \cdot 10^{-6}$ W (@ 300-m)
$= 0.5 \cdot 10^{-7}$ W, (@ 1000-m)
$= 0.54 \cdot 10^{-8}$ W (@ 3000-m)

The shot (or quantum) noise associated with P_r is:

$p_n = [2\, h\nu\, P_r\, B]^{1/2} = [2 \cdot 2 \cdot 10^{-19} \cdot 0.5 \cdot 10^{-5} \cdot 10.2 \cdot 10^{6}]^{1/2} = 4.5$ nW (at 100 m)

where we have assumed $B=\kappa/\tau=0.13/12.7\text{ns}=10.2$ MHz for the bandwidth required to accommodate the Gaussian pulse; and

$p_n = [2 \cdot 2 \cdot 10^{-19} \cdot 0.54 \cdot 10^{-6} \cdot 10.2 \cdot 10^{6}]^{1/2} = 1.48$ nW (at 300 m)

$p_n = [2 \cdot 2 \cdot 10^{-19} \cdot 0.5 \cdot 10^{-7} \cdot 10.2 \cdot 10^{6}]^{1/2} = 45$ pW (at 1000 m)

$p_n = [2 \cdot 2 \cdot 10^{-19} \cdot 0.54 \cdot 10^{-8} \cdot 10.2 \cdot 10^{6}]^{1/2} = 148$ pW (at 3000 m)

The background noise is calculated as the shot noise associated with the background power P_{bg} collected by natural illumination of the scene (see Eq.3.11):

$P_{bg} = \delta\, E_s \Delta\lambda\, NA^2\, (\pi\, d_r^2/4)$,

where E_s = scene spectral irradiance (W/m^{2}μm), usually taken as that provided by the direct sunlight [worst case approximation]; $\Delta\lambda$ = spectral width of the interference filter placed in the receiver lens; NA = arcsin $D_r/2F$ = numerical aperture of the receiver lens, and d_r = diameter of the detector.

For our diode laser telemeter, assuming operation at λ=1μm, we may have (Fig.A3-3) $E_s \approx 500$ W/m^{2}μm in direct sunlight at AM1.5 (sun elevation 42°). Other common design values we may assume are $\Delta\lambda$=10nm (for an 80 to 90% transmission of the filter), NA=0.25, and d_r=0.2-mm. Using δ=1 in the above equation, we get:

$P_{bg} = 1 \cdot 500 \cdot 10^{-2} \cdot 0.25^2 \cdot (\pi 0.2^2 10^{-6}/4) = 0.31 \cdot 3.14 \cdot 10^{-8} = 9.8$ nW.

We need not to compute $p_{nbg}=[2\, h\nu\, P_{bg}\, B]^{1/2}$ because we have already $P_{bg} < P_r$ at the largest distance [3000 m, where $P_r = 0.54 \cdot 10^{-8}$ W = 54 nW]

And, worth being noted, the above assumptions about terms contributing to P_{bg} are very conservative.

Last, about electronic noise, from Fig.3-7 we can see that the typical semiconductor detector, for example an APD as usually employed in

pulsed telemeters, can have a (current) noise spectral density of di_n/df =0.05 pA/√Hz at B= 10 MHz.
With η=0.7 and λ=1μm, so that $\sigma = \eta e/h\nu$= 0.7/0.8=0.87 (A/W), we can go from currents to powers by dividing by σ. Doing so, we get $dp_n/df=(di_n/df)/\sigma$=0.057 pW/√Hz.
When multiplied by $\sqrt{B}=\sqrt{(10\cdot10^6)}=3.1\cdot10^3$, the quantity dp_n/df would provide the total power of the noise equivalent fluctuation due to the electronic circuits, as: p_n=0.057 pW/√Hz $\cdot 3.1\cdot10^3$= 177 pW.
But, we do not need the noise power, rather (page 48) the equivalent P_{ph0} to shot noise, which is given by the relation $dp_n/df=[2\ h\nu P_{ph0}]^{1/2}$.
Solving from here for the circuit-equivalent power yields:
$P_{ph0}= [dp_n/df]^2/2h\nu = [0.057\ pW/\sqrt{Hz}]^2/2\cdot 2\cdot10^{-19}= 8.12\cdot10^{-9}$=8.12 nW
Now, we have all the terms for the time accuracy (cfr Eqs.3.16)
$\sigma_t=(\tau/\sqrt{N_r})[2\kappa/\eta \cdot S_0/s'^2]^{-1/2}[1+(P_{bs}+P_{ph0})/ P_r]^{1/2}$
With the values calculated above, the term $[1+(P_{bs}+P_{ph0})/P_r]^{1/2}$ is evaluated as $[1+(9.8+8.12)/5.4]^{1/2}$=2.08 times worse that the previously found figures, for L=3000m. At L=1000 and less, the term becomes ≈1.

P3-18 *What would be changed in the results of Probl.P3-17 if the peak power of the laser is decreased tenfold, to 2 W ?*

Answ.: The received powers would be scaled down of a decade (cfr Probl.P3-16), becoming

$P_r = 0.5 \cdot 10^{-6}$ W (@ L=100 m)
$= 0.54\cdot10^{-7}$ W (@ 300-m)
$= 0.5 \cdot 10^{-8}$ W, (@ 1000-m)
$= 0.54\cdot10^{-9}$ W (@ 3000-m)

The number of photons would scale down of a decade too decade (cfr Probl.P3-16):

$N_r = 0.32\cdot10^5$ (@ L=100 m)
$N_r = 0.34\cdot10^4$ (@ L=300 m)
$N_r = 0.32\cdot10^3$ (@ L=1000 m)
$N_r = 0.34\cdot10^2$ (@ L=3000 m)

Accordingly, the quantum-noise limited (signal power limited) timing accuracy, at the various distances for a single pulse would, worsen of √10 to:

σ_t =14.2 ns /$\sqrt{N_r}$=14.2 /$\sqrt{(0.32\cdot10^5)}$= 78 ps (@ L=100 m),
or $\sigma_L = c\sigma_t/2= 3\cdot10^8$ m/s$\cdot$78 ps/2= 11.7 mm (@ L=100 m);
σ_t =14.2 ns /$\sqrt{N_r}$=14.2 /$\sqrt{(0.34\cdot10^5)}$= 240 ps (@ L=300 m),
or $\sigma_L = c\sigma_t/2= 3\cdot10^8$ m/s$\cdot$77 ps/2= 36 mm (@ L=300 m);
σ_t =14.2 ns /$\sqrt{N_r}$=14.2 /$\sqrt{(0.32\cdot10^4)}$= 0.78 ns (@ L=1000 m),
or $\sigma_L = c\sigma_t/2= 3\cdot10^8$ m/s$\cdot$0.25 ns/2 = 117 mm (@ L=1000 m);

σ_t =14.2 ns /$\sqrt{N_r}$=14.2 /$\sqrt{(0.34 \cdot 10^3)}$= 2.4 ns (@ L=3000 m),
or $\sigma_L = c\sigma_t /2 = 3 \cdot 10^8$ m/s $\cdot$ 0.77 ns/2= 360 mm (@ L=3000 m).

Of course, background and electronic noise equivalent powers remain unaltered, and their sum, $P_{bs}+P_{ph0}$= 17.9 nW is now comparable to the received power at L=300 m, with the result that the values of accuracy becomes multiplied by the following factors:

$[1+(P_{bs}+P_{ph0})/P_r]^{1/2}=[1+17.9/500]^{1/2} \approx 1$ (@ L=100 m),
$[1+(P_{bs}+P_{ph0})/P_r]^{1/2}=[1+17.9/54]^{1/2} = 1.15$ (@ L=100 m),
$[1+(P_{bs}+P_{ph0})/P_r]^{1/2}=[1+17.9/5]^{1/2} = 2.14$ (@ L=100 m),
$[1+(P_{bs}+P_{ph0})/P_r]^{1/2}=[1+17.9/0.54]^{1/2} = 5.84$ (@ L=100 m),

and for N=1 measurements they are:

σ_L = 11.7 mm (@ L=100 m);
σ_L = 36 $\cdot$ 1.15 = 41.4 mm (@ L=300 m);
σ_L = 117 $\cdot$ 2.14 = 250 mm (@ L=1000 m);
σ_L = 360 $\cdot$ 5.84 = 2102 mm (@ L=3000 m).

These figures show how the effect of background and electronic noises is not very strong but sizeable, except at the shortest distance. And, considering the performance at L=3000 m, it is now really necessary to improve accuracy by averaging on several successive measurements.

P3-19 *How would the use of a better (or worse) photodetector help (or penalize) the accuracy calculated in Probl.P3-16and 3-17 ?*

Answ.: With a PMT (photomultipler tube) we can have a decade less noise in P_{ph0}, whereas with a simple PIN photodiode, the noise term P_{ph0} would worsen of a factor ≈5 (see Fig.3-7).
Accordingly, we would have changes in the calculations only because of the term $[1+(P_{bs}+P_{ph0})/P_r]^{1/2}$, and the changes would affect only the largest distances where the received signal P_r becomes comparable to $P_{bs}+P_{ph0}$.

P3-20 *How atmosphere attenuation affects the received signal in the pulsed telemeter of Probl.P3-15 through P3-17 ?*

Answ.: Referring to Fig.3.5, we can see that the attenuation on the total pathlength 2L is T_{atm}= exp (-2αL), where α, the attenuation coefficient is:
α = 0.1 km^{-1} (exceptionally clear atmosphere)
α = 0.33 km^{-1} (limpid atmosphere)
α = 0.5 km^{-1} (incipient haze)
Using the value of 0.33 km^{-1} the total attenuation is:

T_{atm}= 0.94 @ L=100 m,
= 0.82 @ 300-m,
= 0.52 @ 1000-m,
= 0.14 @ 3000-m

and, accordingly, the received power is modified, respect to the values of Prob.P3-16 as follows:

$P_r = 0.5 \cdot 10^{-5}$ W (@ L=100 m)
$= 0.44 \cdot 10^{-6}$ W (@ 300-m)
$= 0.26 \cdot 10^{-7}$ W, (@ 1000-m)
$= 0.076 \cdot 10^{-8}$ W (@ 3000-m)

This means that on the largest distance, we shall expect a loss due to atmospheric propagation. To mitigate this effect, we have to increase either the peak power of the laser, or the measurement time, or both.

P3-21 *What happens of the resolution of the pulsed telemeter of Problems P3-15 through P3-17 if we use a solid-state Q-switched laser providing 200 kW of peak power, all the remaining parameters being the same ?*

Answ.: A 200-kW peak power in a Gaussian pulse of 12.7 ns (Prob.P3-15) corresponds to a pulse energy of $200k \cdot 12.7n = 2.54$ mJ, a quite reasonable value for a small Nd-rod, pumped by a laser diodes stack.

With a typical repetition frequency f=10 Hz, our solid-state laser supplies a mean power $2.54 \text{ mJ} \cdot 10 \text{ Hz} = 25$ mW, about the same level we have started with in Probl.P3-15.

However, we have now a peak power 10^4 times larger than the previously assumed for the altimeter and therefore we would get the same single-pulse accuracy for a distance $\sqrt{10^4} = 100$ times larger.

P3-22 *Design a sine wave modulated telemeter operating with the frequency-sweep method, using a semiconductor source for a medium-range application (e.g., an altimeter working on a 0-3000 m span with a 10-cm resolution). Evaluate the quantum-limited accuracy at 300 m and 3000 m for a measurement time of 100 ms. Then, evaluate the actual accuracy when the background and electronic noises are taken into account.*

Answ.: We may consider a P_0=1-mW CW laser diode as the source of our telemeter. Such a laser diode is readily available at low cost at several wavelength of operation, from 630 to 1550 nm. In the visible range, the laser is Class 2 by default, and becomes Class 1 when the beam is expanded or propagated on a sizeable distance (so that the eye can intercept only a fraction of it).

We may take L_{NA}=3000 m as the distance of non-ambiguity, so that we need a minimum frequency $f_{m0} = c/2L_{NA} = 3 \cdot 10^8/2 \cdot 3 \cdot 10^3 = 50$ kHz, a very reasonable value.

As we wish a l_R=10-cm resolution out of a phase measurement performed with a 1:100 (or 2-digit) sorting of the 2π angle, we need a maximum frequency $f_m = c/2 \cdot 100 l_R = 3 \cdot 10^8/2 \cdot 1 = 150$ MHz, a very reasonable value.

The block scheme of the telemeter is the same as in Fig.3-22, where the 2-digit phase sorter provides the 10-cm and 1-m digits, and a 3-decade counter provides the 10-m, 100-m and 1-km digits.

About the transmitted signal, we can assume a typical modulation index m=0.7 for a semiconductor laser, and as in problems above, η=0.7 for the quantum efficiency of the photodetector.

Now, we can repeat the calculations of Prob.P3-15 and evaluate the normalized time variance. Let us first assume the ideal case of negligible background P_{bg} and electronics P_{ph0} noises. Then:

$$\sigma_t/(1/2\pi f_m\sqrt{N_r})=(1/m\eta)^{1/2}[1+(P_{bg}+P_{ph0})/P_r]^{1/2}=(1/0.7\cdot 0.7)^{1/2}=1.4$$

and, as $2\pi f_m = 6.28\cdot 150$ MHz $=10^9$ rad/s, the timing accuracy becomes:

$$\sigma_t = 1.4\cdot 10^{-9}/\sqrt{N_r} = 1.4 \text{ ns } /\sqrt{N_r}$$

Going on to evaluate N_r, the number of detected photons, we get the received power P_r as:

$$P_r/P_0 = \delta D_r/4L^2$$

$$= 1\cdot 0.1^2/4\cdot 300^2 = 0.27\cdot 10^{-7} \quad (@ L=300 \text{ m})$$

so that $P_r = 0.27\cdot 10^{-7}\cdot 1 \text{ mW} = 27 \text{ pW}$, and:

$$= 1\cdot 0.1^2/4\cdot 3000^2 = 0.27\cdot 10^{-9} \quad (@ 3000\text{-m}) \text{ so that } P_r = 0.27 \text{ pW}.$$

Now, we can multiply the received power by the integration time T_m(=100ms), and divide it by hν to get the number of received photons N_r. Using λ=1μm so that hν=$1.6\cdot 10^{-19}\cdot 1.24 = 2\cdot 10^{-19}$, we obtain:

$$N_r = P_r\cdot T_m/h\nu = 27\cdot 10^{-12}\cdot 0.1/2\cdot 10^{-19} =$$

$$= 1.35\cdot 10^6 \quad (\text{photons per meas. time @ L=300 m}), \text{ and}$$

$$N_r = 0.27\cdot 10^{-12}\cdot 0.1/2\cdot 10^{-19} = 1.35\cdot 10^4 \quad (\text{photons @ L=3000 m})$$

Finally, we can compute the timing accuracy at the two distances as:

$$\sigma_t = 1.4\text{ns}/\sqrt{N_r} = 1.4\text{n}/\sqrt{(1.35\cdot 10^6)} = 1.2 \text{ ps} \quad (@ L=300 \text{ m}),$$

$$\text{or } \sigma_L = c\sigma_t/2 = 3\cdot 10^8 \text{ m/s}\cdot 1.2 \text{ ps}/2 = 0.18 \text{ mm} \quad (@ L=300 \text{ m});$$

and for the other distance:

$$\sigma_t = 1.4\text{ns}/\sqrt{N_r} = 1.4/\sqrt{1.35\cdot 10^4} = 120 \text{ ps} \quad (@ L=3000 \text{ m}),$$

$$\text{or } \sigma_L = c\sigma_t/2 = 3\cdot 10^8 \text{ m/s}\cdot 120\text{ps}/2 = 18 \text{ mm} \quad (@ L=3000 \text{ m}).$$

These very good values of signal quantum-limited accuracy are much better than the 1-cm performance we have required. However, note that they come out, despite the smaller power available, because of the much larger integration time.

The background P_{bs} and electronic P_{ph0} noise equivalent powers are now no more negligible. The background power increases significantly going from λ=1μm to perhaps λ=0.62-0.85μm as for a CW semiconductor laser for a

sine wave telemeter (the increase, see Fig.A3-3 is a factor 1.5-2.0). However, let's stay with the previous value, see Probl.P3-17, of
P_{bg}= 9.8 nW.
About circuit and detector noise, let's again assume an APD and go back to Fig.3-7 to evaluate the spectral density dp_n/df. From the graph, we get a value
dp_n/df=0.3 pA/√Hz at the modulation frequency f_m=150 MHz.
Solving for P_{ph0} as in Probl.P3-17, we get:
$P_{ph0}= [dp_n/df]^2/2h\nu = [0.3\ pW/\sqrt{Hz}]^2/2\cdot 2\cdot 10^{-19}= 0.0225\cdot 10^{-5}$=225 nW
The multiplying factors of accuracy then become:
$[1+(P_{bs}+P_{ph0})/P_r]^{1/2}=[1+235n/27p]^{1/2}$ = 93 (@ L=300 m),
$[1+(P_{bs}+P_{ph0})/P_r]^{1/2}=[1+235/0.27p]^{1/2}$ = 930 (@ L=3000 m),
or, the accuracy performance is dominated by the electronic noise. The numbers for accuracy are:
σ_t =1.2 ps $[1+(P_{bs}+P_{ph0})/P_r]^{1/2}$=1.2ps 93 = 111ps (@ L=300 m),
or $\sigma_L = c\sigma_t/2= 3\cdot 10^8$ m/s·111 ps/2= 16.6 mm (@ L=300 m);
σ_t =120 ps 930= 111 ns (@ L=3000 m),
or $\sigma_L = 3\cdot 10^8$ m/s·111ns/2= 16.6 m (@ L=3000 m).
The last value we have found is very clearly indicative of what happens in a sine modulated telemeter that uses a low power laser compared to the pulsed telemeter. Indeed, the resolution at short distances is still comparable to that of the pulsed telemeter, because what is lost in peak power is recovered with integration time. But, as the received signal fades away with increasing distance, the overwhelming effect of electronic (and background) noises becomes the driving term of accuracy.
Now, we cannot improve the σ_L=16.6-m @L=3000 m accuracy any more,but using an *equivalent* increased power.

P3-23 *Recalculate the performance of the sine wave modulated telemeter of Prob.3-22 when the target is a corner cube.*

Answ.: With a corner cube, we get a power-equivalent gain of (Eq.3.6b):
$G_c=1/\theta_s^2$.
We can do our best effort to collimate the outgoing beam, so that θ_s is as small as 0.1 milliradian or even less, but, on a sizeable distance of propagation, turbulence effect will widen the beam irrespective of the initial θ_s. Turbulence effects (see App.A3.2) are not so predictable, of course, but we can assume, as a rule of thumb, that in normal clear air

wandering and spot dancing increase aperture of the beam to an effective divergence $\theta_s \approx 10$ mr on distances in the range 0.1 to 5 km.
Thus, let's take $\theta_s \approx 10$ mr as the design value of our corner-cube based sine-wave telemeter, and the gain is $G_c = 1/\theta_s^2 = 1/(10^{-2})^2 = 10^4$.
Then, the power collected at the two distances considered in Probl.3-22 are:

$P_r/P_0 = G_c D_r/4L^2$

$= 0.27 \cdot 10^{-7} \; 1 \cdot 10^4 = 0.27 \cdot 10^{-3}$ (@ L=300 m)

so that $P_r = 0.27 \cdot 10^{-3} \cdot 1$ mW $= 270$ nW, and:

$= 0.27 \cdot 10^{-9} \; 4 \cdot 10^4 = 0.27 \cdot 10^{-5}$ (@ L=3000 m)

so that $P_r = 0.27 \cdot 10^{-5} \cdot 1$ mW $= 2.7$ nW,

After multiplying by the integration time T_m(=100ms), and dividing by $h\nu$, we get the number of received photons N_r as:

$N_r = P_r \cdot T_m/h\nu = 270 \cdot 10^{-9} \cdot 0.1/2 \cdot 10^{-19} =$

$= 13.5 \cdot 10^{10}$ (photons @ L=300 m), and

$N_r = 2.7 \cdot 10^{-9} \cdot 0.1/2 \cdot 10^{-19} = 13.5 \cdot 10^8$ (photons @ L=3000 m)

whence the timing accuracy (signal shot-noise limited) are:

$\sigma_t = 1.4\text{ns}/\sqrt{N_r} = 1.4\text{n}/\sqrt{(13.5 \cdot 10^{10})} = 0.0038$ ps (@ L=300 m),

or $\sigma_L = c\sigma_t/2 = 3 \cdot 10^8$ m/s $\cdot$ 0.0038 ps/2 = 0.0006 mm (@ L=300 m);

and for the other distance:

$\sigma_t = 1.4\text{ns}/\sqrt{N_r} = 1.4\text{n}/\sqrt{13.8 \cdot 10^8} = 0.038$ ps (@ L=3000 m),

or $\sigma_L = c\sigma_t/2 = 3 \cdot 10^8$ m/s $\cdot$ 0.038ps/2 = 0.006 mm (@ L=3000 m).

Now we evaluate the multiplying term as:

$[1+(P_{bs}+P_{ph0})/P_r]^{1/2} = [1+235\text{n}/270\text{n}]^{1/2} = 1.37$ (@ L=300 m),

$[1+(P_{bs}+P_{ph0})/P_r]^{1/2} = [1+235/2.7]^{1/2} = 9.4$ (@ L=3000 m),

whence the accuracy @ L=3000 m becomes

$\sigma_t = 0.038 \; 9.4 = 0.36$ ps and $\sigma_L = 0.06$ mm

As we can see, with the corner cube we obtain very good figures. These figures are however unrealistic in the sense that so small values surely will be masked by other sources of errors and noon-idealities we were allowed to neglect when timing accuracy is in the ns or sub-ns range.
Instead, the interesting consequence of the above considerations is that we can now *decrease* the laser power and match all the way the desired accuracy. This is very desirable, to match the safety standards of outdoor use of the laser telemeter, without any special requirements or installation to protect the generic public.

Going through the numbers, we can see that assuming a CW laser power of P_0=20 μW, i.e. decreased of a factor 50 respect to the starting value of Probl.P3-22, yet using the corner cube as the target, we have:
$P_r = 1.1 \cdot 10^{-3} \cdot 0.02$ mW = 22 nW, $N_r = 1.2 \cdot 10^{10}$, $[1+(P_{bs}+P_{ph0})/P_r]^{1/2}$ =3.4 whence the resolution at 300m: σ_t =0.044 ps, σ_L =0.007 mm;
$P_r = 1.1 \cdot 10^{-5} \cdot 0.02$ mW = 0.22 nW, $N_r = 1.2 \cdot 10^{8}$, $[1+(P_{bs}+P_{ph0})/P_r]^{1/2}$=33 whence the resolutions at 3000m: σ_t =4.3 ps, σ_L=0.64 mm.
Once again, the resolution is quite satisfactory and even better than that of the pulsed telemeter that uses a much larger power. The big gap in powers is recovered through (i) the corner-cube gain; (ii) the increased integration (or measurement) time.

P3-24 *Explain why the PLL is so important in filtering the received signal during the frequency sweep (from the minimum f_m to the maximum f_M) of the sine-modulated telemeter.*

Answ.: In the preceding problems we have dealt with the time devoted to the fine (least-significant 2-digits) measurement of phase shift. Another time interval shall be devoted to the coarse (most-significant 3 or 4 digits) measurement of the zero-crossings of the phase signal, see Fig.3-22.
We now wonder about how fluctuations may affect the detection of the zero crossings.
With the aid of Figure 3, we can make the following reasoning. If spurious zero-crossings are to be avoided, the signal waveform (bottom trace) shall be monotonic. Then, the fluctuation ΔP of received power shall be much less than the variation (dP/dt)/B produced by the mean signal slope dP/dt, in a time interval 1/B equal to the reciprocal of the maximum frequency content of the fluctuation.

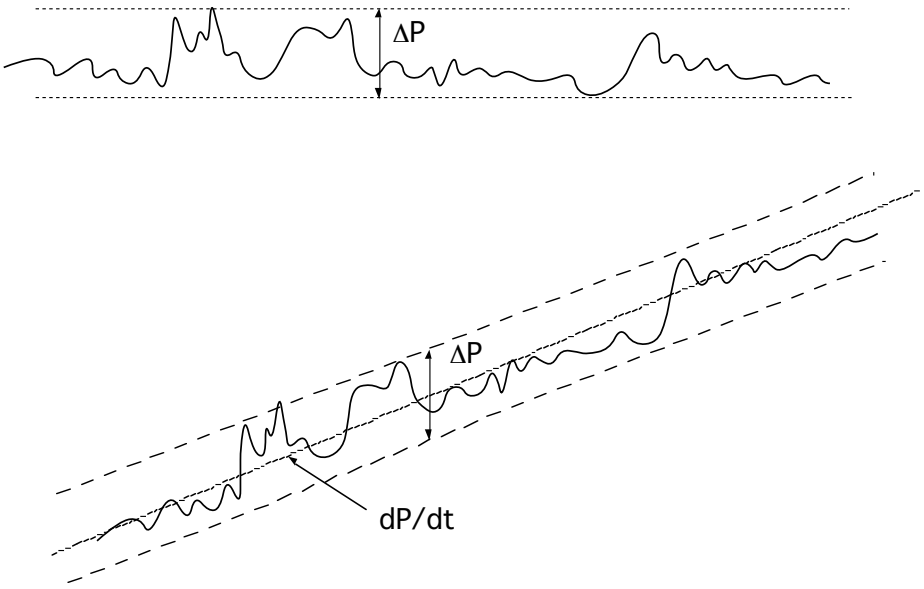

figure 3-1

Considering a modulated signal, $P_r=P_0(1+ m \cos 2\pi f_i t)$, we can write this condition as: $\Delta P \leq P_0 m 2\pi f_i / B$.
Now, the instantaneous frequency f_i sweeps from 50 kHz to 150 MHz, whereas the maximum frequency content B of the fluctuation superposed on the received signal (of mean value P_r), depends on the filtering we apply to the received signal. If no filter is used, then B is as large as 150 MHz, or the maximum signal bandwidth that shall be preserved in the signal. Then when f_i=50 kHz we get $\Delta P \leq P_0 m 2\pi /5000$, with a resulting demand on the S/N ratio. On the contrary, if we dynamically filter the signal with a PLL as in Fig.3-22, the bandwidth of the fluctuation is basically coincident with the instantaneous frequency f_i, and the condition is relaxed to $\Delta P \leq P_0 m 2\pi$.

Q3-25 *Are the calculations of power, number of collected photons and accuracy developed in Problems P3-22 and P3-23 applicable also to a multi-frequency telemeter ?*

Answ.: Yes, they are. In the multi-frequency sine-modulated telemeter, there are three time intervals in which we perform the measurement with three modulation frequencies, e.g. 15 MHz, 150 kHz and 1.5 kHz. As for each interval the measurement is brought down to the same intermediate frequency by the superheterodyne demodulation, the bandwidth of filtering is the same and we shall spend the same time for each of the three periods.

P3-26 *A LIDAR employs a Q-switched laser providing a 10-ns pulse width and the preamplifier and log-converter circuits have a passband of 10 MHz. What is the distance resolution we can achieve?*

Answ.: The pulse width gives a distance resolution
$\Delta L = cT/2 = 3 \cdot 10^{8} \cdot 10^{-8}/2 = 1.5$ m.
The high frequency cutoff B of the electronic circuits is important too, because its inverse $\approx 1/B$ is the response time on which signal is averaged, exactly as for the light pulse duration. More precisely, we can say that the equivalent of the pulse duration is best represented by 1/2B, the time of the Nyquist's sampling theorem.
The distance resolution corresponding to B is then:
$\Delta L = c/4B = 3 \cdot 10^{8}/4 \cdot 10^{7} = 7.5$ m.
This example shows that the bandwidth shall be tailored appropriately, if we wish it not become the factor actually limiting the resolution.

P3-27 *In a LIDAR, the Q-switched laser provides a pulse of E=1 mJ energy and τ=10-ns duration. The collecting objective has a D=30-cm diameter. Calculate the power collected from the atmospheric backscatter with α=1 km^{-1}.*

Answ.: From Eq.3.34 we get, in the case of constant attenuation α and backscatter σ_{bs} coefficient:
$P_{bs}(t) = (E/\tau)\, \sigma_{bs} (\pi D^2/4z^2)\, (\exp - \alpha z)\, (c\tau/2)$
$= (Ec/2)\, \sigma_{bs} (\pi D^2/4z^2)\, (\exp - \alpha z)$
Note that the term $\pi D^2/4z^2$ resembles the attenuation of a telemeter (Eq.3.4), but there is an additional factor π multiplying it. This is not a mistake but comes from the definition of backscatter σ_{bs} coefficient, as the fractional power per unit solid angle (page 408). Thus, the solid angle of collection to multiply is $\pi D^2/4z^2$.
Now we can consider the terms in the above equation:
i) $\exp - \alpha z = \exp - \alpha ct/2$ gives the main dependence with time, a negative exponential with time constant $T = 2/\alpha c = 2/(1 \text{ km}^{-1} \cdot 3 \cdot 10^{5} \text{ km/s}) = 6.6$ μs;
ii) $\pi D^2/4z^2$ is the main attenuation term, equal to $3.14 \cdot 0.3^2/4 \cdot (1 \cdot 10^{3})^2 = 0.07 \cdot 10^{-6}$ at z=1km. There is a time-dependence too, but this is minor, compared to the negative-exponential term.
iii) σ_{bs} term. Assuming small particles, that is the Rayleigh scattering regime (see Appendix A3.1), then the scattering function is isotropic and $\sigma_{bs} = (4\pi)^{-1} \alpha$ (cf. page 408). We then get for the first term, containing the pulse energy E:
$E(c/2)\, \sigma_{bs} = 1 \cdot 10^{-3} \text{J} \cdot 1.5 \cdot 10^{5} \text{ km/s} \cdot (0.08) \cdot 1 \text{ km}^{-1} = 12$ W.

Additionally, because of geometrical attenuation we get, at z=1km:
$P_{bs}(t)$= 12 W $0.07 \cdot 10^{-6} e^{-\alpha_z}$= 0.84 μW exp - τ/6.6μs.

P3-27 *Can the power level found in Probl P3-26 be enough to perform a distance resolved measurement of backscattering, with a resolution of, say, 5 meters ?*

Answ.: To get a 5-m distance resolution, we need a bandwidth B =c/4ΔL = $3 \cdot 10^8$/45 = 15 MHz. At this frequency, a typical PMT (or photomultiplier) can have a noise spectral density of 0.006 pA/√Hz (see Fig.3-7).
Multiplying by √B=$1.22 \cdot 10^3$ and dividing by the typical PMT spectral sensitivity σ_{PMT}= 50mA/W yields p_n=$0.006 \cdot 1.22 \cdot 10^3/50 \cdot 10^{-3}$=0.147 nW.
Respect to the 0.84-μW power level of the received signal, we have a signal-to-noise ratio S/N=0.84μ/0.147n=5720, quite good.

P3-28 *What is the minimum variation of received power and hence of attenuation coefficient you can resolve with the S/N ratio found in the LIDAR of Probl P3-27 ? What is the typical concentration you can resolve accordingly ?*

Answ.: Assuming we get a local variation Δα of the attenuation, then the power variation is ΔαP.
We can trade the S/N ratio found in Problem P3-27 to: i) be able make a good measurement of Δα; ii) be able to appreciate a small variation ΔαP of the received signal. Let assume, for the first point, that a S/N=5 is adequate for our purposes. Then we get a value 5720/5= 1140 as the allowable decrease of signal. This means that we are able to see a small fluctuation of $(1140)^{-1}$=$0.9 \cdot 10^{-3}$ superposed on the received power and due to a small variation Δα/α of attenuation.
Now, we get Δα= $0.9 \cdot 10^{-3} \cdot 1$ km^{-1}= $0.9 \cdot 10^{-3}$km^{-1}.
To determine the concentration, we should make a calibration of the scatterers, or of the substance we are looking for, respect to attenuation. But, by default, we may proceed to a rule-of-thumb calculation as follows. Then, from Eq.A3.2 we get:
α = C A_{sc}L= C Q_{ext}(πr²)L,
where C is the volume concentration (m^{-3}) of the scattering particles, of radius r, as seen along a path of length L, equal to the 5-m resolved pathlength in our case.
To substantiate the evaluation let's take r=1μm, and Q_{ext}=2 (see page 410, that is a λ in the visible). Then we get:
C= Δα/Q_{ext}(πr²)L = $0.9 \cdot 10^{-6}$m^{-1}/2(3.14 10^{-12} m²)5= 2.8 10^4m^{-3}.

To appreciate how small or big this number is, let's recall that cleanliness classes are given as the number of particles (exceeding 10μm) per cubic foot. As 0.3^3=0.027, we have C= 2.8 10^4 m^{-3}0.027=756 ft^{-3}, a fairly low value that becomes very good if we think that it is resolved at 1-km distance and on each 5-m interval.

Problems, Chapter 4

Q4-1 *Does the conversion of field to current really correspond to perform a square of the electrical field, as express by Eq.4.1, and then, why there is no second harmonic generation?*

Answ.: The $I_{ph}= |E|^2$ law is not actually a quadratic-dependence, rather a modulus-square dependence, for the detected current from electric field. Indeed, the detected current I_{ph} is proportional to nothing else than the modulus of the Poynting vector, $|E|^2/2Z_0$, equal to the density of power carried by the optical wave. Therefore, no second harmonic is generated, by no means.

Q4-2 *In the schematics of Fig.4-3, isn't there a phase-shift between transmitted and reflected components introduced by the beamsplitter, that should be taken into account as a π-difference added to the $2k(s_m-s_r)$ arguments in Eq.4.3 ?*

Answ.: That's correct, the π or half-wavelength extra phase-shift should theoretically be added to the difference s_m-s_r of path-length. But, as it is a constant, we can ignore it or think of it as already contained in s_m-s_r.

Q4-3 *What about the reflections from the surfaces crossed by the beams in the schematics of Fig.4-3, can they add to the useful beam ? Don't they alter the operation respect to the case considered, of no reflections?*

Answ.: Undoubtedly, there should be no spurious reflections at all, if we are to get the interferometer operate correctly. To this end, the surfaces crossed by the beam are antireflection-coated, and there angle slightly tilted respect to the perpendicular to the beam, so that the residual minute reflections fall outside the laser as well as the detector.

Despite this provision, some stray light from spurious reflections can still reach the detector, and its effect is a cyclic error (see page 108). We can explain this error by letting $E=E_0 \exp i2ks_m$ be the useful signal, and $E_{sp}=\sqrt{\varepsilon}E_0 \exp i2ks_{sp}$ the spurious reflection, where ε is the fraction of power reflected from a point at a fixed position s_{sp}. Now, by beating on the photodetector with the reference $E_0 \exp i2ks_r$, we get:

$I_{ph}= I_0[1+\cos 2k(s_m-s_r)]+\sqrt{\varepsilon}I_0[1+\cos 2k(s_{sp}-s_r)] +\sqrt{\varepsilon}I_0[1+\cos 2k(s_{sp}-s_m)]$

The first term is the usual signal, the second is a constant (being $s_{sp}-s_r$ =constant) and the third is the cyclic error term, which has a periodicity $\lambda/2$ with the measurement path length s_m, and has an amplitude $\sqrt{\varepsilon}$ referred to the $\lambda/4$ peak-to-peak swing of the signal $\cos 2k(s_{sp}-s_m)$. Another 1/4 factor comes from the splitting of total power into the beams of the two arms, and in conclusion we get an error $\sqrt{\varepsilon}\ \lambda/16$.

P4-4 *How can you implement the multiplier indicated in Fig.4-5, necessary to bring the count measurement to decimal ?*

Answ.: Indeed, the multiplier is not an easy task to implement, as we need a 7 by 7 decades decimal multiplier to apply the $\lambda/8$ scale factor so as to bring the result to a decimal reading.

First approach: we use SS-ICs (small scale integrated circuits), and then we get a decimal digit multiplier, a two-digit buffer, a decimal adder for each of the 7 digits, and a total adder and buffer for the result. We end up with perhaps 160 ICs and a PC board perhaps of 20x30 cm size.

Second approach: it is much better to start with an FPGA (field programmable gate array) or the most modern version of it, the SoC (System on Chip). These devices are ICs (Integrated Circuits) and contain a large number of individual gates, mono/bi-stables, counters, adders and so on, which are interconnected according the desired schematic through a software development program.

The result is a cheap, single chip device, whose overhead cost is the relatively long time spent in programming it, however. As a default estimate, the cost of an FPGA or SoC may be only a few percent of the cost of the SS-IC implementation. But, the cost of developing the program is 3-10 times the cost of the SS-IC product. Thus, we have a break-even point between the SS-IC and the FPGA/SoC at some hundreds part-counts.

P4-5 *Isn't there another approach to implement the multiplication using a reasonably small number of SS-ICs, eventually at the expense of speed of output uptading?*

Answ.: A possible implementation for the decimal-readout multiplier is described in Figure 4.1. Two buffer counters are introduced, one (the λ/8 buffer counter) connected to the main λ/8 counter through a gate, enabled at the start of the conversion (start command setting the JK flip-flop). The buffer counter is decreased by the clock f_1 pulses until it reaches the zero (i.e. all digits equal to zero) content. This is detected by the (6-digit) comparator, which then stops operation of the second counter, which is fed by the clock f_2.
If N_1 is the content of the λ/8 buffer, the time interval to reach zero is $T= N_1/f_1$. Then the content accumulated by the second buffer is $N_2 =Tf_2= N_1 f_2/f_1$. By choosing the frequency ratio $f_2/f_1= 632811/8=0.791014$, i/.e. equal to the λ/8 unit, the content of the second buffer is brought to decimal.

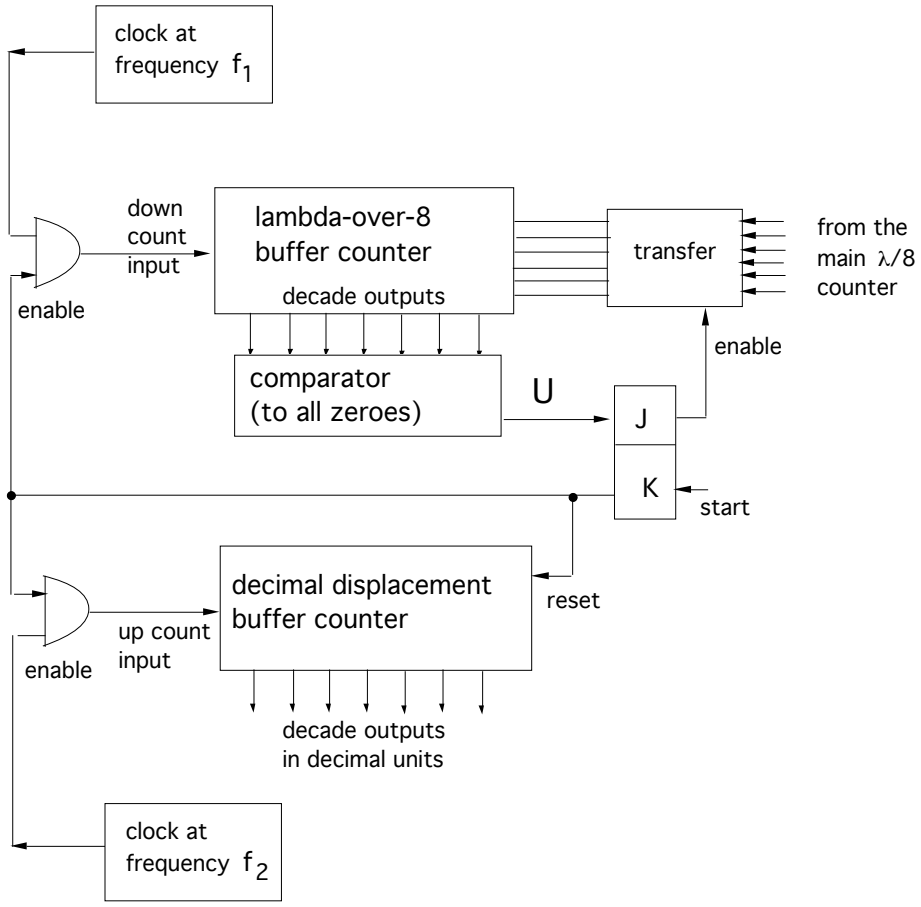

Figure 4.1

P4-6 *Calculate how parallel shall be the stroke of the measurement corner cube respect to axis defined by the propagation vector of the beam, to keep the cosine error below 1 count.*

Answ.: The actual signal we measure with the interferometer is

$I_{ph}= I_0[1+\cos 2\,\underline{k}\cdot\underline{s}_m] = I_0[1+\cos (2\,k\,s_m \cos \Theta_{km})]$

As it is $\cos \Theta_{km} \approx 1-\Theta_{km}^2/2$ for small angle, after a stroke s_m we generate an error:

$\Delta s_m= s_m\, \Theta_{km}^2/2$

Letting $\Delta s_m= \lambda/8$, we get $\Theta_{km}^2=2\,(\lambda/8\, s_m)$, or $\Theta_{km}= (\lambda/4s_m)^{1/2}$.

For example, after a stroke s_m=100 mm, at λ=0.63 μm we need an alignment better than $\Theta_{km}=(0.63\ \mu m/0.1)^{1/2} =2.5\ 10^{-3}$ rad ≈ 8 arc-min.

Note that, if we align at sight the returning beam w, let's say within a fraction ε of the beam itself, we get the desired alignment Θ_{km} at a distance greater than $z \geq \varepsilon\, w/\Theta_{km}$. For 1-mm beam radius and ε =0.2, it is $z \geq 0.2 \cdot 1mm/2.5\ 10^{-3}$ rad= 80 mm.

Q4-7 *Is the cosine error a positive or negative deviation from the true value ?*

Answ.: As it can be seen in Figure 4-2, the actual displacement covered by the corner cube is a, whereas the quantity measured by the interferometer is s cos Θ. Therefore, the measure has a negative deviation from the true value s.

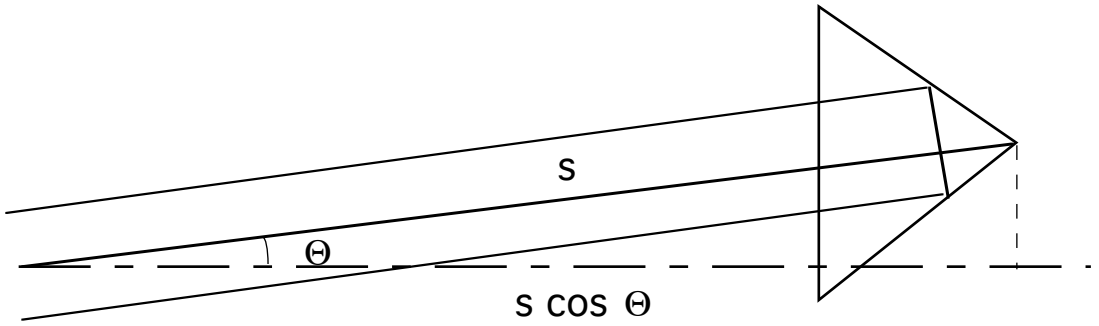

Figure 4.2

Q4-8 *In Fig.4-11 of the text, we have considered a 3-sector phase shifter to provide 3 signals at de-phased by 120 and 240 degrees. Why can't be the same thing be done with just two signals ?*

Answ.: The usual sin and cos interferometric signals have the form:

$I_1= 1+\cos 2ks$, $I_2= 1+\sin 2ks$.

If the dc components were removed, the diagram would be that of Figure 4.3, left, and the pair of co-ordinates x= cos 2ks and y= sin 2ks allow just one solution for 2ks (that indicated with the thick dot).

In the general case, we can represent I_1 and I_2 on a plane as shown in Figure 4.3, right. Indeed, as 2ks varies between 0 and 2π, cos 2ks and sin 2ks swing along -1 and +1 and the figure described by x= cos 2ks and y= sin 2ks is a circle of unit radius. Adding +1 to x and y gives the circle tangent to the x and y axes.
But, for a pair of I_1 and I_2 values, there are two circles passing through the point and being tangent to the x and y axis. We could remove this ambiguity if we are allowed to follow for a while the evolution of the displacement s, so as to sort which of the two circles of figure 4.3, right we are running on. In general, however, we cannot grant any knowledge of the previous evolution of signals I_1 and I_2.
Therefore, the ambiguity can be removed only with a more basic approach, the one using three signals (de-phased of 120°, for example).

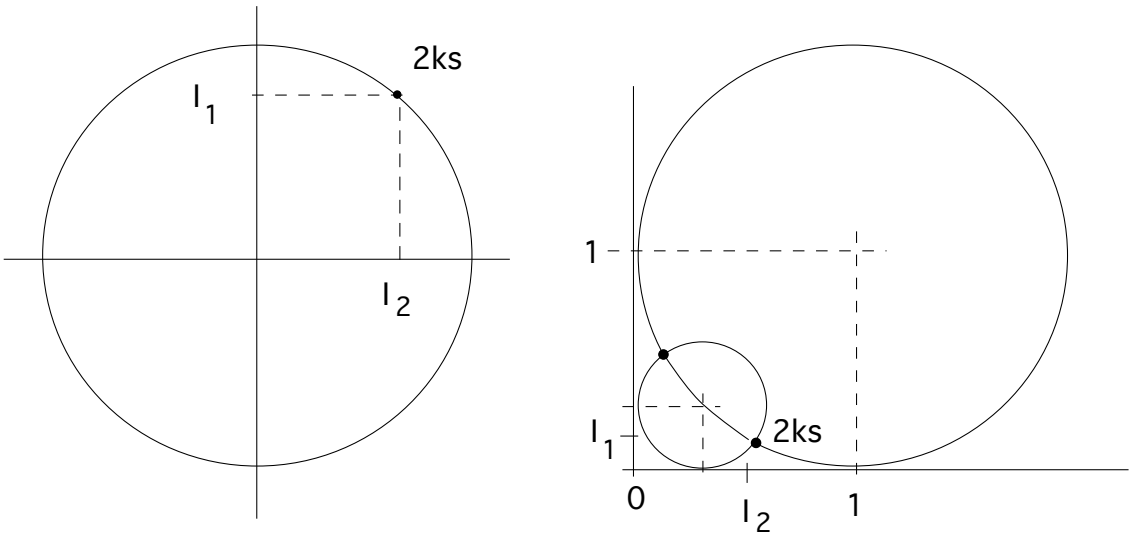

Figure 4.3

P4-9 *A two-frequency laser interferometer shall be measuring a carriage with a corner cube moving at a speed up to 30 cm/s. Determine the required bandwidth of the interferometer signal.*

Answ.:
The speed v=d(Δs)/dt develops a frequency of counts of λ/2 increment:
$f_c=2v/\lambda$,
and, for a velocity ±v, the bandwidth around the central frequency f_1-f_2 doubles at:
$B=2\ f_c=4v/\lambda$,
and in our case B= 4 · 300 (mm/s) / 0.633 μm = 1.89 MHz.

This value can be accommodated easily upon a carrier f_1-f_2 =5 MHz, the value usually chosen in a Zeeman-stabilized He-Ne laser, as it corresponds to a moderate fractional bandwidth, at 5±0.95 MHz.

P4-10 *In Fig.4-12 (text)we see the 3-axis extension of the interferometric measurement. Is it really useful for part saving ? How many more axes can realistically be fed by a single laser source ?*

Answ.: Of course, we save the laser, in a multi-axis arrangement like that shown in Fig.4-12.
Also, if we make a measurement at a time, we can save the electronic circuits as well. This is not the case commonly found however, because in a machine tool we need all the axes of interest simultaneously.
About the maximum number of channels we can extend, this is determined by the minimum signal power that is required at the detector for the counting circuits to function properly. With a 1-mW laser and taking the reasonable value of 50 μW as the minimum signal power, we get 20 channels, theoretically.

P4-11 *The working principle of the planarity-measurement set-up shown in Fig.4-14 is very clear if we look at the angle α as the output, whereas is not so straightforward if we are looking to the height distribution z(x,y). How the data of α(x,y) are used to compute z(x,y) ?*
Answ.: As shown in Fig.4.4 below, as the square is moved along the plane to be tested — let's say along the x-axis to be specific, a lowering Δz of the height is generated, which is related to α.

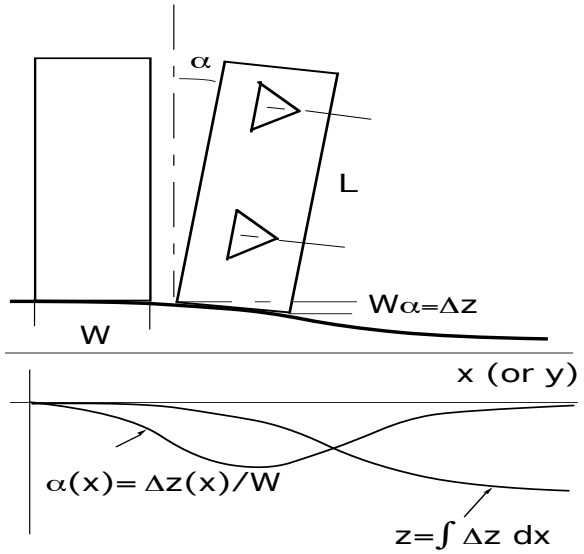

Figure 4.4

The relationship of the total height z to the increment Δz is the integral, of course.
Thus, as also shown in Figure 4.4, the actual height profile or distribution as a function of the coordinate, z=z(x) is found as $z(x)= \int \Delta z(x)\, dx = W \int \alpha(x)\, dx$. In practice, if we perform the measurement in steps of displacements of W, moving the mobile (the right hand side) square along x by W, 2W, 3W, ... and we get a measurement of a_1, a_2, a_3, ... counts of $\lambda/8= 0.08\ \mu m$ at each position, then the profile z_1, z_2, z_3, ... is given by a_1, a_1+a_2, $a_1+a_2+a_3$, ... (in $\lambda/8$ units).

Q4-12 *Can we measure the angles (e.g., roll, pitch, and yaw) of a turret carrying the tools of the machine-tool as in Fig.4-13 so that control in it six axes?*

Answ.: Of course, each angle can be measured by the double-square configuration of Fig.4-14. At large angles, this configuration yields the measurement of $\Delta\phi= 2kL \sin \alpha$, where α is the (roll, pitch or yaw) angle of the turret respect to the fixed frame of the machine-tool. The maximum dynamic range for α is determined by the angular aperture of the corner-cubes and by the distance between the squares (it can go up to 45 deg).

P4-13 *An interferometer operates on a diffuser target like indicated in Fig.4-16. The laser power is P_l=1 mW and we use a lens with F=100 mm and D =30 mm, that focalizes the laser beam (with w_l= 0.5 mm) on the target in a focal spot of w_{tar}=100 μm. What is the collected power P_{ph}, on the 1-mm dia. photodiode ? Does is depend on w_{tar} ? What is the dynamic range of the measurement? What is the loss of sensitivity performance respect to operation on a corner-cube ?*

Answ.: Using the result on page 111, we get
$P_{ph}= P_l\ (w_l/F)^2 = 1\ mW.(0.5/100)^2 = 25\ nW$ as the collected power.
This power does not depend on w_{tar}.
The dynamic range DR is the depth of focus (p.112) $\lambda/\pi NA^2$, where NA=0.5/100, or: $DR=0.6\mu m\ (100/0.5)^2= 24\ mm$.
About sensitivity performances, a reduction of the available power from 1-mW to 25- nW (or 4.6 decade) brings about a worsening of 1/2(4.6)=2.3 decades in the noise-equivalent-displacement, as shown in Fig.4-18.
For example, if we need a 10-kHz bandwidth of measurement, instead of the 0.4 pm (with the corner cube) we may resolve only 0.1-nm.

P4-14 *How the quantum efficiency η of the detector impacts the shot-noise-limited NED? How important is it, compared to visibility and responsivity ?*

Answ.: As $I_0=\sigma P_0= e\eta/h\nu\ P_0$ and the shot noise of the photons gives a power fluctuation $p_n= [2\ h\nu\ P_0B]^{1/2}$, the argument leading to Eqs.4.15 and 4.16 can be repeated with the following result:

$$NED = (\lambda/2\pi)\ [2\ eB/\ \sigma P_0]^{1/2}/RV$$

$$= (\lambda/2\pi)\ [2\ h\nu B/\ P_0]^{1/2}/RV\sqrt{\eta} = (\lambda/2\pi)\ [S/N]_P\ /RV\sqrt{\eta}$$

or, the general expression involving $\lambda/2\pi$, S/N and RV is still valid if we take the S/N ratio as that of the available power, but as a final step we have to divide it by $\sqrt{\eta}$. Thus, the NED is proportional to detector quantum efficiency at power -1/2 whereas R and V affects linearly the NED.

P4-15 *What is the frequency stability Δν of the laser that we need in an interferometer to be able resolving a NED of, say: i) 1-nm on a Δs =1-m distance (arm) imbalance, ii) 1μm on a Δs =10-m distance imbalance ?*

Answ.: We need (Eq.4.21) $\Delta\nu=\nu\ NED/\Delta s$. As ν= 375 THz @ λ=800nm, we get:

$\Delta\nu$= 375 THz 10^{-9}m /1m = .375 MHz for case i), and

$\Delta\nu$ = 375 THz 10^{-6}m /10m = 37.5 MHz for case ii).

These figures basically represent the laser linewidth we need to get.

As a comment, a He-Ne frequency stabilized laser can easily match both figures, whereas using a semiconductor it is likely that we are able to match the specification of case ii) but not that of case i).

P4-16 *Are the spatial-coherence and polarization-state effects the only effects related to beam parameters or other possible errors can arise, for example in wave-front radius mismatch ?*

Answ.: If two beams are recombined with curved wavefront, the radii of curvature shall be the same, otherwise the factor μ_{sp}, as given by Eq.4.22, will be less than one.

P4-17 *If the incoming wavefront is spherical and the detector surface is plane, isn't there an error because of the varying phase of the field along the photodetector surface ?*

Answ.: No, what matters is the phase difference, so the radius matching condition is applicable to the two waves being recombined, not to a wave being compared to the receiving surface.

P4-18 *How large is the error of the interferometric measurement which is caused by an error in wavelength and associated variation of the index of refraction of the air ? Evaluate it for a single mode-hop of a 850-nm semiconductor laser.*

Answ.: Using Eq.4.25, we get after differentiation:
$\Delta(n_{air}-1)= -4.608\ \Delta\lambda_{(\mu m)}/\lambda^2_{(\mu m)} -0.122\ \Delta\lambda_{(\mu m)}/\lambda^3_{(\mu m)}$ (ppm)
and letting for case i) λ=0.85 μm, $\Delta\lambda$=0.3 nm (from the diagram of Fig.A1-13), we get:
$\Delta(n_{air}-1)= -4.608\ 0.3\ 10^{-3}/0.85^2 -0.122\ 0.3\ 10^{-3}/0.85^3 = -\ 1.68\ 10^{-3}$ (ppm)
or, the error is quite negligible. On the other hand, the $\Delta\lambda/\lambda$ error is not negligible at all, being equal to 0.3 nm/850 nm= $0.35\ 10^{-3}$ = 350 ppm.

P4-19 *Evaluate the thermodynamic rms fluctuation arising in a fiber of length L=1000 m in a B=10 kHz bandwidth.*

Answ.: Using Eq.4.28 of the text (page 119), which is rewritten here with the correct multiplicative factor as:
$NED_{th}= \phi_{th}/k= 0.37\ 10^{-5}\ [kT^2LB/\kappa]^{1/2}$
where $k_B T^2=1.2\ 10^{-18}$ J°C, and being κ=0.014 W·cm^{-1}°C^{-1} for silica, the material of which fiber is made. Therefore we find:
$NED_{th}= 0.37\ 10^{-5}\cdot[1.2\ 10^{-18}\times 1000\times 10^4/0.014]^{1/2}$
$= 0.37\ 10^{-5}\cdot 2.90\ 10^{-5}$(cm) = $1.07\ 10^{-10}$ cm
We can also go back to the noise-equivalent-phase ϕ_{th} = k·NED to better understand how this value shall be considered. Assuming λ=850 nm, so that $k=2\pi/\lambda= 6.28/0.85\ 10^{-4}= 7.39\ 10^4$, we get:
$\phi_{th(noise)}= 7.39\cdot 10^4 \cdot 1.07\cdot 10^{-10}= 7.93\cdot 10^{-6}$ rad.
Going back to the diagram of Fig.4-18 with these data, we can see that the thermodynamic fluctuation of 7.93 μrad is equivalent, at B=10kHz, to the shot noise associated with a detected power of ≈1mW. Thus, we shall conclude that, in a sensor with a long fiber, the thermodynamic noise can indeed become the limiting factor.

P4-20 *Evaluate the Brownian rms velocity fluctuation affecting a 1 milligram mass.*

Answ.: Letting T=300 K in Eq.4.29, and being k= $1.38\cdot 10^{-23}$J/K for the Boltzmann constant, we get for a 1-mg mass:
$\langle v^2\rangle = kT/m = 4\cdot 10^{-21}/10^{-3}=2\cdot 10^{-18}$, or $\sigma_v=\sqrt{\langle v^2\rangle}=1.4\cdot 10^{-9}$ m/s.

This is a value well in the reach of a typical interferometer (it corresponds to s=1nm and f=1Hz in the diagram of Fig.4-17).

P4-21 *Evaluate the Brownian rms angular velocity fluctuation affecting a disk of 10 milligram mass and a 1-mm radius.*
Answ.: For a 10-mg mass and 1-mm radius, we get an inertia momentum $I=(1/2)mr^2=5\cdot10^{-3}\cdot10^{-6}=5\cdot10^{-9}$,
and thus we get from Eq.4.30:
$\sigma_\Omega=\sqrt{\langle\Omega^2\rangle}= kT/I =\sqrt{(4\cdot10^{-21}0.2\cdot10^{9})}=0.9\cdot10^{-6}$r/s = 0.18 deg/h,
again a value within the readout sensitivity of a gyroscope (see Ch.7).

Q4-22 *Why there is a speckle-related error when the measurement is performed on a diffusing surface ? How large is it ?.*
Answ.: The error is determined by the speckle-pattern *phase* statistics, which amounts to an interferometric phase error. The error is different for a transversal and a longitudinal displacement, or a lateral shift of the diffuser target. As we have seen from Eqs.4-29 to 31 the amount of the error is primarily determined by the ratio of the displacement Δs we are considering to a characteristic length of the speckle field, e.g., the so-called speckle size. The multiplication factor of this ratio is not far from unity and its actual value is determined by the statistics discussed in Ch. 5.

P4-23 *Calculate the minimum displacement that can realistically be measured with the internal configuration of interferometry working with a L=20-cm He-Ne tube.*
Answ.: The minimum displacement Δs we can detect in an observation time T is that generating at least 1 period of the beating waveform received at the photodetector, or, a frequency $\Delta f =1/T$.
As it is $\Delta f=R_f\ \Delta s$, with the responsivity $R_f=c/\lambda L$ typically as large as $R_f=$ 2.4 MHz/nm for λ=633 nm and L=200 mm, taking T=1 s we get $\Delta s=$[2.4 MHz/nm]$^{-1}$ = 2.4 fm. Of course, for the measurement to be useful, we shall have an adequate S/N ratio, as determined by Fig.4-18.

Q4-24 *The scale factor of the internal configuration of interferometry is $c/L\lambda$. Is L in it the distance (of the rear mirror) to measurement-arm mirror or reference-arm mirror ?*
Answ.: It is the distance of the rear mirror to the measurement-arm mirror if this mirror is the movable one. Should the reference-arm mirror be

moved also, then the associated Δs_{ref} measurement would have a scale factor $c/L_{ref}\lambda$.

P4-25 *A self-mixing interferometer uses a 20-cm He-Ne laser with output mirror reflectivity of 99% and a round-trip gain $2\gamma_0 L=0.02$. Evaluate the AM modulation index and the frequency deviation of the FM signal. Assume a spot size w=0.2 mm and allow for a target either diffusive or reflective, placed at a distance s=50 cm.*

Answ.: Working at s=500 mm distance on a diffuser target, we have a superposition loss $A\eta=w/s= 0.2/500$, whereas for a retroreflector the loss would be $A\eta=L/2s=0.2$ [because A=1 and $\eta=[(w/w_0)^2+(w_0/w)^2]^{-1/2}\approx w/w_0 \approx(\lambda/\pi w_0^2)2s/w_0\approx L/2s$].
Then we have for the diffuser at 500-mm distance:
$m_A=A\eta t_i^2/2\gamma_0\approx(0.2/500)0.01/0.0002540=4\cdot10^{-5}$, and this would then show up as a very minute ripple superposed to the average power emitted by the laser. On the other hand, with the retroreflector, it would be:
$m_A\approx0.20.01/0.00025\cdot40=0.2$, a nicely large amplitude.
Correspondingly, the frequency deviation $\Delta/2\pi$ in the two cases is:
$\Delta/2\pi=ac/2L=750$ MHz$(0.2/500)0.01/6.28=500$ Hz (diffuser), and
$\Delta/2\pi=750$MHz$0.20.01/6.28=250$kHz (retroreflector).

P4-26 *Repeat the calculation of Probl.4-25 for the AM modulation of a semiconductor laser, with output mirror reflectivity of 30% and a round-trip gain $2\gamma_0 L=3$. Assume that an output objective lens makes the beam circular, into a spot size w=0.25 mm. Allow for a target either diffusive or reflective, placed at a distance s=50 cm, and calculate the factor C.*

Answ.: Working at s=500 mm distance on a diffuser target, we have a superposition loss $A\eta=w/s=0.25/500$.
For a retroreflector, the loss is $A\eta=[(w'/w_0)^2+(w_0/w')^2]^{-1/2}$, where $w_0=0.25$ mm is the initial spot size, and w' is the spot size of the beam after having travelled a distance 2s. Hence, $w'=[w_0^2+(\lambda2s/\pi w_0)^2]^{1/2}=[0.25^2+(0.85\cdot10^{-3}\cdot1000/3.14\cdot0.25)^2]^{1/2}=[0.25^2+1.08^2]^{1/2}=1.11$ and we get:
$A\eta=0.225$ for the retroreflector. Then we have at 500-mm distance:
$m_A=A\eta t_i^2/2L\gamma_0\approx(0.25/500)0.3/3=0.5\cdot10^{-4}$ for the diffuser, and:
$m_A\approx0.2250.3/3=0.0225$ for the retroreflector. Thus, both values are larger (but not very much larger) than those of the He-Ne laser.
In addition, assuming for the diode laser a typical cavity length L= 200 μm (=0.02 cm), $n_i=3.5$ and and $\alpha=6$, we can calculate the factor C (see on page

141, the equation following 4.48, and correct accordingly the miswriting of Eq.4.35 on page 127):

$C = A\eta\, s\, (1+\alpha^2)^{1/2}/n_i L = 0.5\cdot 10^{-3}\cdot 50\cdot 37^{1/2}/3.5\cdot 0.02 =$

$= 2.17$ for the diffusing target, and

$C = 0.225\cdot 50\cdot 37^{1/2}/\ 3.5\ 0.02 = 977$ for the retroreflector.

In the first case, the signal already exhibits switching (see Fig.4.28, drawing on the second line from the top) and is adequate to allow a $\lambda/2$-fringe counting mode. The second case shows that, using a retro-reflector, the laser is driven into very high C's at even a moderate (s=50-cm) distance. Thus, the laser will undergo the coherence collapse regime unless we add an optical attenuator along the propagation path so that C is tailored as desired.

If we repeat the calculation for the He-Ne laser, in which $n_i \approx 1$ and $\alpha \approx 0$, using the data of Probl.4-25, we get:

$C = A\eta\, s\, (1+\alpha^2)^{1/2}/n_i L = 0.4\cdot 10^{-5}\cdot 50\cdot 1/1\cdot 20 = 10^{-5}$ for the diffusing target, and $C = 2\cdot 10^{-3}\cdot\ 50\cdot\ 1/\ 1\cdot 20 = 5\cdot 10^{-3}$ for the retroreflector. In both cases, and in general very frequently with He-Ne lasers, we are in the weak-injection regime.

P4-27 *Calculate the speed of response of the AM/FM modulations for an interferometer that uses the He-Ne laser with the data of Probl.4-25, or the diode laser with the data of Probl.4-26. Assume s=50 cm.*

Answ.: Using the He-Ne laser, we have for the time constant τ of the cold cavity: $\tau^{-1}=(1-r)\ c/2L = 0.01\cdot 750$ MHz=7.5 MHz. The gain per pass is $G= 2\gamma_0 L=0.02$, and hence the bandwidth is $B= \tau^{-1}/2\gamma_0 L =7.5/0.02= 225$ MHz. In addition, there is a 50 cm·2/30cm/ns=3.3-ns delay in the response.

For the semiconductor laser, we get $\tau^{-1}= 0.6\cdot 200$ GHz = 120 GHz, and as $2\gamma_0 L=3$, we get $B= \tau^{-1}/2\gamma_0 L =120/3= 40$ GHz. [Of course, it's very difficult to test this large bandwidth with a direct measurement]. In addition, we again have the 3.3-ns delay at s=50 cm.

P4-28 *How can we calculate the minimum-displacement or NED performance of the self-mixing interferometers considered in Problems 4-25 to 4-27 ?*

Answ.: The NED is determined by the smallest of the AM and FM signals. As the AM is usually smaller than the FM signal (see page 130), we are

left with a measurement performed with an average power P_0 (or photodetected current $I_0=\sigma P_0$), on which the useful signal is a cosine with relative amplitude $m_A=A\eta t_i^2/2L\gamma_0$. Thus, we have simply to consider the equivalent power $m_A P_0$ as the value to enter in the diagram of Fig.4-18 and evaluate the NED.

P4-29 *Evaluate accuracy and precision of self-mixing interferometers that use as a source: (i) a frequency-stabilized He-Ne laser; (ii) a monomode He-Ne laser; (iii) a thermal stabilized DFB diode laser; (iv) a Fabry-Perot thermal stabilized laser diode; (v) a normal Fabry-Perot laser diode.*

Answ.: First, we shall note that accuracy is about the uncertainty of the measurement, whereas precision is refereed to the 'true value' of the measurement and involves the possibility of performing a calibration of the instrument. Of course, to achieve a precision of say 10^{-6} or the sixth decimal place, we need the accuracy be at least of the same amount, so in the following we refer to accuracy only.
In the self-mixing interferometers, there is no difference respect to making a normal phase $\phi=2ks$ measurement based on the wavelength $\lambda=2\pi/k$ as the yardstick. So, the accuracy and precision of s are the same of λ or of frequency ν of the source. Thus, left aside the index of refraction correction, the relative uncertainty of s, $\Delta s/s$ is the same of the relative uncertainty of frequency, $\Delta\nu/\nu$. Then we have:
(i) in a typical frequency-stabilized He-Ne laser, $\Delta\nu$ is dependent on the reference chosen and on the control loop gain (App.A1.2). With a simple Zeeman or two-mode mechanism, and a piezo actuation, we easily achieve $\Delta\nu\approx200$ kHz on short term, and proabbly $\Delta\nu\approx2$ MHz on long term. As $\lambda=633$ nm is equivalent to $\nu=500$ THZ, we get a relative accuracy $\Delta\nu/\nu\approx5$ M/ 500 T=10^{-8}. Thus, in principle, we can attain the 8-th decimal place in the measurement with freq-stab He-Ne.
(ii) in a monomode He-Ne laser, mode-wandering under the atomic linewidth $\Delta\nu_{at}$ limits $\Delta\nu$ to $\Delta\nu=\Delta\nu_{at}\approx$ 1.5 GHz, whence $\Delta\nu/\nu\approx1.5G/500T$ =0.3 10^{-5}. Thus, we can get 5,5 digits with unstabilized He-Ne's (the 1/2 digit is for the factor 0.3).
(iii) in a thermal stabilized DFB diode laser, the linewidth is probably a narrow $\Delta\nu_{cav}\approx$1-5 MHz, but we get a much larger wandering of the resonance because of temperature and current-dependence. A typical active thermostat can reduce ambient-related perturbances to, say, ±0.1 °C level, where as a good current stabilizer will reduce current drift around the

working current (20-70 mA) to, say, ΔI=1-μA. As the thermal drift of a diode laser (either DFB, DBR or Fabry-Perot) is $\alpha_\nu = d\nu/dT \approx 3$GHz/°C and the current drift is $\alpha_I = d\nu/dI \approx 2$ GHz/mA (see page 385) summing up the contributions we get:

$\Delta\nu = \alpha_\lambda \Delta T + \alpha_I \Delta I = 3$ GHz $\cdot 0.1 + 2$ GHz $\cdot 0.001 = 302$ MHz.

Accordingly, the resolution at λ=800 nm (or 400 THz) becomes:

$\Delta\nu/\nu \approx 0.3G/400T = 0.75\ 10^{-6}$. Thus, we can get 6,2 digits with a well-stabilized DFB of DBR laser.

(iv) In a Fabry-Perot thermal stabilized laser diode, the coefficients are the same as in (ii), but the Fabry-Perot has additionally the very unpleasant feature of mode-hopping (see Fig.A1-13) This prevents us from assuming $\Delta\nu$=302 MHz as the total linewidth drift. Rather, we shall take conservatively $\Delta\nu$ as that of a single mode hop, or $\Delta\nu = \Delta\nu_{hop} \approx 200$ GHz.

Accordingly, the resolution at λ=800 nm becomes:

$\Delta\nu/\nu \approx 200G/400T = 0.5\ 10^{-3}$. Thus, we get only 3,7 digits with a Fabry-Perot thermal stabilized laser.

10^{-5}. Thus, we can get 5,5 digits with unstabilized He-Ne's (the 1/2 digit is for the factor 0.3).

(iii) in a thermal stabilized DFB diode laser, the linewidth is probably a narrow $\Delta\nu_{cav} \approx 1$-5 MHz, but we get a much larger wandering of the resonance because of temperature and current-dependence. A typical active thermostat can reduce ambient-related perturbances to, say, ±0.1 °C level, where as a good current stabilizer will reduce current drift around the working current (20-70 mA) to, say, ΔI=1-μA. As the thermal drift of a diode laser (either DFB, DBR or Fabry-Perot) is $\alpha_\nu = d\nu/dT \approx 3$GHz/°C and the current drift is $\alpha_I = d\nu/dI \approx 2$ GHz/mA (see page 385) summing up the contributions we get:

$\Delta\nu = \alpha_\lambda \Delta T + \alpha_I \Delta I = 3$ GHz $\cdot 0.1 + 2$ GHz $\cdot 0.001 = 302$ MHz.

Accordingly, the resolution at λ=800 nm (or 400 THz) becomes:

$\Delta\nu/\nu \approx 0.3G/400T = 0.75\ 10^{-6}$. Thus, we can get 6,2 digits with a well-stabilized DFB of DBR laser.

(iv) In a Fabry-Perot thermal stabilized laser diode, the coefficients are the same as in (ii), but the Fabry-Perot has additionally the very unpleasant feature of mode-hopping (see Fig.A1-13) This prevents us from assuming $\Delta\nu$=302 MHz as the total linewidth drift. Rather, we shall take conservatively $\Delta\nu$ as that of a single mode hop, or $\Delta\nu = \Delta\nu_{hop} \approx 200$ GHz.

Accordingly, the resolution at λ=800 nm becomes:

$\Delta\nu/\nu \approx 200G/400T = 0.5\ 10^{-3}$. Thus, we get only 3,7 digits with a Fabry-Perot thermal stabilized laser.
(v) In a normal Fabry-Perot 1 diode, we get several mode-hops in the normal working conditions, and therefore we may have 5-10 times the $\Delta\nu/\nu$ calculated at point (iv), so resolution is very poor, just about 3 digits.

P4-30 *Derive the loop gain and the transfer function of the short-distance vibrometer shown in Fig.4-34. Find the filter response to low-frequency (<100 Hz) components (representative of microphonics)*

Answ.: We may represent the feedback loop of the half-fringe-stabilized vibrometer (Fig.4-34 of the text) as in Figure 4-5.
In this schematic, the displacement signal Δs_{meas} is accompanied by the disturbance from the ambient Δs_{amb}, and the interferometer is a block with transfer function k ($=2\pi/\lambda$); the resulting phase $\Phi = k\,\Delta s$ is read by the photodiode as a signal $I_0\Phi$ (for small Φ) and the front-end preamplifier gives a voltage output signal $V_{out} = RI$. Finally, the low-pass filter has a frequency response $F(\omega)$, let us take it simply as $F(\omega) = 1/\sqrt{[1+(f/f_1)^2]}$, and it feeds the main amplifier with the voltage gain A. \

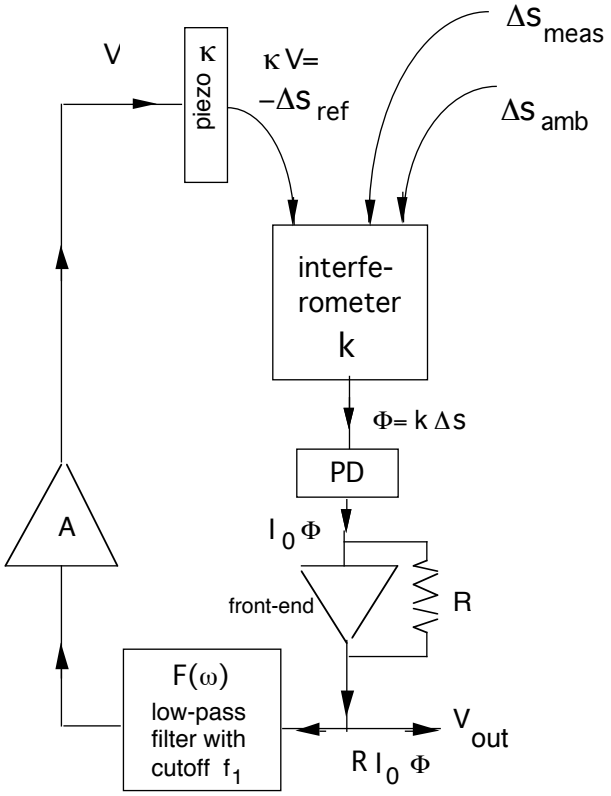

Figure 4-5

Last, the actuator gives a response $\Delta s_{piezo}=\kappa V$, where κ (μm/Volt) is the conversion factor of the piezo.

Now, we can calculate the transfer function between input (the displacement) and output (the front-end output) as:

$V_{out}/\Delta s_{meas}= G_0/(1+hG_0)$, where, from feedback theory, G_0 is the direct transfer gain, and hG_0 is the loop gain. From these definitions we can write by inspection of Figure 4-5:

$G_0= k\, I_0 R$,

$hG_0= k\, I_0 R\, F(\omega)\, A\, \kappa$

When the filter is is cut-off, F=0 for $f>>f_1$, the loop gain hG_0 is zero and we simply get the transfer function G_0 of the normal interferometer, or $V_{out}/\Delta s_{meas}= k\, I_0\, R$. With the typical values I_0 = 0.3 mA (for a 1-mW total optical power) and R=100 kΩ, we get as an example:

$V_{out}/\Delta s_{meas}= 2\pi\ 0.3m\ 100k\ /\lambda= 200$ Volt/wavelength.

On the other hand, when the filter fully effective, F=1 for $f<<f_1$, then the loop gain is $hG_0= k\, I_0 R\, A\, \kappa$ and the transfer ratio becomes:

$V_{out}/\Delta s_{meas}= k\, I_0 R/(1+ kI_0 R\, A\kappa)$

If we neglect the unity respect to $kI_0 R\, A\kappa$, we get

$V_{out}/\Delta s_{meas}= 1/A\kappa$

and, at any rate, the transfer function is reduced respect to the high-frequency normal value, just of the loop gain $kI_0 R\, A\kappa$.

If we let κ= 1 wavelength/ 1000 V and A= 5000, then the loop gain is:

$hG_0= k\, I_0 R\, A\kappa$ = 200 Volt/wavelength × 1wavelength/ 1000 V × 5000

= 1000

As a in conclusion, the ambient induced disturbances Δs_{amb} are reduced by a factor 1000 when they fall in the passband ($f<<f_1$) of the filter.

We can add some further insight in the mechanism of the feedback effect, by expliciting the single-pole expression for $F(\omega)=1/(1+jf/f_1)$ in the transfer ratio:

$$V_{out}/\Delta s_{meas}= kI_0 R/(1+ kI_0 RF(\omega)A\kappa)$$
$$= [kI_0 R/(1+ kI_0 RA\kappa)]\ /[1/kI_0 RFA\kappa +1/(1+jf/f_1)]$$
$$= [kI_0 R/(1+ kI_0 RA\kappa)]\ (1+jf/f_1)/[1/kI_0 RFA\kappa +jf/f_1 kI_0 RFA\kappa +1]$$
$$\approx G_F(1+jf/f_1)/[1+jf/f_{1hG0}]$$

where G_F is the feedback gain.

From this expression we can see that the frequency response is composed as follows: we start from the dc with G_F, then, from the frequency cutoff f_1, there is an increase of the response with frequency (the term jf/f_1), until we

reach the frequency f_{1hG0}, at which the gain has become $G_F f_{1hG0}/f_1 = G_F k I_0 RFA\kappa \approx k I_0 R$, the normal value of the interferometer.

P4-31 *For the short-distance vibrometer shown in Fig.4-34, evaluate the NED when using a 1-mW laser in a 10kHz bandwidth.*

Answ.: To evaluate the NED, let's start considering that half the optical power P_0 supplied by the laser reaches the target.
In the rediffusion process, only a fraction η of it is sent back into a single spatial mode for coherent superposition at the photodetector.
Letting w_1 for the spot size and being $\theta=\lambda/\pi w_1$ the diffraction angle, the power fraction collected back by the photodiode in a single mode is:
η = (solid angle of diffraction)/(Lambert's semispace solid angle), or
$\eta = \pi\theta^2/\pi=(\lambda/\pi w_1)^2$. With typical values for a He-Ne laser, P_0=1mW, λ=0.633 μm and w_1 =0.5 mm, we have:
$\eta=(0.633\mu m /3.14\cdot 0.5 \text{ mm})^2=1.6\ 10^{-7}$. The useful power is then:
$\eta P_0/2=(1mW /2)\cdot 1.6\ 10^{-7}\approx 0.8\ 10^{-10}$ W
From the diagram of Fig.4-18, we can find the minimum measurable amplitude of vibration as:
NED=0.06pm @ B=1MHz and P_{1W}=1W. As the dependence of NED is from $\sqrt{B}$ and $1/\sqrt{P}$, we shall multiply 0.06pm by $\sqrt{1M/10k}$, and divide it by $\sqrt{(0.8\ 10^{-10})}$ thus obtaining:
NED=0.06pm 10^{-2} 1.11 10^5 = 66 pm.

P4-32 *In the vibrometer of Probl.4-31, what would be the NED if we had used a self-mixing interferometer?*.

Answ.: In the self-mixing interferometer we would not have the reference beam, that is, all of the 1-mW power is used in the measurement arm. Therefore, the power impinging on the output mirror in the back travel from the target is: $\eta P_0=(1mW)\cdot 1.6\ 10^{-7}\approx 1.6\ 10^{-10}$ W
In addition, we have to pass through the mirror, and this yields an attenuation equal to t_1 (typ. 0.01 in a He-Ne laser).
We may be attempted, as in Probl.4-25, to take account of the gain factor $2\gamma_0 L$=0.02. But, this is only an extrinsic gain of the modulation signal, not a

true increase of optical power. Therefore, the incoming equivalent power is:
$\eta P_0 t_1 = 1.6 \cdot 10^{-10} 0.01 = 1.6 \cdot 10^{-12}$ W, and we end up with the result:
NED= 66 pm $\sqrt{(0.8 \cdot 10^{-10}/1.6 \cdot 10^{-12})}$ = 930 pm,
a value not so different from that of the external configuration of interferometry.

P4-33 *Suppose you remove the low-pass filter in the vibrometer of Fig.4-34 (and Probl.4-30). What happens of the output signal voltage ? How can we recover the interefrometric signal ? What is its dynamic range ?*

Answ.: By removing the low-pass filter we make the feedback loop effective at all frequencies, or, it is F=1 in the expressions of Probl.4-30 and:
$V_{out}/\Delta s_{meas} = k I_0 R/(1 + k I_0 R A\kappa)$
The output voltage is decreased, from its natural value kI_0R, by a factor equal to the loop gain $hG_0 = kI_0 RA\kappa \approx 1000$ in the example of Probl.4-30. So, we will not see anything (but a dc value) looking at the front-end output. This is because we are tracking the displacement Δs of the target with an equal displacement applied to the piezo. The voltage to the piezo now carries the signal Δs (plus the disturbance Δs_{amb}) and its value is:
$V_{piezo}/\Delta s_{meas} = k I_0 RA/(1 + k I_0 R A\kappa)$
$\approx 1/\kappa$ (=1000V per wavelength, in the example of Probl.4-30)
This value is the low-amplitude scale factor, and we may remark that it is accurate and stable as the piezo-transfer factor κ is.
In addition, if we go to amplitudes larger than the wavelength, $\Delta s > \lambda$, we do not develop the cos $2k\Delta s$ nonlinearity like in a plain interferometer. Indeed, as the signal decreases a little also the feedback from the piezo will decrease, cancelling the nonlinearity.
This result is well-known in feedback theory, and amounts to say that nonlinearity as well as the dynamic range are increased by a factor equal to the loop gain $hG_0 (= kI_0 RA\kappa \approx 1000$ in our example).
Thus, we can reach perhaps $1000\lambda \approx 630\mu$m of dynamic range in the linear regime for Δs, by this servo loop.
The only drawback is that we now shall filter out the Δs_{amb} disturbance *a-posteriori* from the total signal Δs instead of relying on the servo loop to do so as in the scheme of Fig.4-34.

P4-34 *The half-fringe servo loop is incorporated in a self-mixing interferometer operating at s=10 cm from a diffuser target. Calculate the necessary current swing that shall be impressed to the diode drive.*

Answ.: The phase $\Delta\phi$ produced by a $\Delta\lambda$ variation is:
$\Delta\phi=2s\ \Delta(2\pi/\lambda) = 2(2\pi/\lambda^2)s\Delta\lambda$
and, as a good design rule, we may require that the phase swing to be controlled is a full 2π angle, so that
$2\pi = 2(2\pi/\lambda^2)s\Delta\lambda$, and solving for $\Delta\lambda$ we get:
$\Delta\lambda = \lambda^2/2s$
Using λ =0.85μm and s=10 cm we get:
$\Delta\lambda=(0.85^2 /20\ 10^4) = 3.6\ 10^{-6}\ \mu$ m = 0.0036 nm.
The current swing required is found from the relation
$\Delta\lambda = \alpha_I \Delta I$, where α_I (p.387) is typically ≈0.004 nm/mA.
Now, by substituting the previous expressions we then get:
$\Delta I = \Delta\lambda/\alpha_I$=0.0036nm /0.004nm/mA=0.85mA, a quite reasonable value.
With the servo loop, also the self-mixing interferometer can operate as a large dynamic-range vibrometer. The factor hG_0 is now given (by inspection of Fig.4-36) by:
$hG_0 = kI_0 R\ A\ /R_c\ \alpha_I 2(2\pi/\lambda^2)s/2k = I_0(R/R_c)\ A\alpha_I(2\pi s/\lambda^2)$.
as $\alpha_I(2\pi s/\lambda^2)=(\Delta\lambda/\Delta I)(2\pi s/\lambda^2)= \pi/\Delta I$, we also get:
$hG_0 = (\pi I_0/\Delta I)\ (R/R_c)\ A$
Thus, if I_0≈1mA and R≈R_c, the loop gain is primarily given by the amplification A of the block following the front-end (and we can do A≈1000 for this block to duplicate the results of previous problems).
P4-35*Can the feedback loop based on the current control be implemented in a normal Fabry-Perot laser, without detrimental effects from mode-hopping ? What happens if a mode-hop occurs ?.*

Answ.: At a ΔI =0.85mA, and corresponding $\Delta\lambda$=0.0036nm, we are far from the mode hop spacing, which is about ≈0.2 nm, see Fig.A1-13.
At any rate, should a mode-hop occur, the working point settled by the loop control is momentarily lost and the output signal exhibits a spike, losing the correct waveform. But, after getting a new wavelength, the system reacts and converges into a new equilibrium point with the signal returning to the correct value.

Q4-36 *Is the 1/s dependence of the vibrometer scale-factor shown in Fig.4-37 also applicable to a normal (non servo loop) vibromter ? Clarify the point.*

Answ.: The scale factor $\Delta I_{ph}/\Delta s=1/\alpha_{I\ is}$ applicable to the servo-loop vibrometer, either in the external or self-mix configuration. In addition, the 1/s-dependence is that of the *field*-attenuation, in contrast to the $1/s^2$ dependence of the intensity or power-attenuation, for a signal propagated to a distance s and back.
Irrespective from the 1/s or $1/s^2$ dependence, when we go in the fringe-count mode (as in Fig.4-39 and 4-40) it does not matter any more if the signal is eventually decreasing with 1/s or $1/s^2$, because we look at the periods contained in the signal, and therefore the scale factor is *independent* from distance.
This apparent oddity can be easily justified by the following statements:
- in the servo-loop vibrometer we perform an *amplitude* measurement, whereas
- with the fringe counting vibrometer we perform a *phase* measurement.

P4-37 *How can you tell the amplitude of the square-wave driving signal exciting the MEMS in Fig.4-39 and 4-40 from the waveform of the interferometric signal (Fig.4-40) ?*

Answ.: In the cos $2kA_0\cos\omega_0 t$ of Fig.4-40 we can start counting fringes from the rise front (at about 45 on the x-axis) and stop at the fall front (at bout 85). So, we can count $N_{per}=5^1/_2$ (± 0.1) periods, and therefore (assuming $\lambda=0.85\ \mu m$)
$A_0= N_{per}(\lambda/2) = 5.5(\pm 0.1)\ 0.425 = 2.337\ (\pm 0.042)\ \mu m.$
Of course, if we are aiming at our target from an oblique direction, at an angle θ respect to the perpendicular to the target surface, then it would be
$A_0= N_{per}(\lambda/2 \cos\theta).$

P4-38 *An absolute distance self-mixing interferometer is aimed at a target at s=1m. Consider a current sweep of ΔI=0.85mA as in P4-34 and of 10 times as much. How large is the yardstick s_{yst} of the measurement ? How many periods N_{count} are developed aiming at s=1m ?*

Answ.: As with $\Delta I=\Delta\lambda/\alpha_I$ =0.0036nm /0.004nm/mA=0.85mA we were planning to get a 2π phase in s=10cm, thus, even with no calculation we can write that:
$s_{yst} = \lambda^2/2\Delta\lambda = 10cm,$ and therefore $N_{count}= s/s_{yst}= 10$

This working condition requires a small current swing, ΔI=0.85mA. Going to ten times as much, at ΔI=8.5mA, we would get:
$s_{yst} = \lambda^2/2\Delta\lambda$ = 1 cm, and therefore N_{count}= s/s_{yst}= 100.
In a single measurement, the resolution is s_{yst} = 1 cm, and the error is $\sigma = s_{yst}/\sqrt{12}$ =2.88 mm.

P4-39 *How can the resolution and the error of the absolute distance self-mixing interferometer be improved ?*
Answ.: At first sight, we may think that increasing the current-dependence of wavelength, the coefficient α_I , is the best to do. Actually, we can improve resolution and error also by:
- increasing the number of measurements, so to scale errors by $\sqrt{N}$,
- increasing the current swing ΔI.
The current swing is limited by mode hopping (in Fabry-Perot lasers) and by single- to multi-mode transition (VCSELs). Increasing coefficient α_I may result in a two-pole response, one fast due to carrier index-of-refraction dependence, the other slow because due to thermal effects. Increasing ΔI too much also introduces a non-linearity of the scale factor, in the sense that $s_{yst}=\lambda^2/2\Delta\lambda$ then changes with I [as it is $\lambda=\lambda(I)$].

P4-40 *In the angle-measurement scheme of Fig.4-48, how can we change (for example, increase) the dynamic range of the measurement?*
Answ.: We can use a collimating telescope to increase/decrease the spot size w_0 and the divergence $\theta=\lambda/\pi w_0$ accordingly, and recall that the dynamic range of angle measurement is $\approx$1-2 θ whereas the resolution in a (nearly constant) fraction of the resolution.

P4-41*Calculate the maximum value of measurable attenuation a when the weak-echo injection-detector is used (Sect.4.7.3).*

Answ.: We may take the S/N=1 condition to settle the maximum value a_{max} of attenuation.
The signal is given (see Eq.4.39) by:
$S = I_0 \kappa a_{max}$
and the noise is given by the shot-noise associated with the detected current I_0, that is
$N = (2e I_0 B)^{1/2}$
Therefore we get, for S=N:
$I_0 \kappa a_{max} = (2e I_0 B)^{1/2}$ or

$a_{max} = (2eB/I_0)^{1/2}/\kappa$
Using I_0= 1 mA and B= 100 Hz we get:
$a_{max} = (3.2\ 10^{-19}\ 10^2/10^{-3})/\kappa = 1.8/\kappa\ 10^{-10}$
Now, depending on the factor κ=s/nL, and assuming nL=3.5×200 μm=0.7 mm, we may have these representative values:
for and s=1.8×70=126 mm: κ=180 and $a_{max}=10^{-8}$;
for s=1.8×700=1260 mm: κ=1800 and $a_{max}=10^{-7}$

Problems and Questions, Chapter 5

P5-1 *Calculate the transversal and longitudinal sizes of the speckle field generated at distance of 50-cm, 2-m and 10-m by a white diffuser with spot size D=5 mm, using a laser wavelength λ=633 nm. How the longitudinal size changes if, at 2-m distance, we move transversally of 2 meter?*

Answ.: We use Eqs.5.1 and, for the speckle at z=50 cm, on axis, we find:
$s_t = \lambda z/D = 0.633 \times 10^{-3}\ 500/5 = 0.063$ mm
$s_l = \lambda(2z/D)^2 = 0.063\text{mm} \times 2\ 500/5 = 12.7$ mm
If the laser is powerful enough to render the speckles visible (or, we use an image intensifier), we would barely see them as very dots in the laser spot, whereas transversally the speckles are already long enough to be resolved.
At z=2 m the sizes become increased to:
s_t@2-m = 0.063 mm × (2/0.5) = 0.25 mm
s_l @2-m = 12.7 mm × $(2/0.5)^2$ = 203.6 mm
and at z=10 we get:
s_t@10-m = 0.063 mm × (10/0.5) = 1.26 mm
s_l @10-m = 12.7 mm × $(10/0.5)^2$ = 5.08 m
here, as is comparable to z, we are approaching the so called 'last speckle'.
About the off-axis observation at z=2m, with a Δ=2m, we get θ= atan Δ/z = 45° and therefore the longitudinal speckle size are:
s_l@2-m,θ=45° = s_l /cos θ= 203.6 mm/0.707 = 288 mm.

P5-2 *Calculate the distance Z of the 'last speckle' with the data of Probl.5-1. Comment on the relationship of Z to the Fresnel distance.*

Answ. We let s_l=z in the expression of the longitudinal size $s_l = \lambda(2z/D)^2$ and solve for z, obtaining: $Z = D^2/4\lambda = 5^2/4\ 0.633 \times 10^{-3} = 9.87$ m
In classical optics, the quantity $Z=D^2/4\lambda$ is known as the Fresnel distance, separating the Fraunhofer (or far-field) region of diffraction from the

Fresnel near field region. In connection with the speckle property, the last speckle indicates that, from z=Z onward, the result of diffraction from the aperture D doesn't change any more or, the speckle is single. .

P5-3 *Calculate the subjective transversal size of the speckle seen by the eye (D_{eye}=4 mm) when looking at a laser spot of diameter D= of 2 mm projected on a white screen at a distance z=1m (assume λ=633 nm).*

Answ. The transversal size on the speckle on the eye is $s_t = \lambda z/D$ and there are $N^2=(D_{eye}/s_t)^2$ of them in the eye collecting surface. On the focal plane of the eye (the retina), the image has a size (diameter) DF_{eye}/z and dividing by N we get the speckle size on the retina as $(DF_{eye}/z)/(D_{eye}/s_t)=$
$=\lambda F_{eye}/D_{eye}= s_{t\,(retina)}$, the same as if the eye were the new source of speckle.
Projecting back to the object plane, we magnify these speckle (see also Fig.5-3) by a factor z/F_{eye}, thus obtaining $s_{t\,(sub)}=\lambda\ z/\ D_{eye}$ as the subjective speckle dimensions. Inserting the numbers we get:
$s_t = \lambda z/D = 0.633 \times 10^{-3}\ 1000/2 = 0.316$ mm
$s_{t\,(retina)}=\lambda F_{eye}/D_{eye} = 0.633 \times 10^{-3}\ 14/4 = 1.4\mu$m (having taken F_{eye}=14 mm)
$s_{t\,(sub)}=\lambda\ z/D_{eye} = 0.633 \times 10^{-3}\ 1000/4 = 0.158$ mm
This figure tells us that the speckle will be well visible, as a random dotting on the average brilliance of the laser spot projected on the diffuser screen.

P5-4 *How many speckles are contained in the spot imaged back on the photodetector of a triangulation telemeter? What about their effect on the accuracy of the measurement ?*

Answ.: To simplify, let us assume that the collimating telescope projects a diffraction-limited spot size $w_{tar} =\sqrt{(\lambda L/\pi)}$ on the target at distance L.
The objective lens in front of the photodetector demagnifies the target spot size by a factor F_{rec}/L (F_{rec}=focal length, D_{rec}=diameter). The result is a spot of size $w_{fp}=w_{tar}\ F_{rec}/L= F_{rec}\sqrt{(\lambda/L\pi)}$ on the detector plane [this result is correct provided $w_{fp} >> \lambda F_{rec}/D_{rec}$, the diffraction limit of the objective].
On the focal plane, the subjective speckle has a transversal size
$s_{f(fp)}=\lambda\ F_{rec}/D_{rec}$.
Thus, the number of speckles inside the received spot is:
$N= [w_{fp}/s_{f(fp)}]^2= [F_{rec}\sqrt{(\lambda\ /L\pi)/\lambda F_{rec}/D_{rec}}]^2= D_{rec}^2/(\lambda L\pi)$
With L=3 m, λ=0.633μm, D_{rec}=10mm, we get:
$N= 100\ /[0.633 \cdot 10^{-3}\ 3000\ 3.14]= 16.7$.
As the number of speckles is small, the effect on the accuracy of the measurement should be considered. As the speckle intensity is a negative-

exponential distribution, the collection of the speckle-spots has a median shifted of a random amount respect to the spot centre w_{fp}. The error decreases with $\sqrt{N}$, and is of the order of $w_{fp}/\sqrt{N}$.
As L decreases, or the spot size on the target increase, the error becomes negligible.

P5-5 *How frequent are the bright speckles in the speckle field? Calculate the probability of finding the intensity 2.5 times the average. Are dark speckles less frequent that bright ones ?*

Answ.: Using Eq.5.8, the probability of having $I \geq 2.5\langle I\rangle$ is found as:
$P\{I \geq 2.5\langle I\rangle\} = \exp -I/\langle I\rangle \big|_{5\langle I\rangle} = e^{-2.5} = 0.082$.
We get as much as 8.2% chance of having a speckle brighter than the average.
On the other end, we may assess quantitatively a dark speckle as one with ≤25% average intensity. In this case the probability is:
$P\{I \leq 0.25\langle I\rangle\} = 1 - \exp -I/\langle I\rangle \big|_{0.25\langle I\rangle} = 1 - e^{-0.25} = 0.22$
and we can say that oddly, or, at least on the subjective judgement of the eye observing the speckle distribution, dark speckles are more probable (22%) than bright ones (8.2%).

QP5-6 *Doesn't the bright speckle violate the principle of invariance of the brilliance in those points where a bright speckle is found ?*

Answ.: No, because the principle is applicable to the *total* value of radiant power P or to the *average* value of power density I.
If we want to connect power density of the field to the black-body temperature of a collector, then we write $\sigma T^4 = I$ or $T = (I/\sigma)^{1/4}$. A speckle brighter than average then means a higher than average (absolute) temperature. This sounds awkward and dangerous, but actually is no wonder: a thermal reservoir at average absolute temperature T will anyway have a fluctuation, and the speckle-related temperature fluctuation is just a manifestation of this circumstance.

P5-7 *Consider a point, in a bright speckle, having 2.5 times the average intensity. What is the average intensity of a nearby point, correlated to the starting one with m=0.8 ? What is the phase variance ?*

Answ.: Using the diagrams of Fig.5-7 and 5-8 (or, Eqs.5.27) we find:
$I_2 \big|_{I1} = 1.96\ (2\sigma^2)$ and $\sigma^2_2 \big|_{I1} = [0.13 + 1.28\ 0.36\ 1.96](2\sigma^2) = 1.03(2\sigma^2)$

The point close (or internal) to an intense-speckle has a relatively smaller variance than the normal field, $\sigma^2_{2}\,|_{I1}/[I_{2}\,|_{I1}]^2=0.268$ in place of the normal (=1) value.
In addition, from the diagram of Fig.5-9 (or from Eq.5.29) we get for I_1 =2.5 and I_2=1.96, the phase variance as:
$\sigma^2\phi\,|_{I1,I2}=(\pi^2/3)\ 0.05$,
a value substantially less than the unconditioned (=1) value and of the 'free' value (=0.32 from Fig.5-9).

P5-8 *Consider a point, in a dark speckle, having 0.2 times the average intensity. What is the average intensity of a nearby point, correlated to the starting one with m=0.8 ? How about the phase variance ?*

Answ.: Using the diagrams of Fig.5-7 and 5-8 (or, Eqs.5.27) we find:
$I_2\,|_{I1}=0.368\ (2\sigma^2)$ and $\sigma^2_{2}\,|_{I1}=[0.13+1.28\ 0.36\ 0.368](2\sigma^2)=0.30(2\sigma^2)$
This time, the weak-speckle has a variance a little bit larger than the normal field, $\sigma^2_{2}\,|_{I1}/[I_{2}\,|_{I1}]^2=2.21$ in place of the normal (=1) value.
In addition, from the diagram of Fig.5-9 (or from Eq.5.29) we get for I_1 =0.2 and I_2=0.368, the phase variance as:
$\sigma^2\phi\,|_{I1,I2}=(\pi^2/3)\ 0.45$,
a value less than the unconditioned (=1) value, but larger than the 'free' value (=0.32 from Fig.5-9).

P5-9 *An interferometer works on a diffuse target to make a measurement of displacement. Let the spot size be, like in Probl.P5-1 D=5 mm, and assume a distance of 50-cm, and a wavelength λ=633 nm. Calculate the amount of: (i) longitudinal displacement, (ii) transversal displacement; (iii) spot shift on the target; (iv) detector aperture that are allowed for a 1-λ (or 2π) phase error each.*

Answ.: With the data, from Probl.P5-1 we get s_t =0.063 mm and s_l=12.7 mm, and from Eq.5.35, the allowed displacement is Δ=0.063mm and 12.7 mm in the cases (i) and (ii).
From Sect.5.1.7, we get Δ=0.063mm also for case (iii).
Last, using Eq.5.58 and following lines, we get: $\lambda=\Delta z(D_{det}/4)^2/z^2$ whence, assuming $\Delta z=z/2$, we can solve for $D_{det}=2z\sqrt{\lambda}/\Delta z=1000\ \sqrt{0.633\ 10^{-3}}\ /250=1.59$ mm.

P5-10 *In an interferometer, amplitude fading due to speckle statistics is mitigated by operation in space diversity. We use two photodetectors,*

placed apart of a speckle size, so to have uncorrelated amplitudes. What is the probability of fading (and incorrect operation) in this case ?

Answ.: The probability of having a signal intensity less than $\eta\langle I\rangle$ is:
$P\{I \le \eta \langle I\rangle\} = 1\text{-}\exp\text{-}I/\langle I\rangle \big|_{\eta\langle I\rangle} = 1-e^{-\eta} \approx \eta$ (for small η).
We may recover the amplitude $I=\eta\langle I\rangle$, for example by means of an automatic gain control, and bring it to a level adequate for processing.
If one detector has a signal $I<\eta\langle I\rangle$ too low, we switch on the second detector. Then, the probability of not working is that of having two independent intensities smaller than $\eta\langle I\rangle$, or:
$P\{I_1 \le \eta \langle I\rangle,\ I_2 \le \eta \langle I\rangle\} = \{1\text{-}\exp\text{-}I/\langle I\rangle \big|_{\eta\langle I\rangle}\}^2 = (1-e^{-\eta})^2 \approx \eta^2$ (for small η).
Therefore, if we recover with an AGC amplitudes down to 10^{-2}, the probability of not working becomes 10^{-4}, a value very small but not zero.

P5-11 *We are using the extension of Fig.4-16 for the operation of the interferometer on a diffuser. The focussing lens receives a collimated beam of waist w_0 and has a focal F and diameter D. What is the transversal dimension of the speckle exiting from the lens?*

Answ.: If the lens receives a beam of size (radius) w_0, it focuses it in a spot, on the focal plane, given by:
$w_{fp} = \lambda /\pi NA = \lambda F/\pi w_0$
where NA is the numerical aperture presented by the lens, as seen at a distance F by the beam radius w_0.
As w_{fp} is the radius of the spot re-radiating the field at the diffuser, we can calculate the transversal speckle size at the distance z=F as:
$s_t = \lambda F/2w_{fp} = \lambda F /2(\lambda F/\pi w_0) = (\pi/2)\, w_0$
Apart from the $\approx$1 multiplying factor, we can see that the transversal speckle size is equal to the (single-mode) impinging beam size.
The same conclusion holds if we use a collimating telescope to cast the beam from the laser output facet onto the remote target. If the target is conjugated to the beam waist w_0, then the transversal speckle size returning from the diffuser is equal to w_0, irrespective of magnification.

P5-12 *I don't like the approximation to 1 of the multiplying factor in Probl.5-11. How can you reconcile the results outlined in Probl.5-11 without the need to introduce this approximation?*

Answ.: The focussed spot of size $w_{fp}=\lambda F/\pi w_0$ implies that the beam is a Gaussian mode distribution, such that the divergence is $\theta=\lambda/\pi w_0$, then giving the spot size w_{fp} at the distance F (or, $w_{fp}=\theta F$). If we consider, as in

the derivation of the speckle pattern sizes, a rectangular-distributed intensity for the source, the divergence is $\theta=\lambda/D= \theta=\lambda/2w_0$ and thus $w_{fp}= \lambda F/2w_0$. The transversal speckle size is therefore:
$s_t= \lambda F/2w_{fp}= \lambda F /2(\lambda F/2w_0)= w_0$
Conversely, if we assume working with Gaussian beams, we get $\theta=\lambda/\pi w_0$ and $w_{fp}=\lambda F/\pi w_0$ as already noted, but the speckle transversal size is no more $s_t= \lambda F/2w_{fp}$. We shall repeat the calculation of the size (as carried out on pages 189-191) for a Gaussian source. Doing so, we obtain the result:
$s_t= \lambda F/\pi w_{fp}$
and consequently we get, once again:
$s_t= \lambda F/\pi w_{fp}= \lambda F /\pi(\lambda F/\pi w_0)= w_0$

P5-13 *How can we ensure that, on the distance swing Δ_{max} to be covered by an interferometer operating on a diffuse-surface target, the speckle phase error is minimized ? Specialise to the case $\Delta_{max}=1m$ and calculate the attenuation of the returning signal.*

Answ.: To minimize the speckle-phase error, we need to keep the largest possible speckle size, or the minimum spot size on the target throughout the distance swing.
Using the external configuration, we collimate the laser beam on the full dynamic range $z=2\Delta_{max}$, and get a spot size as (see Eq.2.4):
$w=\sqrt{(\lambda\Delta_{max})}$
The longitudinal speckle size then follows as:
$s_l=\lambda(2\Delta_{max}/w)^2$
and, inserting w in it, turns out to be $s_l=4\Delta_{max}$.
In this way, we stay inside a single speckle on the full dynamic range. The phase error is then $\sigma_\phi \leq 2\pi$ throughout the measurement range.
The signal of this last speckle is very weak, however.
Indeed, if P_L is the laser power, half of it is sent in the reference path, and the intensity at the target is $P_L/2\pi$. Thus, the power collected by the receiver is $(P/2\pi)\pi(w/\Delta_{max})^2$.
The attenuation respect to the power leaving the laser is accordingly:
$(w/\Delta_{max})^2=\lambda/\Delta_{max}$.
Using $\lambda=1\mu m$ and $\Delta_{max}=1m$, we get
$(w/\Delta_{max})^2= 1\mu m / 1m = 10^{-6}$ (or, we get a –60 dB loss).

P5-14 *Try to mitigate the attenuation effects found in Probl.5-13 while keeping the error at no more than a few λ's on the entire measurement range $\Delta_{max}=1m$.*

Answ.: Assuming a not-so-small diameter of the objective lens, let's say D_L =30mm, then the loss is
$\pi D_L^2/4/\Delta_{max}^2 = 3.14 \cdot 900/4\ 10^{-6}\mu m = 0.7\ 10^{-3}$ (or, it's a –35 dB loss).
However, we are faced with a small longitudinal speckle size, which is evaluated as:
$s_l = \lambda(2\Delta_{max}/D_L)^2 = 4mm$.
In a 1-m=Δ_{max} dynamic range, this means we will find 250 speckle passages (each with a $\approx 2\pi$ or λ error).

P5-14 *In the bright-speckle tracking techniques, we not only oppose amplitude fading, but also have a better phase statistics. Is there a simple physical reason why a bright speckle should have a smaller phase error whereas a dark one have a larger one ?*

Answ.: From the statistical point of view, the diagrams of Fig.5-8 and 5-9 tell us that large intensity is correlated to small phase variance.
In addition, we may think of the total speckle field as the result of a random-walk addition, in which several small vectors are added with random phases (as depicted in Fig.5-2).

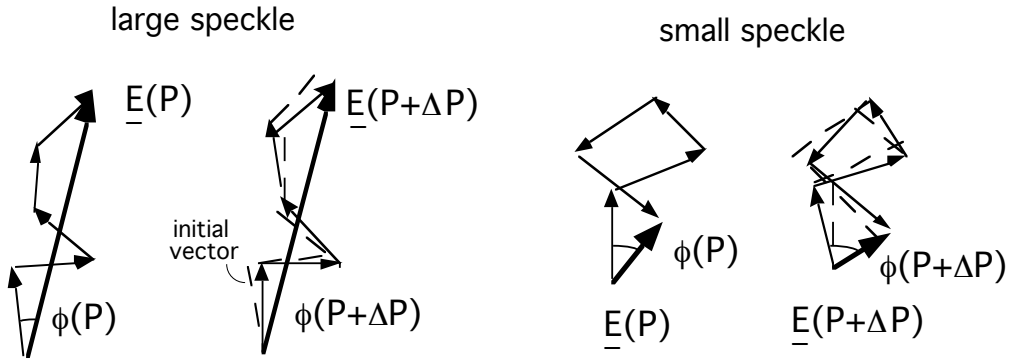

figure 5-1

We can represent the addition as in figure 5-1, where the same small phase variation is impressed to the individual vectors (with alternate sign), from point P to point P+ΔP.
Then, we can see that, on a large speckle with the nearly aligned vector-sum, the phase variations has little effect on the new result, and therefore passing from P to P+ΔP the phase ϕ does change, but not so much.
On the other hand, on a small speckle with the nearly zero net vector sum, the phase variations has a large effect on the new result, and therefore phase ϕ appreciably changes passing from P to P+ΔP.

Problems and Questions, Chapter 6

P6-1*To design the electronic part of a LDV, we start assuming a superposition angle θ ranging from 5 to 30 degrees, a wavelength λ ranging from 0.35 to 0.70 μm. , and want to evaluate To make a speed measurement covering the range 1 μm/s to 200m/s, which frequency range has to be secured ?*

Answ.: Using the basic formula,
$f = v / 2\lambda \sin\theta$
we get $2\lambda \sin\theta$ = (0.7-1.4)μm (0.1-0.5)= (0.07-0.7)μm
and therefore
f = (1μm/s-200m/s) /(0.07-0.7)μm = 14 Hz- 280 MHz
This range is not so difficult to achieve in a frequency meter following front-end detection and signal validation.

P6-2 *Consider an LDV that shall probe a fluid at a 200-mm depth, with a θ= 14° superposition angle. What is the size of the sampling region? What is the number of fringes and the accuracy ?*

Answ.: From the angle of superposition, we get
$\tan\theta = 0.25 = R_{os}/F$.
As F=200 mm, we get R_{os} = 50mm, calling for a lens with a diameter D_{lens} = $2R_{os}$= 100mm (and with a reasonable F-number F/ =0.5).
With a laser spot size w_L= 1mm on the focusing lens, we obtain a number of fringes (Eq.6.4): 50/1 =
$N_F=(2/\pi)\, R_{os}/\, w_L = 0.636$ 50/1 =31.8
The accuracy of the single velocity measurement then follows (Eq.6.3) as:
$\sigma_v/v = \sigma_f/f_D = (2\pi\, N_f)^{-1} = 1/200 = 0.5\%$.
At the He-Ne wavelength λ=0.633μm, the fringe spacing is evaluated as D= 0.633μm/2(sin14°)= 1.30μm,
and the scale factor of the measurement is:
R= 2sinθ/λ= 0.766 Hz/(μm/s) [or, 0.766 kHz/(mm/s) or MHz/(m/s)].
The focused spot size is w_f = (0.633μm) 200/π·1= 40μm. The sizes of the sensing region are, from Eqs.6.5 and 6.6:
$w_m = w_f$ /0.97= 41μm, and $w_l = w_f$/0.24 = 166 μm.

As we can see, these central design values provide a good intrinsic accuracy and a small sampling volume. The sampling volume is located 200-mm away, in front of the objective lens of the instrument.

P6-3 *Repeat the calculation of Probl.6-2 using a larger distance to the sampling spot, say 500 mm.*

Answ.: To sense the fluid farther away, we may use a larger focal length, for example F=500mm.
With this value, the angle of superposition is tan $\theta = 0.1$, or $\theta = 5.7°$.
Again using a beam size w_L=1mm on the lens, the number of fringes N_F is unchanged, because it only depends on R_{os} and w_L (not from F), as well as the accuracy $\sigma_v/v = 1/2\pi N_F$.
Fringe spacing and scale factor are increased (by the $\tan^{-1}$ ratio) to: D=3.16μm, and $R = 0.316$ Hz/(μm/s).
The focused spot size changes to:
$w_f = (0.633\mu m)\ 500/\pi 1 = 100\mu m$,
and the sizes of the sensing region becomes
$w_m = w_f /0.995 = 101\mu m$, and $w_l = w_f/0.1 = 1000\ \mu m$.
Should this large value of the longitudinal size w_l be inconvenient, we can always trim it by the a-posteriori validation of fringe (see Sect.6.3.1).

P6-4 *With the LDV data of Probl.6-2, calculate the amplitude of the signal supplied by the photo-detector. Assume the detector is forward-looking at the sampling region, seeded by 0.25 μm particles, and the solid angle of collection by he detector objective be Ω=0.1 sr.*

Answ.: We take the result (Eq.6.7) of the power budget calculation:
$I_{ph} = \sigma\ (P_L/w_l^2)\ Q_{ext} \pi r^2 4\pi f(\theta_{meas})\ \Omega$
and substitute in it: σ=spectral sensitivity=0.7 A/W, Q_{ext}=extinction factor =0.3, f(0)=scattering function =0.1sr, $\Omega = \pi\ D_{obj}^2/4F_{obj}^2 = 0.1$, P_L=20 mW, getting as a result:
$I_{ph} = \sigma\ (P_L/w_l^2)\ Q_{ext} \pi r^2 4\pi f(\theta_{meas})\ \Omega$
$= 0.7\ (20m/1mm^2)\ 3.14\ 0.25^2 \mu m^2 \cdot 12.560.1 \cdot 0.1 = 0.34$ nA
This is a small but still reasonable value to carry out a low-noise measurement of the frequency contained in it.

P6-5 *Our laboratory has a 10.000 class-level of air cleanness. Calculate how many particles are found in the sampling volume of the LDV of Probl.6-2.*

Answ.: The sampling volume is given by (page 238)
$V = w_I^3/\tan\theta = 0.166^3\ mm^3\ /0.25 = 18.3\ 10^{-3}\ mm^3$
The class-level number expresses the concentration of (≥1μm) particles per cubic foot, so the concentration per mm^3 is:
$C_V = 10.000/(308)^3 = 0.34 \cdot 10^{-3}\ mm^{-3}$
and the average number of particle per sampling volume follows as:
$N = C_V\ V = 0.34 \cdot 10^{-3}\ mm^{-3}\ 18.3\ 10^{-3}\ mm^3 = 6.26\ 10^{-6}$
Thus, we need to increase the sampling volume, or only rarely will a particle be measured. This implies a long measurement time [unless we funnel the particles in a forced flux, thus amplifying the concentration].

P6-6 *Changing the parameters of the LDV in Prob.6-5 appropriately, estimate which class of cleanness can be measured by the Doppler technique .*

Answ. We can assume an expanded w_L=5-mm laser beam, and split it and superpose with prisms, so as to keep $w_I \approx w_L$. With a reasonable θ=0.1 we get as s superposition volume:
$V = w_I^3/\tan\theta = 5^3\ mm^3\ /0.1 = 1250\ mm^3$
Additionally, instead operating the LDV in free air, we funnel it with a 20:1 ratio of input to output diameters. Thus we obtain a concentration factor C_F = 400. The average number of particle per sampling volume now follows as:
$N = C_V\ C_F\ V = 0.34 \cdot 10^{-3}\ mm^{-3} \cdot 400 \cdot 1250\ mm^3 = 170$
Setting at 1 particle the lower limit of the measurement, we get the class 1000/170= 59 (i.e. better than 100 but not yet 10 or 1).

P6-7 *In the fiberoptics LDV of Fig.6-15 (bottom), isn't the fiber detrimental to the beam wavefront quality needed in the superposition region ?*

Answ.: We need a mono-mode fiber for adduction of the beam, of course, whereas the returning fiber may be multi-mode as well, because it shall just carry the collected power, originating from the particle scattering - thus posing no phase requirements.

Problems and Questions, Chapter 7

P7-1 *When read as a phase difference, the signal out from an electro-optical gyro is proportional to the area or R^2 (Eq.7.5), whereas when read as a frequency difference it is proportional to the radius R (Eq.7.6). Isn't it a contradiction?*

Answ.: No, it isn't, as we can see starting from Eq.7.6, here written for convenience:
$\Delta f_s = 2\Omega R/\lambda$
We note that frequency f is related to wavenumber k as f=k/c, hence:
$\Delta f_s = \Delta k_s/c$
In addition, the phase difference is given by the product of wavenumber difference times the perimeter $2\pi R$ of the gyro, or:
$\Delta\Phi_s = \Delta k_s\, 2\pi R$
and, inserting the expression written above for Δk_s we get:
$\Delta\Phi_s = c\Delta f_s 2\pi R = c\ 2\Omega R/\lambda\ 2\pi R$
From here we can see that Δf_s and Δk_s are proportional to the radius R (or, to the linear size of the gyroscope), whereas $\Delta\Phi_s$ is proportional to πR^2 (or, to the area of the gyroscope) because of the multiplication of Δk_s by $2\pi R$.
Thus, for a very large area (or radius) it may be better to read the gyro as an external interferometer (with output $\Delta\Phi_S$) whereas a (relatively) small area device will be best read as an internal interferometer (with output Δf_S). This is a possible explanation of why the FOG is an external interferometer and the RLG is an internal interferometer.

Q7-2 *Why no basic limitations other than the quantum noise are considered to influence the gyro performance, like we have done for interferometers in Sect.4.4 ?*

Answ.: In principle, all the factors considered in Sect.4.4 shall be scrutinized, of course. But, for a normal, central design gyroscope, either the FOG or the RLG type, the effects other than quantum noise are negligible.
In fact, we don't have to care about temporal coherence, because the Sagnac or ring interferometer is balanced (App.A2.1), nor about spatial coherence, as we work either in a laser cavity supporting one mode, or in a mono-mode fiber.

Dispersion of the medium and propagation effects are negligible errors in a RLG, whereas they will be actually considered as a source of GDV, PMD and XPM (Sect.7.5.2.8) in the FOG.
Thermodynamic phase noise, and Brownian motion effects could be of importance, but only if we go to unusually small size for our device. Last, speckle errors are absent as we don't deal with diffuser in the gyro.

P7-3 *Calculate the maximum and minimum angular velocity that can be measured at the limit of discretization with a He-Ne RLG gyroscope having a radius (or apothem) R=6.33 cm. Find the associated dynamic range of measurement.*

Answ. At a radius R, the Sagnac frequency we get is:
$\Delta f_S = 2\Omega R/\lambda$
and the responsivity $R_F=\Delta f_S/\Omega$ is, inserting numbers:
$R_F= 2R/\lambda = 2 \cdot 63.3/ 0.633 \cdot 10^{-3}= 200$ kHz/(rad/sec).
A very slow rotation, say Ω_0=1 deg/h (= 4.7 μrad/s) is translated in a frequency difference $\Delta f_s = R_F\Omega_0 = 200$ kHz 4.7 μrad = 0.96 Hz.
Considering the 1-count criterion as the lower limit of measurement set by discretization, and taking T_{max} =15 minutes as the longest practical observation time, we get a minimum readable angular velocity as
$\Omega_{min}= \Omega_0/\Delta f_s\, T_{max}$=1 deg/h /(0.96 · 15 · 60)= 0.00116 deg/h.
On the other side, the maximum frequency that can be measured without entering ambiguity problems is determined by the mode spacing
$\Delta f_{smax} = c/2\pi R = 3 \cdot 10^8/6.28 \cdot 63.3\, 10^{-3}= 754$ MHz.
At this frequency, there corresponds an angular velocity
$\Omega_{max}= \Delta f_{smax}/ R_F= 754$ M/ 0.2 M =1500 rad/sec.
As we cab see, the maximum angular velocity is a very large one, hardly found in a mobile vehicle because it would require unusually large accelerations. The ratio of maximum to minimum, that is the dynamic range DR is a huge number indeed, perhaps seldom attained but revealing the potentiality of the gyroscope:
DR = $\Omega_{max}/\Omega_{min}$ = 1500 rad/sec/0.00116 deg/h
$= 1.3 \cdot 10^6/4.7 \cdot 10^{-6}= 2.76 \cdot 10^{10}$

P7-4 *Repeat the calculation of the minimum detectable angular velocity (Probl.P7-3) considering now the noise limits. Assume an output power P=1-mW from the laser, and a mirror reflectivity r_i=0.995.*

Answ. We calculate the equivalent power as $P/(1-r_1)^2\ [1+\alpha_{en}^2]$ (Eq.7.10). Being in addition $\alpha_{en} \approx 0$ in He-Ne lasers, we get:
P_{eq} = 1mW/0.095^2= 100 mW.
The RLG area is $\pi R^2 = 3.14 \cdot 63.3^2 \cdot 10^{-6} = 1.26 \cdot 10^{-2}\ m^2$
Then, using the diagram of Fig.7-6, and entering with a B=100 Hz band-width, we get:
$\phi_n = 10^{-8}$ rad
Translating the phase ϕ_n into a frequency signal Δf_n through the conversion factor $c/p = c/2\pi R$ = 754 MHz (as in Probl.7-3), we get:
$\Delta f_n = (c/p)\ \phi_n/2\pi$ = 754 MHz 10^{-8}rad /6.28 = 1.2 Hz
As we can see, we have obtained a result about the same lower limit of measurable signal calculated in Probl.7-3. In addition, we have:
$NE\Omega = \Delta f_n / R_F$=1.2 Hz/ 200 kHz/(rad/sec)
= 6 μrad/s = 1.27 deg/h (B=100 Hz)
Now, if we go to the minimum reasonable bandwidth of integration, $B_{min}=1/2\pi T$ where T (=15 min) is the integration time of Probl.7-3, we get:
B_{min}=1/ 6.28 · 15 · 60 = 0.00018 Hz
and , corresponding to this bandwidth:
$NE\Omega_{@Bmin} = NE\Omega\ [B_{min} / B]^{1/2}$
= 1.27 deg/h $[0.00018/100]^{1/2}$= 0.0017 deg/h.
Here, we can appreciate the performance currently achieved by real-world RLG gyroscopes, by underlining that they actually approach the quantum noise-limit.

P7-5 *The He-Ne RLG gyroscope considered above is rigidly mounted (or, strapped-down) on a mobile vehicle. We get n=5 counts (or periods) of the difference frequency, in a certain unspecified time interval. What can be say about the rotation undergone by the vehicle ?*

Answ. By integrating the frequency difference $\Delta f_S = 2\Omega R/\lambda$ we get:
$n = \int \Delta f_S\ dt = \int 2\Omega R/\lambda\ dt = 2R/\lambda\ \Psi$
where Ψ is the (inertial) rotation angle (see also Eq.7.13). This quantity can be solved for with the result:
$\Psi = n/[2R/\lambda] = n/R_F$
Letting numbers in it, we obtain the rotation angle as:

Ψ =5 / 2·10^5= 2.5 μrad = 0.53 arc-sec.
Note that we don't need to know the time interval in which the counts are developed, but just their total final number. Note also that the integration of

frequency by a counter does not suffer from low-frequency errors or dc cut-offs, a very nice feature of the measurement.

P7-6 *In a He-Ne RLG there is a residual diffusion $\delta=10^{-4}$ at one of the mirrors. Does it produce locking ? What is the frequency band of signal washout ?*

Answ.: We always get locking, no matter how small the coupling coefficient is. The coupling due to diffusion is given by Eq.7.16, that is:
$a_c = (\lambda/\pi w_0)\sqrt{\delta}$
With w_0= 0.5 mm and $\lambda=0.633 \cdot 10^{-3}$ mm, we get:
$a_c = (0.633 \cdot 10^{-3}/3.14 \cdot 0.5)\sqrt{10^{-4}}=0.4 \cdot 10^{-5}$
Using the condition K<1 in Eq.7.15, we get the minimum frequency separation Δf_0 that prevents locking as:
$\Delta f_0 < a_c(c/p)= (c/p)(\lambda/\pi w_0)\sqrt{\delta}$.
Hence, we get the value:
Δf_0=754 MHz $0.4 \cdot 10^{-5}$=30.4 Hz, or, translated in equivalent angular velocity of locking, we get:
$\Omega_0 = \Delta f_0/R_F$= 30.4 Hz /[200 kHz/(r/s)] = 0.15 mr/s = 32 deg/h.
Note that we have used a very good figure, representative of low-scatter mirror, yet the locking range entails a very poor sensor performance, if not tackled appropriately.

P7-7 *Calculate the responsivity of a FOG gyroscope made by L=300-m fiber wound on a 2R=8-cm diameter coil, when we read the coil with a source at λ=850 nm.*

Answ. Using Eq.7.5 we get:
$R_F = \Phi_s/\Omega = 8\pi A/\lambda c$,
where we can compute the area as $A=N\pi R^2$, N being the number of turns, given by $N=L/2\pi R$. Upon substitution it is $A=(L/2\pi R)\pi R^2 = LR/2$ and then:
$R_F = 8\pi A/\lambda c = 4\pi LR/\lambda c$
$= 12.56 \cdot 300 \cdot 4 \cdot 10^{-2}/(0.85 \cdot 10^{-6} \cdot 3 \cdot 10^{8}) = 0.591$ rad/(rad/s)
This figure is close to unity and is typical. Thus, as a default estimation of the signal out of a FOG gyro it is customary to use the $R_F \approx 1$ rule-of-thumb.

P7-8 *Calculate the amplitude of the signal expected from a FOG (with the data as in Probl.7-7) when the rotation is 1 deg/hour.*
Answ.: As a phase signal, recalling that 1 deg/h=4.7 μrad/s, we get:
$\Phi_s = R_F\,\Omega = 0.591 \cdot 4.7 \cdot 10^{-6} = 2.78$ μrad.

If we now consider that the Sagnac interferometer signal swings from 0 to a full V_{bb} in the photodiode preamplifier receiver, where V_{bb}=10 V is the typical large-signal swing, then we get for the output signal:
$V_{out}= RI_{ph}= RI_{ph0}[1+ \cos (\phi_{bias}+\Phi_s)]$
and letting ourselves to the most favourable condition, $\phi_{bias}=-\pi/2$, we get:
$V_{out}= RI_{ph0} \sin \Phi_s \approx RI_{ph0} \Phi_s = V_{bb}\Phi_s$
In conclusion, a Φ_s= 2.78-μrad signal will show up, on the quiescent voltage RI_{ph0}, as an amplitude variation of:
$V_{bb}\Phi_s= 10\ V \cdot 2.78 \cdot 10^{-6}= 27.8\ \mu V$,
a very small value indeed, that is not yet the lower limit we would like to approach.

P7-9 *Take into account a fluctuation of 0.1% of the loss of the launch coupler, and calculate the error generated in the output signal.*

Answ.: If the beamsplitter is loss-less, the phase shift between transmitted E_t and reflected E_r fields is π/2. With no lack of generality, we may suppose the two components are of equal amplitude, $E_t=E_r=E_{in}/\sqrt{2}$, or that $R= (E_r/E_t)^2=(E_{in}/E_t)^2= 0.5$.
For a generic loss p, the angle between E_r and E_t is found as [see *'Photodetectors'*, page 261]:
$\phi_{err}= \pi/2+p/2\sqrt{R(1-R)}$, where R is the power reflection.
Taking R=0.5 we get: $\phi_{err}=\pi/2+p$, or, the angle deviates from π/2 by a quantity equal to the loss p. In our case, the deviation is 0.1%=1 mrad. This figure is reduced because of the Sagnac configuration, but we take it now as a conservative estimate. Letting Φ_s=0 and $\phi_{bias}= \pi/2+\phi_{err}$, the output signal fluctuation would be:
$V_{bb}\phi_{err}= 10\ V \cdot 10^{-3} =10\ mV$,
i.e., much larger than the signal considered in previous Problem, and this tells us how careful we shall be about sources of inadvertent phase-shifts, in the FOG.

Q7-10 *Since the FOG works on the Sagnac configuration, a balanced interferometer, the phase shift ϕ_{err} supposed in Probl.7-9 should actually be cancelled out when the beating of the two counter-propagating beams is considered. How do you comment about it ?*
Answ.: Indeed, the error generated is not the total ϕ_{err}, but the difference $\phi_{err}(t)-\phi_{err}(T-t)$ where $T=2\pi NR/c$ is the time delay of propagation through the coil (see Eq.7.23).

To get further insight, we can assume that $\phi_{err}(t)$ is a random process with white spectral density up to a corner frequency f_ϕ, characteristic of the device. Then, the actual error becomes:

$\sigma_\phi^2 = \sigma_{\phi_0}^2 [1-\text{sinc}^2 2\pi fT]$

where is σ_ϕ the rms error, $\sigma_{\phi_0}^2$ its low-frequency value, and sinc(..)= sin(..)/(..) is the function summing up the suppression effect due to the delayed subtraction.

As a consequence of the above consideration, the dc (or zero frequency) error is suppressed, the cancellation is partial for intermediate frequency up to $1/2\pi T$, and there is no cancellation for $1/2\pi T < f < f_\phi$.

Q7-11 *Can any other waveform different from the sinusoidal be employed to drive the dither excitation (Fig.7-13 and 14) of the piezo actuator to unlock the gyro ?*

Answ.: Several options other than the sinusoidal can be considered. For example, a sinusoid plus a square wave can superpose a pedestal to the half-periods indicated in Fig.7-14, resulting in a better linearity of the dithered response. However, the optimum waveform depends on the locking range, which on its turn is not that stable in time. So, after all, no sophistication of the dither waveform is worth the added complication.

P7-12*Would you prefer a gyroscope tagged with a noise of 0.01 deg/h or one with 0.01 deg/√h ?*

Answ.: The specifications are different. The former is the rms error or MDΩ of the device, whereas the latter stands for the spectral power density of the fluctuation, S_Ω.

As the relation between the two (see Eqs.7.20) is:

$MD\Omega = S_\Omega/\sqrt{T} + \Omega_{ZB}$

where Ω_{ZB} is the zero-bias error. In the comparison, it is clear that it is better to have the former figure (0.01 deg/h) provided T<1-h, because the latter figure will become increased, when divided by a number <1 to get the total MDΩ.

P7-13 *In the right-hand side of Fig.7-17, the levelling down to nearly constant of the diagrams is due to the zero-bias error coming into play or to other reason ?*

Answ.: May be due to Ω_{ZB}, but also to non-white (that is, 1/f or $1/f^2$) noise components. No general rule exists to tell one case from another.

P7-14 *We read the FOG gyro of Probl.7-7 (L=300-m, 2R=8-cm, λ=850 nm.) with the open-loop configuration based on a PZT phase modulator. What is the optimum value of the frequency modulation? What is the typical drive voltage required by the PZT ? What is the signal amplitude obtained at the output?*

Answ.: We use the criterion of maximising the signal output $\sin\Phi_s$ (page 280):

$2J_1(\Phi_0) = \max$

The maximum is found at $\Phi_0=1.8$, and recalling (Eq.7.25) that:

$\Phi_0= 2\Phi_{m0} \sin \omega_m T/2$

we see that we can actually trade frequency (term $\sin \omega_m T/2$) for drive amplitude (term Φ_{m0}) of the PZT phase modulator. However, if we take full advantage of the first term, we have to maximise the sine dependence choosing

$\omega_m T/2= \pi/2$, or, solving for frequency: $f_m =1/2T$

Using T=nL/c in this expression, we get:

$f_m=1/2T= c/2nL = 3\cdot10^8 /2\cdot1.5\cdot300= 333$ kHz, a very reasonable value.

Now, returning back to $\Phi_0=2\Phi_{m0} \sin\omega_m T/2$, having $\sin\omega_m T/2=1$, we need a phase amplitude

$\Phi_{m0}=\Phi_0/2 \sin\omega_m T/2=1.8/2 = 0.9$ rad.

This is a very reasonable value, too.

We can calculate the drive voltage required for a phaseshift $\Phi_{m0}=0.9$ rad from the data published in literature (page 282). A typical relationship to voltage is $\Phi_{m0}=\kappa N V_{dr}$, where N is the number of turns wound on the PZT cylinder, and κ is a conversion coefficient depending on PZT material and geometry, but that usually is in the range 0.05..0.2 rad/V. Assuming:

$\kappa=0.1$ and N=5 we get the drive voltage amplitude as:

$V_{dr}=\Phi_{m0}/\kappa N = 0.9/0.5 = 1.8$ Volt

[Note: if we wish so, we can now trade amplitude V_{dr} for frequency f_m leaving unchanged the other quantities, for example: $V_{dr}=1.8\cdot10=18$ V and $f_m=333/10=33.3$ kHz. This allows us to lower f_m below the high-frequency cutoff of the PZT].

The signal output (see Eq.7.27) is now:

$$I_{ph}/ I_{ph0} = 1+[J_0(\Phi_0) + 2 J_2(\Phi_0) \cos 2\omega_m t + \text{hoh}] \cos\Phi_S + \\ + 2 [J_1(\Phi_0) \cos \omega_m t + \text{hoh}] \sin\Phi_S$$

where hoh =higher-order harmonics. So, besides the dc component $\approx 1+ J_0(1.8)=1.34$, there is a minor $2 J_2(1.8)=0.62$ second-harmonic component in

$\cos\Phi_s$, and then the term of interest, a $\sin\Phi_s \approx \Phi_s$ signal of amplitude 2 $J_1(1.8)=1.16$.
If the detected signal is sent to a front-end amplifier with (Probl.7-8) $V_{bb}= R I_{ph0} =10V$, we would get:
$V_{out}=R I_{ph}= V_{bb} 2 J_1(\Phi_0) [\cos \omega_m t] \sin\Phi_s \approx 11.6 \Phi_s$
and, for Ω=1 deg/h whence $\Phi_s = 2.78$ μrad, the amplitude of the $\cos \omega_m t$ carrier is
$V_{out}=11.6 \cdot 2.78$ μrad =32.2 μV,
a value not so different from the amplitude estimated in Probl.7-8.

P7-15 *Should we wish to get the cosΦ in addition to the sinΦ signal in the FOG external configuration, how large shall we expect is it ?*

Answ.: From previous Problem, we have in the output signal I_{ph} a second-harmonic component $\cos 2\omega_m t$ with amplitude: =0.3/100
$V_{out}= R I_{ph} = V_{bb} 2 J_2(\Phi_0) [\cos 2\omega_m t] \cos\Phi_s$
$=10 \cdot 0.62 \cdot [\cos 2\omega_m t] \cos\Phi_s$
The amplitude of the $\cos\Phi_s$-modulated second-harmonic component is therefore $10 \cdot 0.62=6.2$ V, not so different from the amplitude of the fundamental component.

P7-16 *How can we derive the datum of CW/CCW mode coupling due to fiber backscattering (page 285) at -55 dB/m, typically?*

Answ.: To calculate this figure, we start considering the attenuation of a good communication or FOS fiber, typically α=3dB/km (or, a factor 2 for L=1-km) at λ=850 nm.
Inserting in $P=P_0 \cdot 10^{-\alpha_{L/10}}$ we get: $\text{Log}_{10}2=\alpha$(1-km)/10 whence $\alpha=0.3/100 = 0.003$ m^{-1}. To convert to Neper units, we compare with Lambert-Beer law written as $P=P_0 e^{-\alpha' L}=10^{-0.43\alpha' L}$ and find $0.43\alpha'=\alpha/10$, or $\alpha'=\alpha/4.3 =0.00069$ m^{-1}. As in general we have α=a+s (App.A3.1), and near a minimum of attenuation we may expect s=0.8 α, we get a scattering coefficient: s=0.00055 m^{-1}. The scattered power is radiated isotropic in space according to Lambert cosine law, on 2π sterad. The capture angle for backscattering is $\Omega_{bsc}= \pi(\lambda/\pi w_0)^2$ where w_0 is the fiber core radius. Taking w_0=2.5μm and λ=0.85μm, we get the fraction of collected backscatter light as:
$\Omega_{bsc}/2\pi=0.5(\lambda/\pi w_0)^2= 0.5(0.85/3.14 \cdot 2.5)^2=0.5(0.108)^2=5.8 \cdot 10^{-3}$,
Now, the total coupling due to backscattering is given by:
$A_{tot}=\alpha' \Omega_{bsc}/2\pi=0.00055 \cdot 5.8 \cdot 10^{-3}$ $m^{-1}=3.2 \cdot 10^{-6}$ m^{-1}
This is equivalent to say that the A_{tot} is $10\text{Log}_{10}3.2 \cdot 10^{-6}$=-55 dB/m

P7-17 *Estimate the contribution, to the zero-bias error, of the Rayleigh backscattering from the fiber in a FOG gyro, when using a laser source with linewidth $\Delta\nu$=10 MHz and when using a SLED with spectral width $\Delta\lambda$=50 nm.*

Answ.: On the 200-m=L length of the fiber, the strength of the Rayleigh backscattering amounts to:
$A_L = A_{tot} + 10\text{Log}_{10}L/(1\text{-}m) = -55 + 23 = -32$ dB. In power, this means a backscattered fraction given by $10^{A_{tot}} = 10^{-32/10} = 0.63 \cdot 10^{-3}$. If the coherence length were larger than L=200m, this power will sum coherently with the useful signal, and the angle of wandering (see Fig.7-22) would be:
$\phi_{bs} = \sqrt{A_L} = \sqrt{(0.63 \cdot 10^{-3})} = 25$ mrad,
an enormous error, absolutely unacceptable.
Actually, using the laser diode with $\Delta\nu$=10 MHz, we get a coherence length $L_c = c/\Delta\nu = 3 \cdot 10^8/10$ MHz= 30 m,
and in a first approximation can state that only a fraction L_c/L of the total backscattering is added coherently. Then, we get
$A_L = 0.63 \cdot 10^{-3} \cdot 30/200 = 0.95 \cdot 10^{-4}$ and the phase error
$\phi_{bs} = \sqrt{A_L} = 9.7$ mrad (LD) still a very large, intolerable value.
Considering the SLED, we get for the coherence length:
$L_c = \lambda^2/\Delta\lambda = 0.85^2/0.05 = 14.4$ μm. Now the coherent field fraction is
$A_L = 0.63 \cdot 10^{-3} \cdot 14.4 \cdot 10^{-6}/200 = 4.5 \cdot 10^{-11}$ and $\phi_{bs} = \sqrt{A_L} = 6.7$ μrad (SLED).
So, with the SLED, we have slashed down the phase error due to backscatter to a reasonable low value.

P7-18 *An Integrated Optics FOG is made up with N=10 turns of 4-cm=R radius waveguide on a SOS substrate. What is the responsivity of the FOG ? What the expected phase and NEΩ performance ?*

Answ.: We go back to Eq.7.5 or Probl;7-7 and write:
$R_F = 8\pi A/\lambda c = 8\pi^2 NR^2/\lambda c$
$= 78.87 \cdot 10 \cdot 4^2 \cdot 10^{-4}/(0.85 \cdot 10^{-6} \cdot 3 \cdot 10^8) = 0.005$ rad/(rad/s)
a value much smaller than that [0.591 rad/(rad/s)] of a typical fiber FOG.
Assuming now the same power available at the detector, that is P=1mW, from the diagram of Fig.7-6 we can find, at B=100Hz:
ϕ_n=0.1 μrad.
This is a relatively minute angle, not very easily resolved. Anyway, assuming to detect it, the corresponding noise-equivalent angular velocity is found as:

$NE\Omega = \phi_n / R_F = 0.1 \cdot 10^{-6}/0.005 = 20$ μrad/s = 4.2 deg/hour.
This example is of more general validity than the numbers tell. Indeed, reducing the responsivity implies a reduction of performances, because what is relatively independent from the chosen configuration is the minimum detectable phase, typically 0.1 to 1 μrad.

Q7-19 *Number out the advantages of the closed-loop, digital readout FOG compared to the open-loop configuration. Consider: NEDΩ, linearity, dynamic range, signal swing of the electronic circuit, and bandwidth.*

Answ.: The main advantage of CL-FOG (closed-loop) compared to OL-FOG (open-loop) is the output format, digital instead of analogue. When lot of bits are involved (the FOG readily provides a dynamic range of 6 decades, or 20 bit) the digital readout removes all the errors and limitations faced with the A/D converter.
Second, closed loop operation provides the best linearity, because even at large signals that would entail a $\sin\Phi_s$ distortion, working dynamically at $\Phi_s \approx 0$ cancels out the error.
The signal swing in the circuits is the same as for an open-loop, so is the voltage swing feeding the PZT. Bandwidth required to preserve the waveform is higher than the Φ_s signal bandwidth, because of the $\Delta\phi$ steps making up the digital ramp. Bandwidth of the Φ_s signal is the same in the two cases.

P7-20 *A MEMS gyroscope has a mass m=2μg and the resonant frequency is f_0=10 kHz. Find the spring constant and how large is the comb displacement undergone by application of a constant force F=1μN. Assuming then a readout comb made by 60 fingers, 2x300 μm in area and 2 μm in gap, calculate the capacitance variation obtained. Last, calculate the Coriolis force induced by a Ω=1rad/s angular velocity.*

Answ.: The spring constant is solved out from $\omega_0=\sqrt{k/m}$ as:
$k=m\,\omega_0^2 = 2 \cdot 10^{-9} \cdot (6.28 \cdot 10^4)^2 = 7.9$ N/m
The comb displacement occurring when a constant force F is applied is:
$x = F/k = 10^{-6}/7.9 = 0.126$ μm.
The capacitance of the comb structure is:
$C = \varepsilon_0 N A/w = 8.86 \cdot 10^{-14} 60 \cdot (600 \cdot 10^{-4})^2/2 \cdot 10^{-4} = 0.159$ pF
Now we can apply the virtual work principle to the comb, when they move from a separation w to a new separation w+dw, and equate the change of electrostatic energy to the elemental work performed F dw:

$\delta L = (1/2)\, dCV^2 = -F\, dw$
Differentiating C we obtain: $dC = -\varepsilon_0 NA/w^2 dw = -(C/w)dw$, and:
$(1/2)\,(C/w)dw\, V^2 = F\, dw$, whence
$F = (C/2w)\, V^2$
Now, let's take V=10 V as the bias and find:
$F = (0.159\ pF/2 \cdot 10^{-4})\ 100 = 0.08 \cdot 10^{-6}$ N, whence a displacement Δz:
$\Delta z = 0.08 \cdot 10^{-6}\ N/7.9 = 0.01\ \mu N$,
a value that is about 1% of the constant force assumed above.
Using Eq.7.35 we get the Coriolis force as:
$F_c = 2m\, \Omega\, v$.
To find the excitation velocity v, let us assume a Q factor Q=10. Then the velocity due to a force applied at the resonance frequency is calculated as:
$v = \omega_0 Q\, F/k = 6.28 \cdot 10^4 \cdot 10 \cdot 10^{-6}/7.9 = 7.91 \cdot 10^{-2}$ m/s, and accordingly
$F_c = 2m\, \Omega\, v = 2 \cdot 2 \cdot 10^{-9} \cdot 1 \cdot 7.91 \cdot 10^{-2} = 0.32$ nN
This is barely measurable, being about a few percent of the force between the combs.

Problems and Questions, Chapter 8

Q8-1 *How would you classify a hypothetical optical-fiber-sensor (OFS) for SARS detection, based on the colour change induced in an organic tracer cemented to the fiber end face ?*

Answ.: This sensor would be a kind of *optrode*. As a OFS, it would be classified as *extrinsic*, *indirect* sensor, of the *intensity-readout* category.

P8-2*How can I design a balance for weighting small (<500g) weights, based on an intensity readout OFS ?*

Answ.: We can do that with two fiber pigtails, whose end faces are separated by about one fiber diameter (so that $z/2a \approx 1$ in Fig.8-6), and bearing a helical spring slipped axially upon the fibers. Eventually, we take advantage of sleeves (or ferules) to cement the spring and distribute the load along the fiber length.
When a weight is applied to the arrangement laid vertically, the spring pulls closer the fiber end faces. The signal attenuation is given by the diagram of Fig.8-6, where the quiescent point is chosen according to the desired range and linearity. As the diagram is nearly logarithmic versus the

displacement, a log-attenuation circuit will bring to about linear the measurement.

P8-3 *Can additional measurand other than force be measured with the arrangement of fiber misalignment ?*

Answ.: In addition to force and pressure (Fig.8-7) we can measure angular displacement and torque, by taking advantage of the angle misalignment loss A (Fig.8-6 bottom left). Mounting two fiber pigtails on a rotary stage, one pigtail being fixed to the stage and the other free of moving, we get an $A=A(\alpha)$ dependence from loss [seen in (Fig.8-6 to be almost quadratic].
The torque sensor is implemented in a similar way, by adding a spiral spring to the fixture holding the fiber.

P8-4 *Can the intensity readout OFS considered in Probl.8-1 and 8-2 be implemented by a single-ended access, using just one fiber pigtail ?*

Answ.: Yes, it can be done using a mirror in place of the second fiber pigtail end face, and the result looks like the arrangement depicted in Fig.8-8 (right) for the pressure sensor.
At the expense of an increased part count (we need an input/output coupler) and some extra loss (6dB for the go-and-return passage through the coupler), we get a more compact and easily deployed sensor.

Q8-5 *Two common problems of intensity-readout OFS are the lack of a reference and the poor linearity. How can we mitigate them with a minimum of added complexity?*

Answ.: To be able adding a reference, we need getting a separate 'channel' of measurement, that is, another variable or 'degree of freedom' of the optical measurand.
Perhaps the easiest and most frequently available degree of freedom is wavelength. We can reference an amplitude or intensity measurement by taking advantage of the wavelength-dependence of the measurand, let's say, strong at λ_1, and weak or vanishing at λ_2. If we find such a circumstance, then the interval around at λ_1 will be the measurement channel, and the interval around at λ_2 will be the reference channel. A subtractor stage will perform the referencing, better if preceded by a log-converter stage - so that the log-and-difference operation amounts to make the ratio of measurement to reference.
About linearity, a common cure is already performed with the log conversion as far as the optical readout is attenuation proportional to the

physical measurand. In other cases, we have to correct the readout with a look-up table.
Examples of development of the above concepts are: the temperature OFS (Fig.8-10), the Nd-fiber high-temperature OFS (Fig.8-11), and the pH-measurement optrode (Fig.8-14).

P8-6 *How large is the circular-birefringence rotation induced in a fiber subjected to a 1-Ampere-turn magnetic field intensity?*

Answ.: Assuming λ=850 nm and a normal silica fiber, we have (see Table 6-1) for the Verdet constant:
V= 3 μrad/A
then, the angle of rotation of a linear SOP (state of polarization), induced by a magnetic field along a piece of fiber of length L is (Eq.8.3):
$\Psi = V \int \underline{H} \cdot \underline{dl} = VHL$
and when we consider a wire carrying a current I, linked to the fiber with a number of turns N, we get:
$\Psi = VNI$
Now, if N=1 and I = 1 Amp, we get a rotation Ψ= 3 μrad
This is a quite small value, and explains why the magneto-optical current sensor is difficult to implement, at least when a sensitivity comparable to that of usual electrical instruments.
Indeed, if we use the setup of Fig.8-16 to read the birefringence, the amplitude of the output signal is $\sin 2\Psi \approx 2\Psi$ in power. Thus, we are going to read a power $\approx 2\Psi = 6 \cdot 10^{-6}$ of the input power P_0, a minute signal that we should check from the point of view of noise.

P8-7 *How can we increase the small value of the rotation angle of Probl. P8-6 ?*

Answ.: We can link more turns N_f of fiber to the conductor carrying the current, as well as more turns N_w of wire to the fiber. Doing so, we get:
$\Psi_{multiturns} = N_f N_w \Psi_{1\text{-}turn}$
As an example, for 30 wire turns linked to 30 fiber turns, we get
$\Psi_{multiturns} = 30 \cdot 30 \cdot 3$ μrad= 2.7 mrad
still a small value but much easier to be measured.
Another possibility is using a YIG crystal (yttrium iron garnet), which has a Verdet constant $\approx 10^3$ time that of the silica. In this case, however, we have N_f =1 because we can't wind the crystal, and additionally, the OFS becomes of the *external* type.

P8-8 *Can we sense a magnetic field produced by a normal magnet, say supplying B=1000 Gauss, with the following: (i) a short piece (10-cm) of fiber; (ii) a coil of N=100, 1-cm dia. fiber turns; (iii) a 1-cm long YIG garnet ?*

Answ.: We recall that an induction of B=1000 Gauss corresponds to a magnetic field intensity of H= 1000 Oersted, and that being 1 Oe = 80 A/m, we get H=80 000 A/m= 800 A/cm.
Now, using a 1-cm fiber we get
$\Psi = V \int \underline{H} \cdot \underline{dl} = VHL = 3 \cdot 10^{-6} \cdot 800 \cdot 10 = 24$ mrad, a small but measurable angle; in case (ii) we get
$\Psi = V \int \underline{H} \cdot \underline{dl} = 0$, because the liner integral of the magnetic field H is zero on the closed path of the coil (unless H is produced by a current and the coil is linked to the wire); and in the case (iii):
$\Psi = VHL = 3 \cdot 10^{-3} \cdot 800 \cdot 1 = 2.4$ rad, a large value, that tells us how the YIG can be useful indeed in magnetic field measurements.

P8-9 *Calculate the minimum current we are able to measure (with a S/N=1) using a fiber coil linked to the current wire, with N_f =25 turns, using an optical power P_0=1mW and a measurement Bandwidth B=10 Hz*

Answ.: Entering in Fig.8-21 (or using Eq.8.7) we can read the NEI (noise equivalent current) and the corresponding noise-rotation angle Ψ_n at 100 Hz and 1 mW (or 1 mA). To read our data, we shall only mind the correction factor, respect to the N=50 case of the diagram. For N_f =25, we shall multiply by 2 both NEI and noise Ψ_n. Doing so, we obtain:
NEI = 2 mA, $\Psi_n = 4 \cdot 10^{-7}$ rad
If we were able to resolve such a small angle (Ψ= 0.4 μrad), a milliAmp capability of current OFS would be obtained. Unfortunately, several disturbing effects (like in the FOG) impede us from attaining the quantum limit of performance.

P8-10 *A 1-cm long fiber is loaded with a small weight F=0.01 N. Knowing that the photoelastic birefringence coefficient is q=0.3 rad/N, calculate the signal amplitude that is read with the basic scheme (Fig.8-23) using a 1-mW power.*

Answ.: The coefficient q comes from the analysis of the elasto-optical deformation of the fiber, with the final result expressed as:
$\Delta\Psi_{lin} = 2n^3(1+\nu)E^{-1}(p_{11} - p_{12})\, F/r\lambda$

where E and ν are the Young's and Poisson's moduli, n is the effective index of refraction and the p's are the strain elasto-optical coefficients (p_{11}=0.121 and p_{12}=0.270 in silica fiber). Inserting the values, we get the phase as $\Delta\Psi_{lin}$= 0.3 rad/N.
Now, in the scheme of the linear birefringence readout (Fig.8-23 and 24) we get an output signal
$\sin 2\Psi \approx 2\Psi$,
or, we are going to read a power fraction of the initial power P_0:
$\approx 2\Psi$= 0.3 rad/N ·0.01 N= 3 mrad
This is about 0.3% of the input power, an easily detected quantity. Note that 0.01 N is about 1gram in weight.

P8-11 *Can we develop an OFS hydrophone sensitive enough to beat the human hearing ?*

Answ.: We can assume to employ a reasonable length of fiber, say L=5 m, wound on a coil as 82 turns of 2πR= 6.28 cm. A coated monomode fiber may have a sensitivity, to isotropic hydrostatic pressure (see p.347):
s_{ac}= 300 μrad/Pa ·m
whence an optical phase developed per unit pressure:
$\Delta\phi = s_{ac}L$ = 300 μ5= 1.5 mrad/Pa.
Now, the threshold of human hearing in normal working conditions is about +10 dBa (@ 3kHz) respect to the 0-dBa level, equivalent to a pressure of $10 \cdot 2 \cdot 10^{-5}$ Pa = $2 \cdot 10^{-4}$ Pa (see also page 348). Thus, at the acoustic threshold we get a typical phase:
$\Delta\phi$= 1.5 mrad $2 \cdot 10^{-4}$= $0.3 \cdot 10^{-7}$ rad.
This is a very small value that amounts to have, on a 1mA average value (detected from a ≈1mW power), a minute signal current, specifically i≈ $0.3 \cdot 10^{-7}$ rad ·1mA= 30 pA.
But, as this current is alternate, not continuous, and on a moderate (audio) bandwidth, so it is much easier to amplify and detect it down to the level of quantum noise. Indeed, the quantum noise limit associated to 1mA, on a 1-Hz bandwidth, is:
$i_n = (2eIB)^{1/2} = (2 \cdot 1.6 \cdot 10^{-19} \cdot 10^{-3})^{1/2} = 1.8 \cdot 10^{-11}$=18 pA.
So, at least from this very preliminary evaluation, our OFS hydrophone can indeed equal or surpass the performance of the human ear.